Studies on RNF168 and CXCL5 Expression by Epithelial Cell lines during RSV Infection

By Jonathan Jeyatheswaran

This thesis was submitted according to the requirements of the University of Liverpool for the Master of Philosophy Degree

By Jonathan Jeyatheswaran

August 2013

CONTENTS

Acknowledgements

First and foremost I would like to thank my supervisors Dr Paul McNamara and Dr Brian Flanagan for their invaluable support and guidance during my first year of laboratory based research. I also wish to thank other members of the Respiratory Research team, Angel Hackett, Rachel Corkhill, Katie Rose, Gemma Saint and Wael Alturaiki for their advice with regards to mastering the laboratory techniques that I have learnt throughout the year. I would also like to take this opportunity to thank other staff members at the Institute of Child Health including Angela Midgley, Lucy Ballantine, Graham Jeffers, Moira Saphier and Jean Maguire for their continual support throughout the year. I would like to express my gratitude to my fellow MPHIL students James Braniff, Rosanne Pickles and Bethan Griffith for their encouragement throughout the year. Finally, I would like to thank my family and friends for their great level of support throughout this year of research.

Abbreviations

ARI	Acute Respiratory Infection
BAL	Bronchial Alveolar Lavage
BPD	Bronchopulmonary Dysplasia
BSA	Bovine Serum Albumin
CCA	Chimpanzee Coryza Agent
CF	Cystic Fibrosis
CHD	Chronic Heart Disease
CLD	Chronic Lung Disease
COPD	Chronic Obstructive Pulmonary Disease
DC	Dendritic Cells
DDR	DNA damage response
DFA	Direct Immunofluorescent Antibody Titres
DMEM	Dulbecco's Modified Eagle Medium
DNA	Deoxyribonucleic acid
DSBs	DNA double strand breaks
dsRNA	Double stranded RNA
DTT	Dithiothreitol
ELISA	Enzyme-linked immunosorbent assay
ENA-78	Epithelial cell-derived neutrophil-activating peptide-78
FCS	Fetal Calf Serum
HECT	Homologous to the E6-AP Carboxyl Terminus

HPA	Health Protection Agency
HRP	Horse Radish Peroxidase
HSV-1	Herpes Simplex Type 1
IFN	Interferon
IFNAR	Interferon alpha/beta receptor
IL-6	Interleukin-6
Il-8	Interleukin- 8
IRF	Interferon regulatory factor
ISGs	Interferon-stimulating genes
JAK	Janus Tyrosine Kinase
LRTI	Lower Respiratory Tract infection
MAVS	Mitochondrial antiviral signaling proteins
MDA5	Melanoma Differentiation-Associated protein 5
MHC	Major Histocompatibility Complex
MIU	Motifs Interacting with Ub
MOI	Multiplicity of Infection
mRNA	Messenger RNA
NF-*k*B	Nuclear factor kappa-light-chain-enhancer of activated B cells
NLRs	nucleotide-binding oligomerisation domain (NOD)-like receptor
NOD	nucleotide-binding oligomerisation domain
NPA	Nasopharyngeal aspirate
PAMPs	Pathogen Associated Molecular Patterns
PBS	Phosphate Buffered Saline
PCR	Polymerase Chain Reaction
PICU	Paediatric Intensive Care Unit

Poly I:C	Polyinosinic:polycytidylic acid
PRR	Pattern Recognition Receptors
RADT	Rapid antigen detection testing
RIDDLE syndrome	radiosensitivity, immunodeficiency, dysmorphic features, and learning difficulties syndrome
RIG-1	Retinoic acid inducible gene – 1
RLR	Retinoic acid inducible gene – 1 (RIG-1)-like receptor
RNA	Ribonucleic Acid
RNP	Ribonucleoprotein
RSV	Respiratory Syncytial Virus
RT-PCR	Reverse Transcriptase Polymerase Chain Reaction
SDS	Sodium Dodecyl Sulphate
SH	Small hydrophobic protein
STAT	Signal Transducer and Activator of Transcription, or Signal Transduction And transcription
TBS	Tris Buffered Saline
TLR	Toll-like Receptors
TRAM	TRIF-related adaptor molecule
Ub	Ubiquitin
USA	United States of America
WHO	World Health Organisation
WT	Wild Type

List of Figures

List of Tables

Table 3.2.3: P-values for 24 Hours RSV to determine whether there was any statistical significant ($p<0.05$) difference between samples and the control

Table 3.2.4: P-values for 4 Hours IFN-beta stimulation to determine whether there was any statistical significant ($p<0.05$) difference between stimulated samples and the control

Table 3.2.5: P-values for 24 Hours IFN-β to determine whether there was any statistical significant ($p<0.05$) difference between samples and the control

Abstract

Background: During herpes simplex virus type 1 (HSV-1) infection, the protein ICP0 causes degradation of RNF168 during infection, preventing the ubiquitination of histones proteins and a subsequent DNA damage response to double strand breaks. Our laboratory has shown that during RSV infection in vitro, RSV replication as measured by RSV N gene expression increased considerably when SiRNA were used to knock down RNF168 gene. This suggests that RNF168 activity may be affected by RSV expression or act to limit RSV replication normally during infection as part of a host cell intrinsic antiviral defence. Identifying and understanding the mechanism by which this occurs may be useful in the development of future drug therapies for RSV.

Aims: To investigate the effect of RSV infection, interferon beta stimulation and polyI:C on RNF168 expression. To investigate how the duration of RSV infection affects the concentration levels of CXCL5.

Methods: A549 cells were infected with RSV in a 24-well plate. Cells were also stimulated with IFN-β and the TLR3 ligand polyI:C**.** Real-time PCR for RSV N gene expression and Sandwich ELISAs for IL-6 and IL-8 were carried out to provide evidence that samples have been infected. Western Blotting was carried out to measure RNF168 expression. A Sandwich ELISA was applied to measure the concentration levels of CXCL5.

Results: At a MOI of 1:1, 4 hours RSV infection suggested that there was an increase in RNF168 expression. This increase was not statistically significant (p=0.13). At 24 hours after RSV infection, MOI 1:1 the level of RNF168 expression decreased in comparison to control but this decrease was not statistically significant (p=0.14). However, at a MOI of 0.025:1, 24 hours after infection, RNF168 expression increased in comparison to the control. This change was not significant (p=0.29). IFN-β stimulation for 4 hours suggested that higher concentrations of IFN-β increased RNF168 expression. This was not a significant change (p=0.17). IFN-β stimulation for 24 hours suggested that higher concentrations caused a decrease in RNF168 expression in comparison to the control (p=0.6 for 100ng/ml). An increase in CXCL5 concentration in infected samples was seen at 6 hours in comparison to control, which supports previous proteonomic data results.

Conclusions: The results of this investigation suggest that RSV and IFN-β affects RNF168 expression at 4 and 24 hours. The preliminary experiment with polyI:C must be repeated to gain more evidence but suggests that TLR3 may be involved in regulating RNF168 expression. For the changes noted in RNF168 expression by RSV, IFN-β and polyI:C to be more significant, repeat experiment could be done to increase the samples size of data obtained. The CXCL5 experiment will have to be repeated but supports previous laboratory findings that CXCL5 is involved in neutrophil recruitment.

1. Introduction

1.1Respiratory Syncytial Virus Background

1.1.1 Overview Respiratory Syncytial Virus

Respiratory syncytial virus (RSV) is a major cause of viral lower respiratory tract infections (LRTI) in children worldwide (1-3). This virus contains a single stranded negative sense ribonucleic acid (RNA) consisting of an estimated 15,000 nucleotides. RSV is part of the family *Paramyxoviridae* and the subfamily *Pneumovirinae* (3, 4). However, this virus is not solely linked to paediatric respiratory illness, with significant respiratory symptoms commonly seen in the elderly and immunosuppressed. RSV disease severity tends to be worse in those with comorbidities such as asthma, Cystic Fibrosis (CF) and Chronic Obstructive Airway Disease (COPD) (3, 5, 6).

1.1.2 Origins of RSV

In Minneapolis during the year 1937 an outbreak of pneumonia occurred in two hospitals with 32 infants affected. Dr John Adams studied these cases, discovering the presence of cytoplasmic inclusions in bronchial epithelium of all dead babies. These findings led to Dr Adams suggesting that the outbreak was due to a virus. Approximately, two decades later in 1961 Dr Adams and his colleagues described a similar episode of lower respiratory tract infection (LRTI) in infants, this time identifying the virus that was to become known as RSV (7, 8).

In 1956 a colony of chimpanzees were noted to be suffering with cold-like symptoms such as coughing, sneezing and mucopurelent discharge. Investigations carried out on throat swab samples taken from one of the chimpanzees identified a cryptopathic agent, which was later named “Chimpanzee Coryza Agent” (CCA). A laboratory worker who came into contact with the infected chimpanzees developed fever and frontal headache. The finding of positive CCA antibody titres in the worker indicated that this disease was transmittable between animals and humans (3, 9, 10).

A year later, Chanock and Finberg identified 2 agents in infants with lower respiratory tract disease indistinguishable from CCA. These agents were named Long and Snyder viruses. The Long agent was a CCA-like virus from an infant with bronchopneumonia and the Snyder agent was a CCA-like virus from an infant with bronchiolitis. It was noted that a prominent characteristic of both viruses was the production of giant cell syncytia in tissue culture. This lead to the suggestion that the agents identified in this study should be grouped together with CCA virus and named "Respiratory Syncytial Virus" (7, 9-12).

1.1.3 Epidemiology of RSV

According to the World Health Organisation (WHO) there are about 64 million cases of RSV with approximately 160,000 deaths per year worldwide (13). Other studies report that there 33.8 million new cases of RSV per year leading to 3.4 million hospital admissions and figures as high at 199,000 deaths per year (99% which occur in the developing world) (14, 15). Laboratory reports, 4 weekly received by the Health Protection Agency (HPA) Colindale for England and Wales from 1991 to 2013 show that the number of reports of RSV is approximately 3200 in 2013 (Figure 1.1.1) (16). According to the HPA the most number of laboratory reports between 2012 and 2013 was 750 for children< 1year old in England and Wales (Figure 1.1.2) (17). RSV is the leading cause of hospitalisations among infants, with those 1 month old at greatest risk of RSV hospitalisation. In comparison, up to 144,000 infants with RSV are hospitalised annually in the United States of America (USA) (13, 18-21). Admissions for RSV make up around 70% of bronchiolitis and 25% of pneumonia cases that have been hospitalised (13, 20, 22).

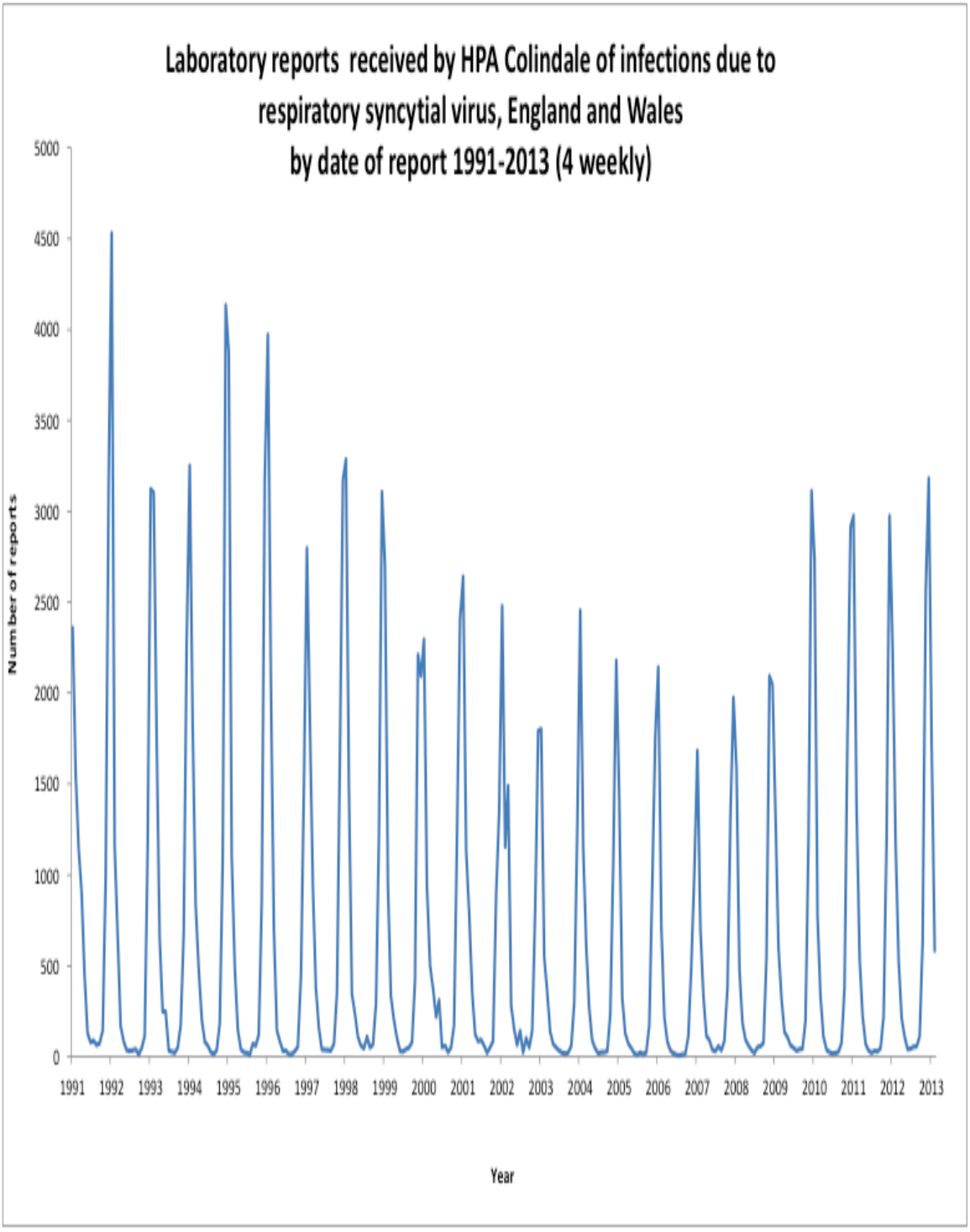

Figure 1.1.1: Laboratory reports due to RSV infection from 1991to 2013, 4 weekly (16).

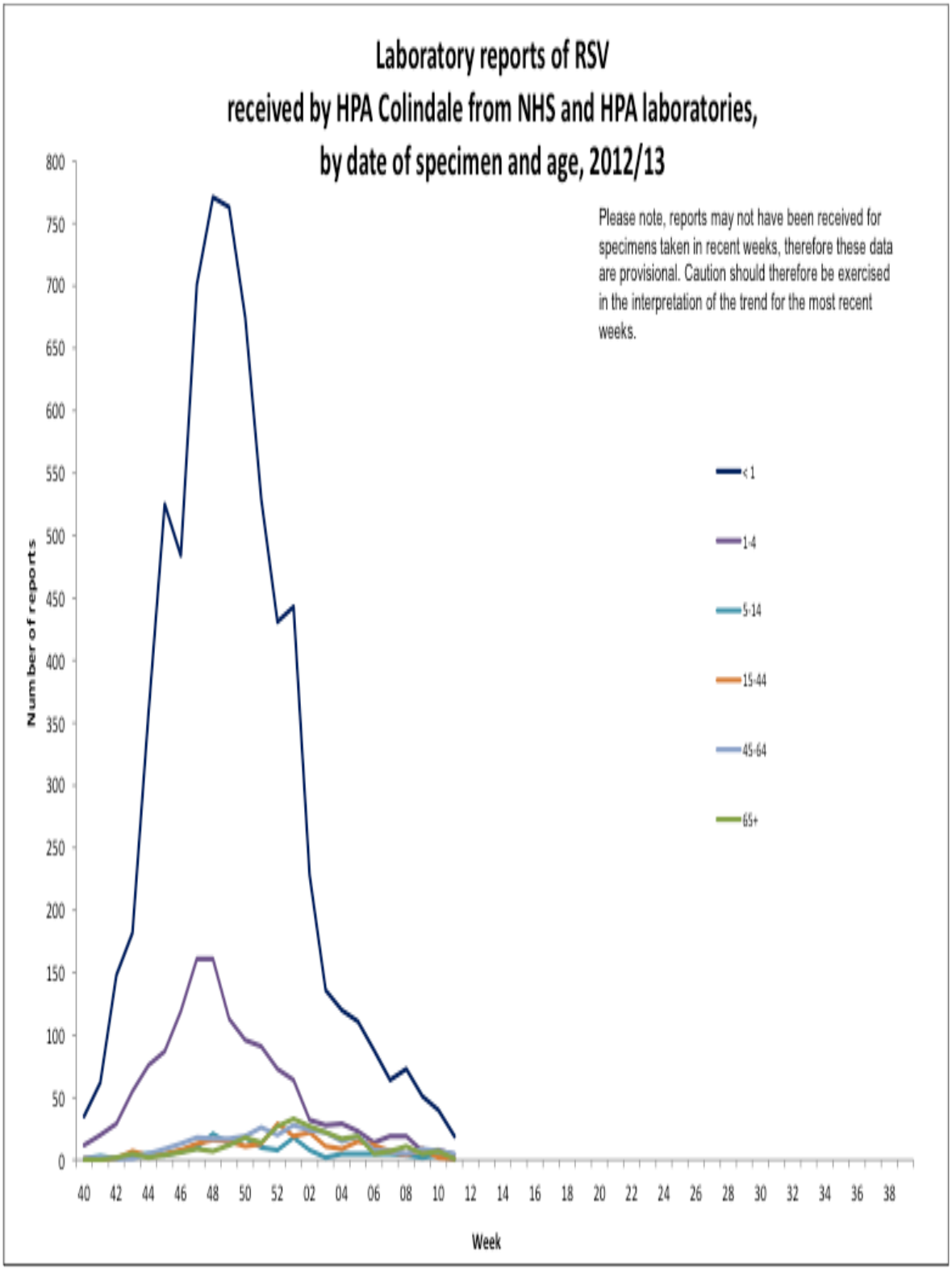

Figure 1.1.2: Laboratory reports for RSV received by data of specimen and age in 2012/13 for England and Wales (17).

Overall, studies have shown that males are more likely to be infected with RSV and hospitalised than females with the ratio at approximately 1.5:1 (23-26). Infants who are in higher socioeconomic groups have a lower chance of developing severe disease as they acquire primary RSV later (23). Pre-term infants tend to be a group associated with an increased risk of severe RSV-related illness and hospitalisation. The main factors contributing to an increased likelihood of hospital readmissions in pre-term children were those with lower gestational age, with siblings attending school and children with Chronic Lung Disease (CLD) (23, 27, 28).

Apart from children, the elderly are also at risk of severe RSV infection. Information provided by WHO states that there are an estimated 14 000 to 62 000 RSV-associated hospitalisations of the elderly occurring annually in the USA. However, cases of RSV are rarely diagnosed in the elderly. This could be due to greater focus and importance being stressed on the effects of the virus in paediatric population (13, 29). In USA nursing homes, RSV 'attack' rates are approximately 5%-10% per year with a 2%-8% case fatality rate. This amounts to approximately 10,000 deaths per year among persons >64 years of age (13).

The incidence in developing countries of RSV is more than twice that of industrialised countries with the virus accounting for a high proportion of Acute Respiratory Infections (ARI) in children. For example, studies in Brazil and Thailand suggest that RSV causes 30% of ARI cases in children between 1 and 4 years of age (13, 15). A study based in Kenya estimated that over half of severe infections occur between 6- 30 months of age rather than< 6 months of age as previously thought, possibly because many children get reinfection with RSV (30).

In the developed world, RSV bronchiolitis is the leading cause of hospitalisations for infants less than 1 year of age. In the winter season, RSV bronchiolitis is a common cause of admission to the Paediatric Intensive Care Unit (PICU) (31). Of the number of children hospitalised with RSV related bronchiolitis in the USA, 15-35% require admission to PICU with 9% requiring mechanical ventilation (32, 33). A recent study found that due to RSV the median length of PICU admission was 5 days with the median length of hospital stay being 9 days (34).

Outbreaks of RSV occur throughout winter in areas with temperate climates coinciding with outbreaks of influenza. In European countries, epidemics have been noted to occur from approximately mid-November to late March (13, 35-37). In comparison, high numbers of RSV cases are reported during the rainy season in tropical countries when the temperature drops (38).

1.1.4 Risk Factors

Some of the main predisposing factors of severe RSV disease include Chronic Lung disease (CLD), Congenital Heart Disease (CHD), neurological disorders, metabolic disorders, birth before 24 weeks gestation and immunodeficiency (Table 1.1). Bronchopulmonary Dysplasia (BPD), Cystic Fibrosis (CF) and severe asthma increase the risk of severe RSV infection. Due to their immune status and the structural prematurity of distal air spaces, children less than 2 months tend to be more susceptible to RSV than older children (Tables 1.1 and 1.2) (39-41).

In developed countries, lack of breastfeeding, day care exposure, older siblings in households, male sex and birth during the RSV season are risk factors for RSV and severe RSV bronchiolitis (Table 1)(42). In comparison, the main risk factors for severe disease found in developing countries are indoor smoking pollution, crowding and malnutrition (Table 1.2) (37, 39, 43-45). A universal recognised risk factor for RSV infection is smoking. In particular maternal smoking was noted to be more harmful than paternal smoking. Studies have found that maternal smoking during pregnancy was noted to be an independent risk factor for reduced lung function and increased airway reactivity presenting during adulthood (39, 46).

Table 1.1: Conditions and resultant pathophysiology leading to increased risk of RSV in children (42)

Children at risk of Severe RSV disease	
Condition	**Pathophysiology**
Premature birth	Altered airway anatomy Absence of maternal antibody
Chronic Lung Disease	Bronchial hyper-responsiveness Reduced lung reserve
Congenital Heart Disease	Pulmonary hypertension
Neuromuscular disease	Decreased respiratory muscle strength and endurance
Immune deficiency	Decreased host defence

Table 1.2: Main Risks Factors contributing to Severe RSV infection (37, 39, 43-45)

Main Risk Factors contributing to Severe RSV infection
Social Determinants: • Infant environmental smoke exposure. • Maternal exposure to environmental tobacco smoke during pregnancy. • Maternal tobacco use during pregnancy. **Significant Illness:** • Severe neurological disorders. • Severe metabolic disorders. • Chronic lung disease (CF, BPD, Asthma). • Haemodynamically significant Congenital Heart Disease (CHD) • Disorder of cellular immunity. **Environmental Factors:** • Malnutrition • Presence of siblings • Crowded living conditions • Low socioeconomic status • Day care exposure • Outdoor air pollution • Indoor smoke (due to burning wood or coal) **Other:** • Male sex • Current weight <5kg • Premature birth (before 35 weeks gestations)

1.1.5 Clinical Features

The symptoms of RSV infection range from mild cold-like symptoms to those of severe pneumonia or bronchiolitis. Upper respiratory tract symptoms such as coryza, rhinitis and coughing have been known occur in patients. Low-grade fever and rhinorrhoea is usually present with some children developing otitis media. Children who suffer with more severe infection display signs of nasal flaring, grunting and intercostal recessions (47-49). Infants often have an increased respiratory rate and hyperinflated chest because of increased air trapping. Cases of bronchiolitis can result in severe hypoxia and acute respiratory failure (48, 50).

1.1.6 Investigations

RSV infection can be tested for using the following methods (51, 52):

- Serology
- Cell culture
- Direct immunofluorescent antibody tests (DFA)
- Enzyme linked immunoassays
- Nucleic acid amplification (using PCR)
- Rapid antigen detection testing (RADT)

In acute illness, serological testing and cell culture are not useful. Cell culture also requires precise collection and processing techniques and is time consuming. In comparison DFA and PCR require specialist equipment and staff, making it difficult to provide timely results 24 hours a day. Rapid antigen detection testing is the most frequently used test for RSV in clinical settings. This is because it is inexpensive, easy to perform and the results are available quickly in comparison to other tests (53, 54).

Nevertheless, in comparison to laboratory-based tests such as DFA, rapid antigen detection has proven to be less sensitive. In comparison to RT-PCR, RADT has only 50-85% sensitivity. It should be noted that the clinical utility and overall performance of rapid immunoassays depends on many factors. These include method of specimen collection, time of specimen collection in relation to onset of symptoms and patients age. Additional factors that affect rapid performance detection and utility include

subjective visual interpretation of results and a low positive predictive value when testing is performed during periods of low disease prevalence (52, 54).

Other clinical investigations can be used to provide supporting evidence for RSV infection such as arterial oxygen saturation, respiratory rate and chest X-rays (Figure 1.1.3) (55).

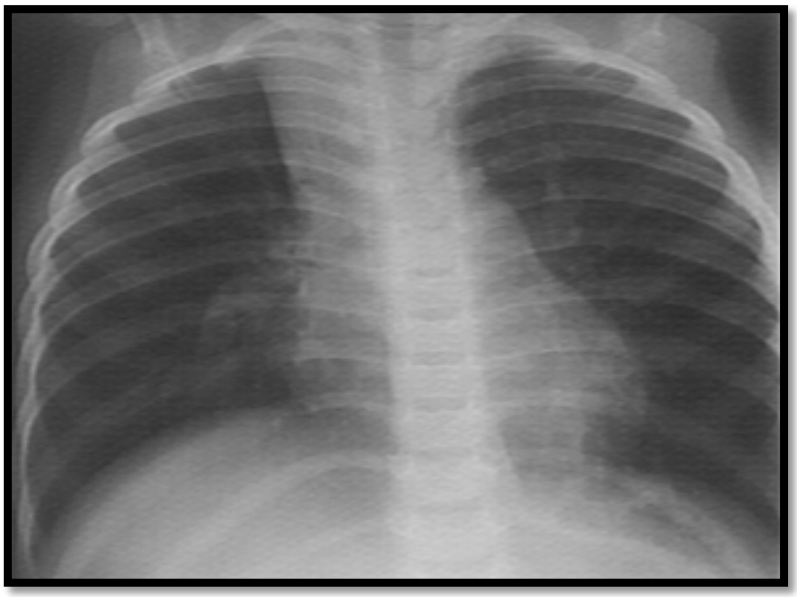

Figure 1.1.3: X- ray showing hyperinflation in RSV patient with bronchiolitis. However, diagnosis tends to be made based on clinical picture supported by RSV detection. This image was kindly provided by Dr P McNamara

1.1.7 Prevention and Prophylaxis

1.1.7.1 Sterilisation and barrier methods

Simple methods such as hand washing can be applied with regards to preventing the spread of RSV infection. This virus in known to be mainly transmitted by hand to hand contact instead of droplet inhalation. Hands should be washed before and after contact with a patient or any contaminated objects (43, 56, 57). The mother must avoid smoking around children and during pregnancy. It has been suggested that breastfeeding can produce benefits with regard to a child's general health with lipids in human milk displaying some antiviral activity (58). The key issue with vaccination is developing a cost-effective vaccine with vaccination viewed as cost-effective only with patients at increased risk of severe RSV infection (59).

1.1.7.2 Palivizumab

Palivizumab (trade name Synagis) is a humanised murine monoclonal antibody directed against RSV. It is the first monoclonal antibody to provide immune prophylaxis of infectious disease in humans (43, 57, 60, 61). However, it is not widely used as it is only given to high risk infants in 5 separate monthly jabs and is expensive (62).

Palivizumab binds to the RSV fusion (F) protein at a highly conserved region between amino acids 258 and 275 known as antigenic site A. Palivizumab prevents RSV from fusing with the respiratory epithelial cell membrane, preventing virus entry and therefore replication (43, 60, 61, 63).

In the UK, palivizumab is used as a preventative measure against RSV infection in children from the following three high-risk groups. (43):

1) Infants born before 35 weeks gestation.
2) Infants with chronic lung disease.
3) Infants born with haemodynamically significant Congenital Heart Disease.

Palivizumab is given as 5 monthly intramuscular injections (15 mg per kg). Some children may receive fewer than 5 injections but no more than 5 should be administered. Despite palivizumab's use as a primary means of prophylaxis, no benefit has been seen in terms of RSV mortality rate. Nevertheless, significant benefits are seen in RSV prophylaxis by the reducing the number of hospitalisations (43, 64).

A recent study has found that palivizumab treatment resulted in a significant reduction in wheezing days in preterm infants during the first year of life (65). Therefore, it could be said that RSV offers some benefit in preventing post RSV respiratory symptoms. Ribavirin is the only drug licensed for therapy of RSV infection but its toxic effects, relatively high cost and nonspecific anti-RSV activity limit its clinical use (66).

1.1.8 Management

The management of hospitalised cases of severe acute bronchiolitis consists of supportive care, such as nasal suction, nasogastric or intravenous fluids, supplemental oxygen, and nasogastric feeding. The management of bronchiolitis in children is provided by UK Signs the National Clinical Guidelines for Bronchiolitis in Children (67).

Nasal suction is used to clear secretions in infants hospitalised with acute bronchiolitis who exhibit respiratory distress due to nasal blockage. For infants with acute bronchiolitis who cannot maintain oral intake or hydration nasogastric feeding should be considered. Infants suffering with cyanosis or severe respiratory distress or have oxygen saturation level ≤ 92% should receive supplemental oxygen by nasal cannula or facemask. Previous research has identified that there is no significant benefit of nebulised epinephrine, inhaled corticosteroids, systemic steroids, leukotriene receptor antagonists and chest physiotherapy for the treatment of acute bronchiolits is infants (67). Alder Hey Children's Hospital has a specific care management pathway for the management of bronchiolitis in children (Figure 1.1.4).

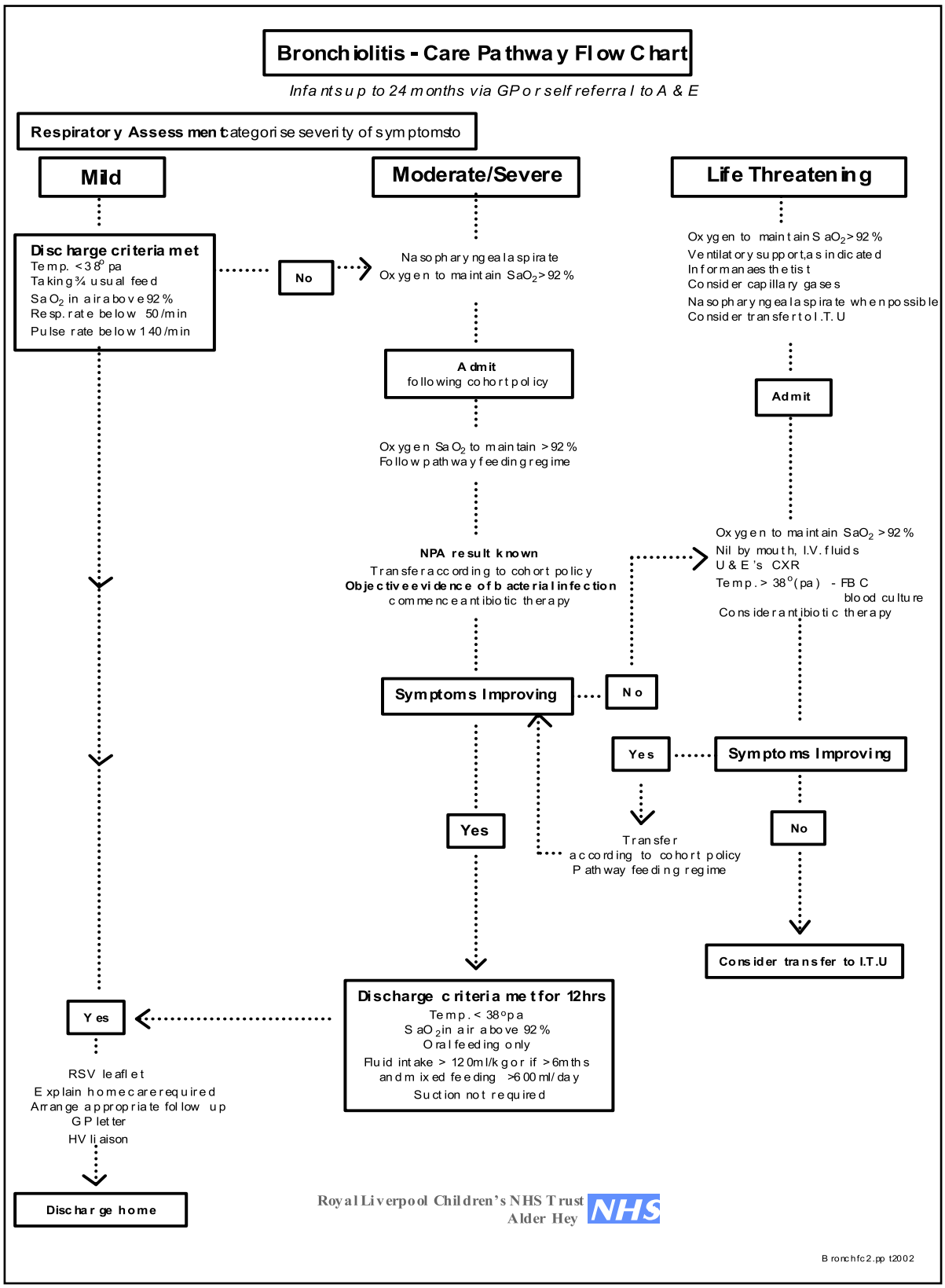

Figure 1.1.4: Care management pathway for children suffering from bronchiolitis at Alder Hey Children's hospital provided by Dr Paul McNamara.

1.1.9 RSV in Adults

All adults get RSV infection on mean every 18 months to 3 years, they will often be asymptomatic. Clinical feature include nasal congestion, cough, wheeze and low-grade fever. It is difficult to diagnose RSV infection in adults because viral cultures and antigen detection are insensitive due to low viral titres in nasal secretions. Treatment of RSV is largely supportive. Ribavarin and gamma immunoglobulin are associated with increased survival in the immunosuppressed. Infection control by good hand hygiene and gloves are effective preventative measures (49, 68).

1.2 Virology

1.2.1 Key Components of RSV Virus

RSV has a RNA genome and is composed of 15,000 nucleotides. RSV contains 10 genes, which encode 11 viral proteins (3, 69). There are 11 proteins because 2 overlapping reading frames in M2 mRNA yield 2 distinct matrix proteins M2-1 and M2-2.The attachment (G) protein is involved in host cell attachment and the fusion (F) protein is involved in fusion and cell entry. The SH protein is not involved in either of these processes. The other 5 structural proteins are nucleocapsid (N), large (L) polymerase protein, phosphoprotein (P), matrix (M) and M2-1 and the 2 non-structural proteins NS1 and NS2 (Figure 1.1.5). It is not know M2-2 functions in mature virus assembled particles (3, 69-71). The details about the functions of these proteins are provided (Figure 1.1.6).

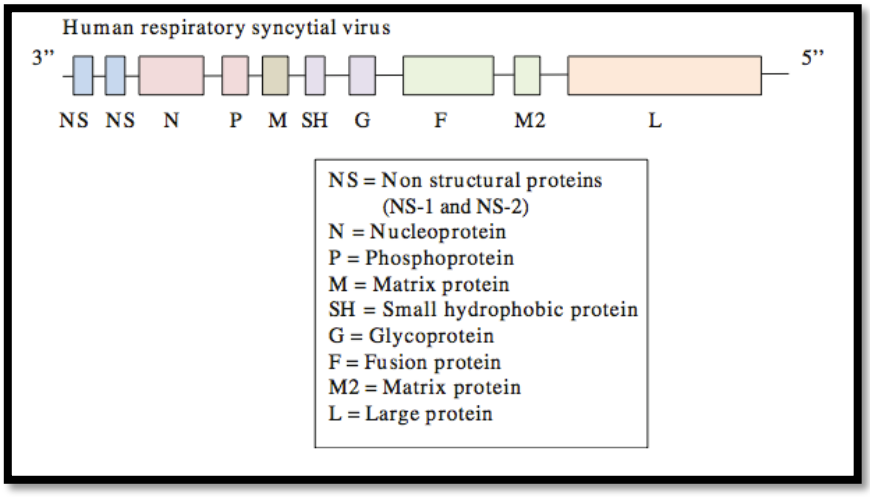

Figure 1.1.5: Basic RSV genetic structure and 11 viral proteins (3).

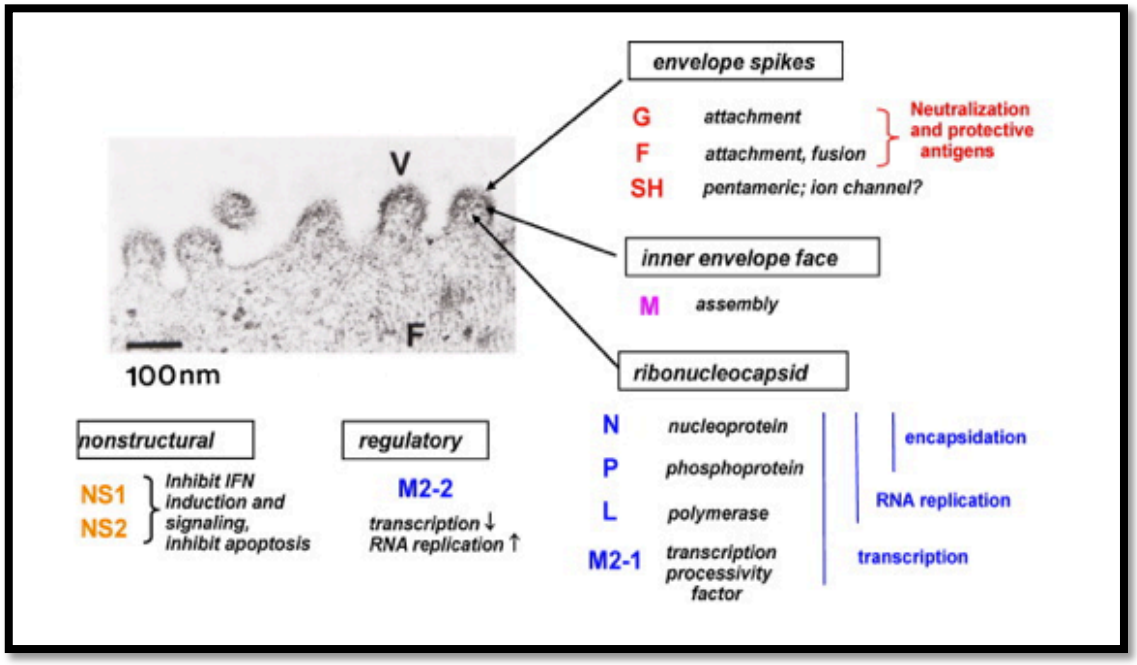

Figure 1.1.6: Negatively stained electron micrograph of budding RSV virions. F indicates filamentous cytoplasmic structures thought to be nucleocapsids and V indicates a budding virion. The locations of viral proteins in the virion, and their known functions are indicated (69).

The following overview of function of viral proteins is taken from the journal article *Progress in understanding and controlling respiratory syncytial virus: still crazy after all these years* (69). RSV transcription and RNA replication follow the Mononegavirales model. The polymerase enters the genome at the 3′ end, which begins with a 44-nucleotide leader region. Genes are transcribed in succession guided by short gene-start and gene-end signals to produce individual messenger RNA (mRNAs). During RNA replication, the polymerase yields a complete positive sense replicative intermediate called the antigenome, which serves as the template for producing progeny genomes (69, 72, 73).

RNA synthesis is carried out by the large L polymerase protein, which performs mRNA capping and polyadenylation (3, 74). The actual template is viral ribonucleoprotein (RNP) or nucleocapsid, a complex of viral genomic or antigenomic RNA tightly bound by N protein. This stops degradation of these RNAs. It has been suggested that encapsidation reduces detection of these RNAs by pattern recognition receptors in the host cell (69, 73).

The P protein is a homotetramer, which is known to interact with N, L, and M2-1 and is an essential co-factor of the polymerase (3, 75). Though much shorter than other Paramyxoviridae counterparts, RSV P has similar activities. The C-terminus of P interacts with the C-terminus of N to open the RNP structure so the polymerase, tethered by P, can reach bases in the viral RNA. The P protein also interacts with newly synthesized N to prevent illegitimate assembly of the latter and to deliver it to the nascent chain during genome replication. Promoter clearance and chain elongation by the viral polymerase during transcription seem to be dependent on the P protein (69, 73, 75).

M2-1 and M2-2 are RNA synthesis factors. M2-1 is a transcription processivity factor. When M2-1 is absent, transcription terminates prematurely and non-specifically within several hundred nucleotides. M2-1 is a homotetramer that binds to the P protein. It is suggested that P associates with soluble M2-1 and delivers it to the RNA template. The other factor involved in RNA synthesis, M2-2 protein, is a small, non-abundant species that accumulates during infection and appears to shift RNA synthesis from transcription to RNA replication (69). M protein lines the inner surface of the viral envelope. M has a central role in budding and may silence viral RNA synthesis in preparation for packaging (69, 76).

The NS1 and NS2 proteins both interfere with the induction of interferon beta (IFN-β) (77, 78). The NS1 protein has the greater effect on inhibiting IFN induction. These proteins impede the signal transduction pathway leading to up-regulation of IFN-β at multiple steps: NS2 binds to the cytoplasmic receptor RIG-I; either protein mediates a decrease in TNF receptor-associated factor 3 (TRAF3); and NS1 mediates a decrease in IKKε. The NS proteins strongly suppress IFN-induced signal transduction from its receptor through the Janus Tyrosine Kinase (JAK)/STAT pathway. This suppression is mediated by proteosomal degradation of the signal transducer and activation of transcription (STAT) 2 by NS2. However there also is evidence that NS1 can assemble ubiquitin ligase enzymes to target STAT2 (69, 78-80).

1.2.2 Key Proteins in RSV Infection

There are three main surface lipid envelope glycoproteins encoded by RSV that are components of the virion: fusion protein F, attachment protein G and small hydrophobic protein SH (69, 81, 82).

1.2.2.1 Fusion Protein (F)

The F protein is made up of 574 amino acids its inactive form. The fusion of both viral and cell membranes is promoted by the F protein, resulting in the transfer of viral genetic material (48, 83). The importance of this protein has been highlighted by the ability of the virus to attach to a cell with the F protein present but the G and SH proteins absent. When a RSV virus particle attaches to the target cell, the F protein becomes activated by an unknown mechanism. This activation causes the F protein to undergo conformational changes, allowing the fusion peptide of the F protein to be inserted into the plasma membrane of the target cell. As a result, infected cells express RSV F protein on the their plasma membrane and this mediates cell to cell fusion resulting in multinucleate syncytia formation which is the characteristic feature of RSV infection (48, 69, 81, 84, 85).

1.2.2.2 Attachment Protein G

G proteins consist of about 299 amino acids and are an essential component for viral attachment to the cell. It is naturally expressed as membrane bound and anchored forms. This protein is responsible for the differences between the two major RSV strains A and B. This is due to the protein's antigenic variability, with the G protein of the A and B strains differing by 47%. The G proteins of the same strain differ by 20% (48, 69, 83, 86).

RSV has developed multiple mechanisms to evade host immune response. The G protein, which is a RSV antigen that induces neutralising antibodies, is heavily glycosylated and this interferes with antibody recognition. The G protein can be secreted in truncated form, which acts as a decoy for neutralising antibodies (Figure 1.1.7) (3).

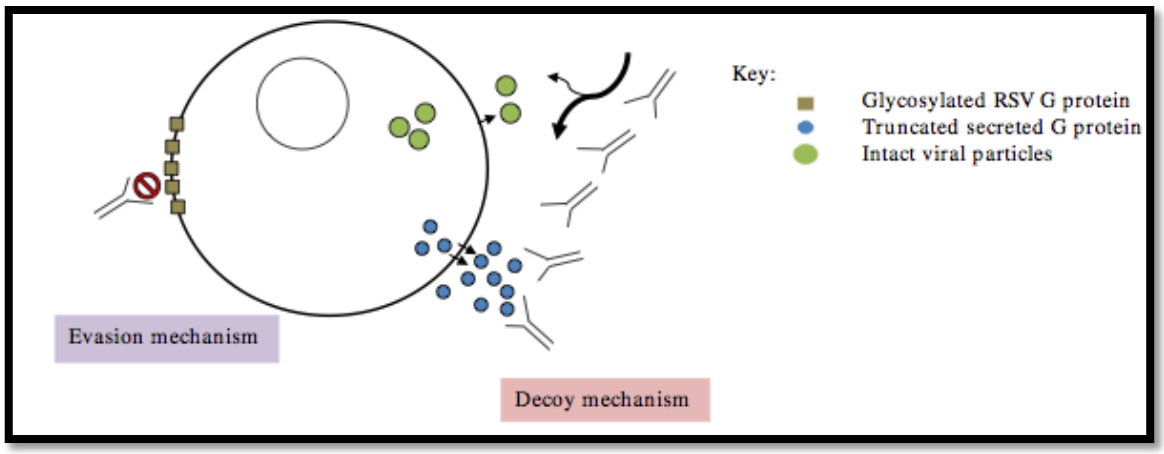

Figure 1.1.7: Viral G protein evasion strategies (3).

1.2.2.3 Small Hydrophobic Transmembrane Protein SH

The small hydrophobic (SH) transmembrane protein is 64 amino acids, type 2 integral membrane protein. The role of the protein is unclear but it is known that this protein does facilitate fusion. In infected cells most SH protein accumulates at the membrane of Golgi complex but is also found in the plasma membrane and the endoplasmic reticulum(48, 87). The SH protein has the ability to permeabilise membranes. Recent studies have shown that the SH protein functions as a viroporin which as act as a proton or ion channel, enhancing the membrane permeability of the host cell (48, 69, 87-90).

1.3 Immune Response

Previous work on RSV has suggested that immunological mechanisms could be the key to the severity of RSV bronchiolitis in infancy (48). This is because the disease is most prevalent when the infant is least immunologically mature despite the possession of maternally derived specific RSV antibody. The immunological response to RSV infection in humans can be divided into innate and adaptive (48, 91).

1.3.1 Innate Immunity

The innate immune system is the body's first line and earliest phase of defence (92). It consists of a cellular response and an activation of mechanisms that defend the host from a wide range of organisms in a generalised rather than pathogen specific manner. Pulmonary surfactant, which is made up of a layer of phospholipids together with several surfactant proteins is one example of this first line of innate defence in the airway. Surfactant protein A has been shown *in vitro* to neutralise RSV by binding to F protein but not G protein (32, 48).

Pattern recognition receptors (PRRs) are involved in the recognition of microbial products by host cells and initiate an innate immune response. There are 3 types of PRRs associated with RSV, which are toll-like receptors (TLRs), retinoic acid inducible gene (Rig-1)-like receptors and nucleotide-binding oligomerisation domain (NOD)-like receptor (NLRs). Rig-1 like receptors are critical sensors of viral infection initiating an interferon beta production in response to RSV. NOD-like receptor are also involved in an antiviral response through interferon production (93).

The TLRs have a central role in innate immunity, initiating an innate immune response through the production of interferon beta, proinflammatory cytokines and cause neutrophil migration. TLR2, TLR3, TLR4, and TLR7 are linked to RSV infection. TLR2 acting as a functional receptor of RSV and TLR4 specifically detects the RSV F protein. TLR7 detects singles stranded RNA (ssRNA) and therefore would be involved in the detection of RSV which is a negative stranded ssRNA. TLR3 is responsible for recognizing viral double stranded RNA (dsRNA), which in this case will be the dsRNA, generated during the RSV replication cycle (93, 94).

Interleukin-8 (IL-8) and interleukin-6 (IL-6) are proinflammatory cytokines produced by respiratory epithelial cells in response to RSV infection (48, 95). Raised levels of IL-8 are seen in serum and bronchoalveolar lavage samples from infants ventilated with RSV bronchiolitis (96). Serum levels of IL-6 are increased during RSV infection. IL-6 and IL-8 have important roles in initiating neutrophil and macrophage chemotaxis (48, 97, 98).

1.3.2 Interferon in Innate Immunity

1.3.2.1 Interferon role in antiviral defence mechanism

Type 1 interferon (IFN), a soluble cytokine and represents one of the first major barriers to infection in terms of innate immunity, exhibiting potent antiviral effect. Interferon has a significant role in antiviral defence by inhibiting replication (79, 80, 99). Type 1 IFNs initiate a bimodal response, which firstly involves the secretion of IFNs in response to detection of an invading virus. Secondly IFNs act in a paracrine and autocrine manner to induce 300 IFN-stimulated genes (ISGs), which ultimately leads to the production substances, that disruption of viral replication (Figure 1.1.8). As a result, of the protective effects of IFNs, viruses have adapted to form strategies for overcoming anti-viral responses (100).

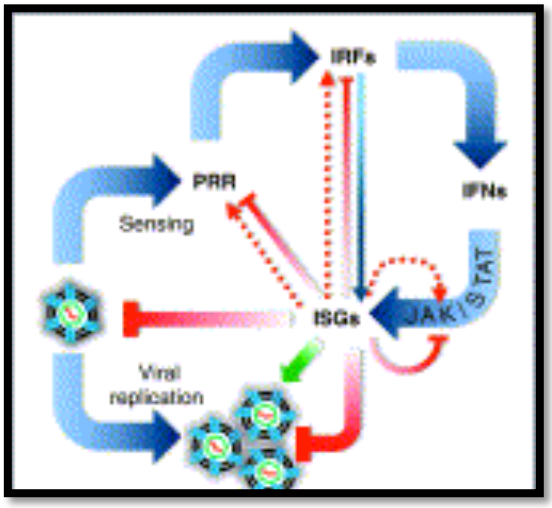

Figure 1.1.8: The role of interferon stimulating genes. Viruses are detected by PRRs, which leads to activation of interferon regulatory factors (IRFs) and the transcriptional induction of IFNs. The IFNs signal through the JAK/STAT pathway inducing ISG production. ISGs can also be induced by some IRFs acting through an IFN independent pathway (thin blue line).

Some ISGs block viral replication whilst other can actually promote it in some viruses. Subsets of ISGs are a component of the interferon pathway and promote its signalling (red dotted arrows). ISG induces several negative regulatory factors to target PRR, JAK/STAT and IRFs to dampen down the response (thin red lines) (100, 101).

1.3.2.2 Viral recognition and Interferon response pathways

Pathogen associated molecular patterns (PAMPs) present on the virus particles are recognised by a cell's pattern recognition receptors (PRR) in a biphasic type 1 interferon response (80, 102). The PRRs involved include Toll-like receptors (TLRs), which detect viral components such as nucleic acids and glycoproteins. TLRs act through toll interleukin-1 receptor (TIR) domains to recruit TIR-containing adaptors such as TIR-domain-containing adapter-inducing interferon beta (TRIF), Mal and TRIF-related adaptor molecule (TRAM). This leads to the activation of NF-ϰB (nuclear factor kappa-light-chain-enhancer of activated B cells) and interferon regulatory factor 3 (IRF3), which ultimately leads to interferon production (80).

The second class of PRRs is retinoic acid inducible gene – 1 (RIG-1)-like receptor (RLR) family, including RIG-1 and melanoma differentiation-associated gene 5 (MDA5). The function of RLRs is to detect cytoplasmic double stranded RNA (dsRNA). They interact with adaptor mitochondrial antiviral signaling proteins (MAVS) and activate nuclear factor kappa-light-chain-enhancer of activated B cells (NF-*k*B) and IRF3. In RSV the N protein is responsible for inhibiting MDA5 and MAVS (80, 103).

1.3.2.3 IFN Expression due to Transcription Factor Activation

If a virus is sensed by a PRR, then the transcriptional factor activation occurs leading to interferon production (Figure 1.1.9) (80).

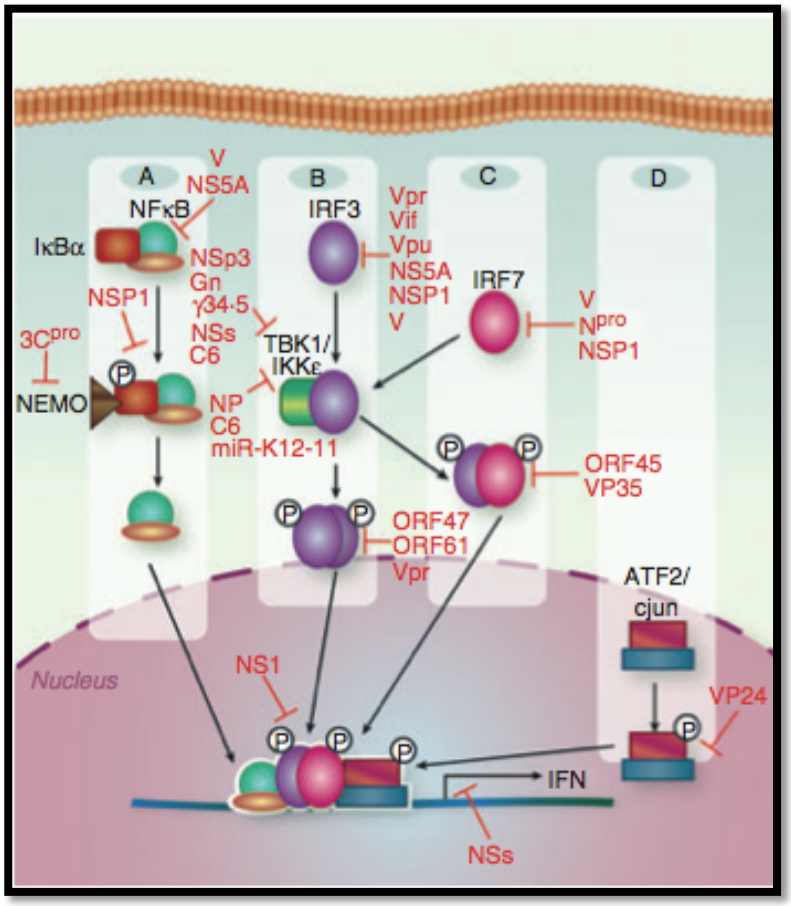

Figure 1.1.9: Transcription activation leading to IFN production. Detection of viral components by PRR leads to activation of transcriptional factors. (a) NF-ϰB is held in an inactive cytoplasmic complex due to the inhibitor IϰB alpha**.** IϰB alpha is degraded upon viral recognition resulting in its degradation. This frees the NF-ϰB to translocate to the nucleus where it binds to IFN-promoter. (b) When the virus is detected, kinases phosphorylate IRF3 leading to its dimerisation and translocation. (c) Low level of IFN production induces IRF7 expression leading to its phosphorylation by kinases, heterodimerization with IRF3, nuclear translocation and increased IFN expression. (d) When the virus is detected, stress activated members of the mitogen-activated protein (MAP) kinase family phosphorylated nuclear ATF2/cjun leading to activation of this complex. The combined binding of NF-KB, IRF3 and IRF7 leads to full expression of type 1 IFN genes (80).

1.3.2.4 Interferon Signaling

The second phase of biphasic interferon response is where interferon binds to its interferon alpha/beta receptor (IFNAR) and activates ISG induction (Figure 1.2.1) (80).

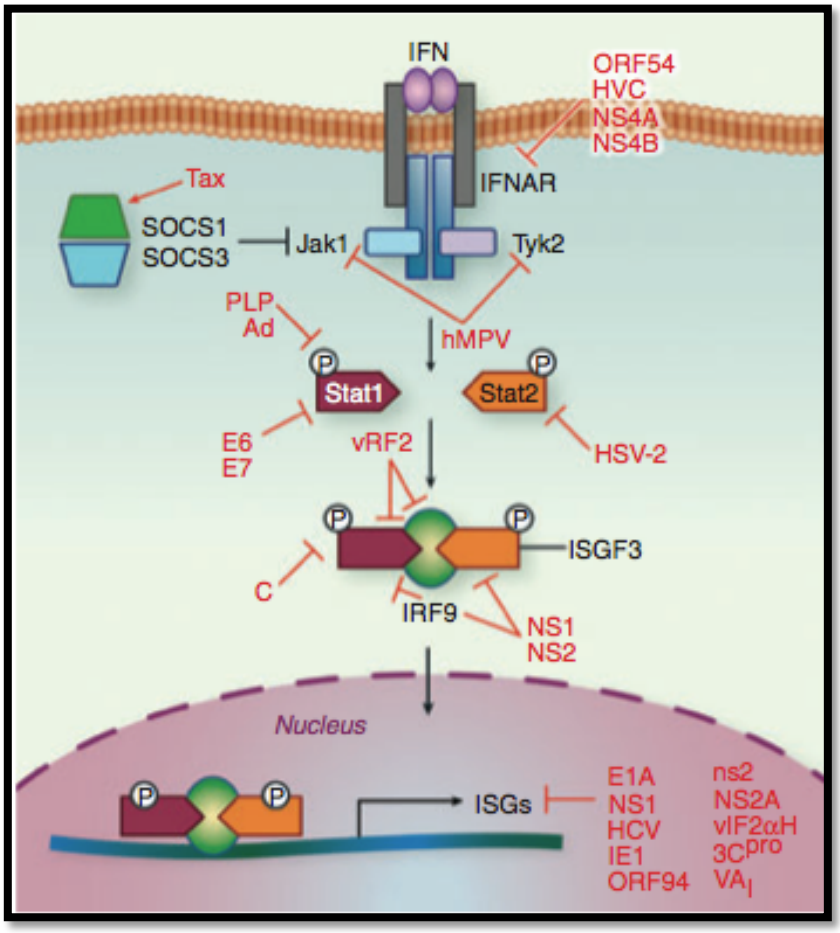

Figure 1.2.1: Interferon signalling resulting in ISG expression. When interferon is secreted, it binds to the cell surface receptor interferon-α/β receptor (IFNAR). Kinases are activated, resulting in the phosphorylation of signal transducer and activation transcription (STAT) 1 and STAT2. This results in the formation of a heterotrimeric complex containing interferon regulatory factor 9 (IRF9) which is also referred to as IFN stimulated gene factor 3 (ISGF3). The binding of ISGF3 to promoters of ISGs leads to their transcriptional activation. The collective actions of hundreds of ISGs induced by IFN inhibit the spread and replication of virus (80).

1.3.3 Adaptive Immunity

Adaptive immunity can be divided into humoral and cell-mediated responses. (48).

1.3.3.1 Humoral Immunity

Humoral response to RSV infection occurs resulting in the production of antibodies. The production of serum neutralising antibodies is higher in older children and adults in comparison to children. Antibodies are produced in response to F and G proteins, which acts as RSV antigens. The antibodies produced are IgE, IgM, IgA and IgG (48). IgM is produced 5 days post infection and stays elevated for around several weeks after infection. IgG is produced 10 days after infection and remains elevated for several months. IgA in adults is elevated 3 days post infection. There has been evidence that IgE levels are affected in bronchiolitis (3, 104).

1.3.3.2 Cell-mediated Immunity

The relationship between T cells and RSV infection with respect to immune response, immunomodulation and immunopathology is complex. A basic overview has been provided (Figure 1.2.2) (14). There are four main types of helper T cells are Th1, Th2, Th17 and T regulatory (regs). These types of T cell all function in response to RSV infection (Figure 1.2.3). IFN-γ, IL2, TNF-α and IL-4, IL-5, IL-10, IL-13 are released as part of TH1 and TH2 response to an incoming pathogen (14).

Human observational studies implicate T cells in viral clearance. In children with severe infection, accumulation of CD8+ antigen-specific T cells in the peripheral blood and airways, peaking at around nine days after symptom onset is seen. A prospective study examining RSV infected children under the age of five where individuals were immunocompromised due to chemotherapy or had primary immunodeficiencies affecting T cell function were found to shed virus at higher levels for several months, compared to the 7–21 days in normal children and suffered more severe disease. This study provides evidence suggesting that T cells are involved in viral clearance (3, 14, 104).

Dendritic cells (DC) are major antigen presenting cells which and act as an interface between the innate and adaptive arms of the immune system (105).

RSV infected human DCs have been found to impair CD4+ T cell proliferation and have been shown to inhibit the production of cytokines, including IFN gamma. The mechanism for this phenomenon is currently unclear. RSV infection of DCs renders them unable to activate T cells as a result of failure to assemble the immunological synapse required for antigen recognition (14, 105)

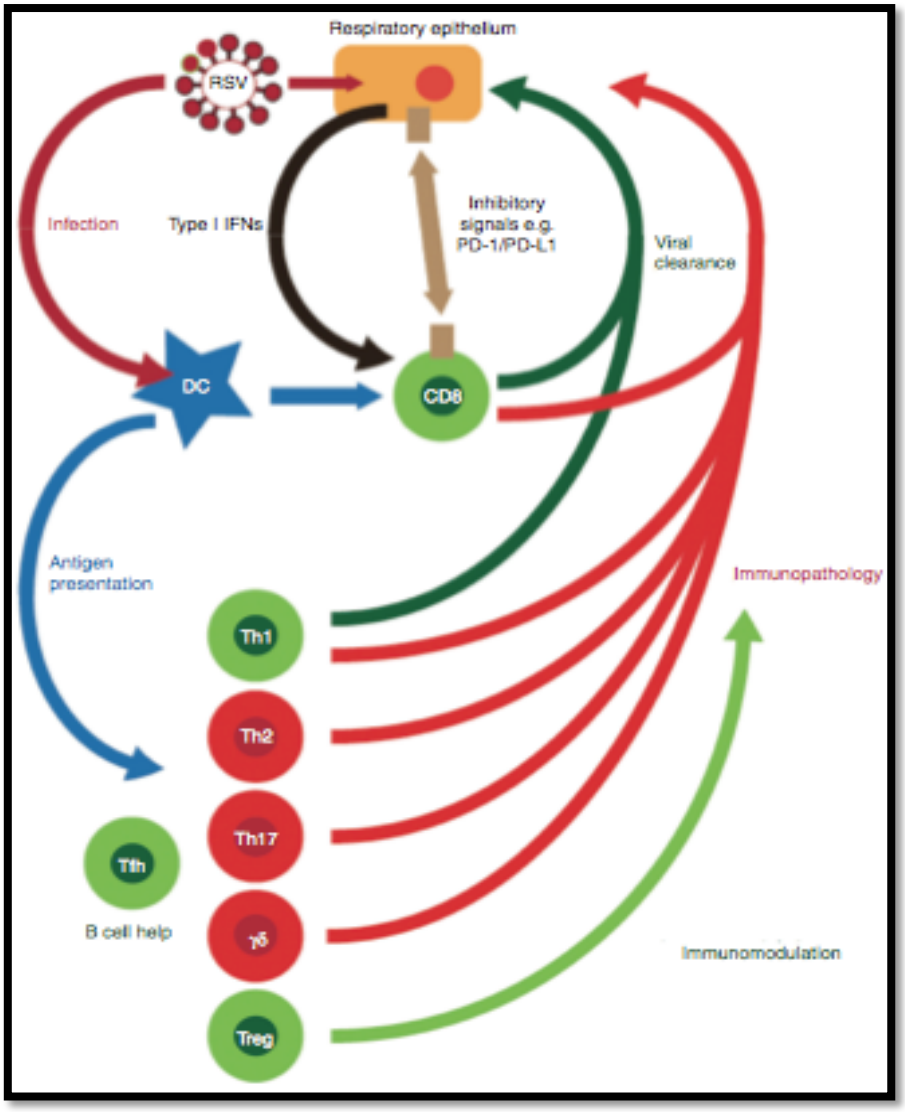

Figure 1.2.2: Role of T cells in RSV clearance, protective immunity and immunopathology. RSV infects respiratory epithelial cells, inhibiting type I interferons. Direct infection of dendritic cells also causes interferes with antigen presentation, leading to impaired T cell function, reduced viral clearance and memory formation. T cell subsets that enhance immunopathology but which may be limited by regulatory T cells (Treg) (14).

Several T cell subsets have been implicated in the immunopathology seen during RSV infection. These include nonclassical T cells, such as γδ T cells. Increases in γδ T cells are associated with increased disease severity. These cells make Th1-like cytokines early post infection, but more IL-4, IL-5 and IL-10 at later time-points (14).

It has been shown that Th17 cells may play a role in regulating inflammation in the RSV-infected lung. This CD4+ T cell subset is characterised by production of IL-17, a cytokine that induces chemokine production by respiratory epithelial cells and resultant leukocyte infiltration. In vitro, bronchial epithelial cells infected with RSV cause the differentiation of peripheral blood lymphocytes to Th2 and Th17 phenotypes. Members of the IL-17 family are induced following RSV infection and cause neutrophil recruitment to the airway, mucus production, and impairment of viral clearance as seen in mouse models. Th17 cytokines have also been found to be critical for RSV associated airway hyperresponsivness (14, 106).

The control of T cell-associated autoimmunity and immunopathology is mediated by the regulatory T cell (Treg) subsets, in RSV disease. Tregs are essential modulators of the adaptive immune response, making up 5–10% of CD4+ T cells in the mouse and regularly characterised by the expression of the transcription factor FoxP3. Absence of CD4+ FoxP3+ Treg cells in both mice and humans leads to autoimmunity, and defective or suboptimal Treg function during RSV infection may cause immunopathology. In RSV-infected mice, Tregs proliferate and accumulate in the lungs, upregulating activation markers and CTLA-4 in RSV infected mice.. Tregs lead to anti-inflammatory cytokines such as IL-10 being produced in abundance by this subset, which also limits pulmonary inflammation. Studies have concluded that Tregs are essential for the control of mucosal inflammation during RSV infection. Thus, Tregs appear to limit immunopathology in RSV disease and may provide new opportunities for interventions to limit inflammatory disease (14).

1.4 Purpose of Study

1.4.1 RNF168 Investigation

1.4.1.1 Ubiquitination

Ubiquitination regulates a host critical cellular function often through mediating the selective degradation of master regulatory proteins by proteasomes by labelling these proteins with ubiquitin (Ub) (107). Some of the processes regulated by the ubiquitin/ proteasome dependent proteolysis include cell cycle progression, induction of inflammatory response and antigen presentation. Apart from the degradation of proteins, ubiquitin tagged proteins are involved in ribosomal function, post replication DNA repair and the function of certain transcription factors.

Ubiquitin (Ub) is a 76 amino acid polypeptide chain. A cascade of enzymes is required for the ubiquitination reaction. Ubiquitination usually results from a formation of a bond between the C terminus of ubiquitin and e-amino group of substrate lysine residue. The reaction requires sequential actions of three enzymes.

The activating enzymes (E1), which contain an active-site cysteine attaches to the ubiquitin carboxy-terminal glycine through a reactive thioester bond (108). The conjugating enzyme (E2) transiently carries the activated ubiquitin molecule as thiol ester. The ligase enzyme (E3) transfers the activated ubiquitin from E2 to the substrate (or ubiquitin) and catalyses the attachment of Ub to a lysine in the target protein. This mechanism involving the three enzymes are responsible for all known ubiquitination reactions and are independent of every various process that each substrate bound ubiquitin will mediate (Figure 1.2.2) (108-112).

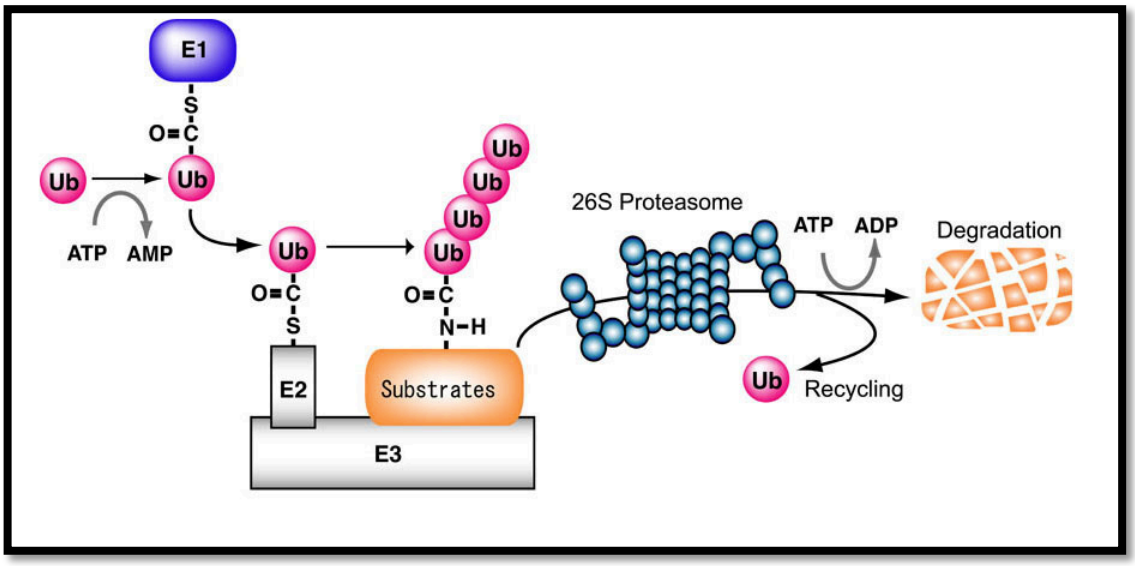

Figure 1.2.3: Biochemical reactions of ubiquitination. This image was taken from Hokkaido University Graduate School of Medicine website (113).

Monoubiquitination (monoUb) is where a single Ub molecule attaches to a substrate. Ub contains seven lysine residues that can themselves be a substrate of ubiquitination, giving rise to polyubiquitinated (polyUb) chains that according to the type and position of inter chain linkages are recognised differently by the cell. For example, polyubiquitin chains built via lysine 48 (K48) have been extensively characterised (107, 108, 114).

The E3 ligases are an enzymatic family consisting of 600 proteins. They are the final enzymes of the in the ubiquitination conjugating cascade and have substrate specificity. Two known large groups of E3 are Homologous to the E6-AP Carboxyl Terminus (HECT) domain and Really Interesting New Gene (RING) finger domain (107, 115). RING E3 ligases are specified in over 600 human genes and play a critical role in controlling many critical cellular processes and have been implicated in multiple human diseases (116).

1.4.1.2 RING Finger E3 Ligase

The basic sequence of the canonical Really Interesting New Gene (RING) is Cys-X2 -Cys-X(9-39) -Cys-X(1-3) -His- X(2-3) -Cys-X2 -Cys-X(4-48) -Cys-X2 –Cys as seen in (Figure 1.2.3). RING domains function as enzyme E3 ligase in the process of ubiquitination, binding to ubiquitin-conjugating enzymes and promoting direct transfer of ubiquitin to the substrate (115-117).

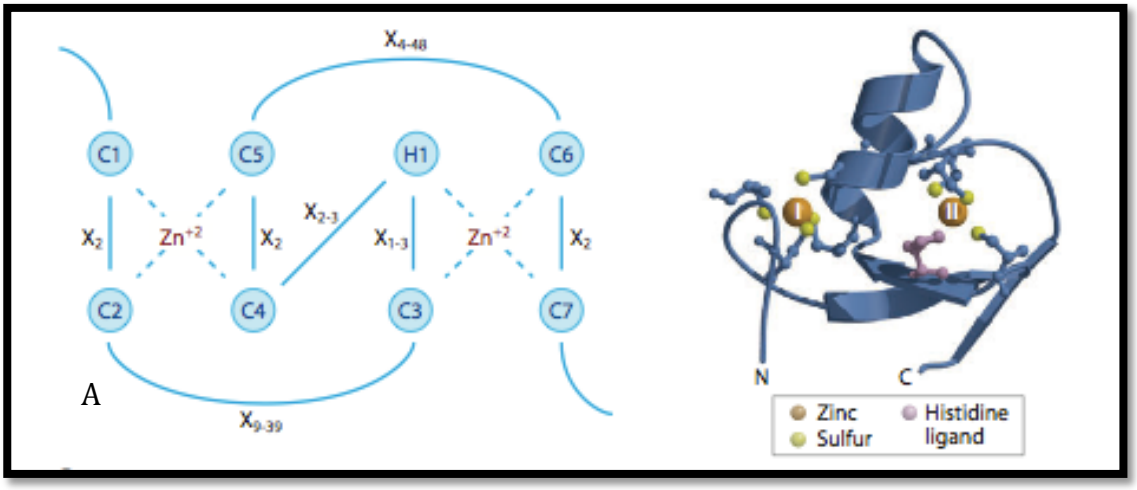

Figure 1.2.4: Primary sequence and 3-dimensional structure of the RING finger domain. (a) Basic sequence for canonical RING (b) Three dimensional structure of the RING finger where it is shown that cysteine and histidine residues are buried within the domains core where the overall structure is maintained by binding to zinc atoms (116, 117)

RING E3 ligases bind both substrate and E2–ubiquitin (E2–Ub) thioester. In terms of the E2-E3 association RING ubiquitin ligases should be considered to be bisubstrate enzymes that have two substrates and two products. The substrates can be are the lysine residue on the target protein (substrate) and the E2 thioesterified with ubiquitin (E2~Ub). The two products are the target protein linked to ubiquitin and the discharged E2 (1.2.4) (116, 117).

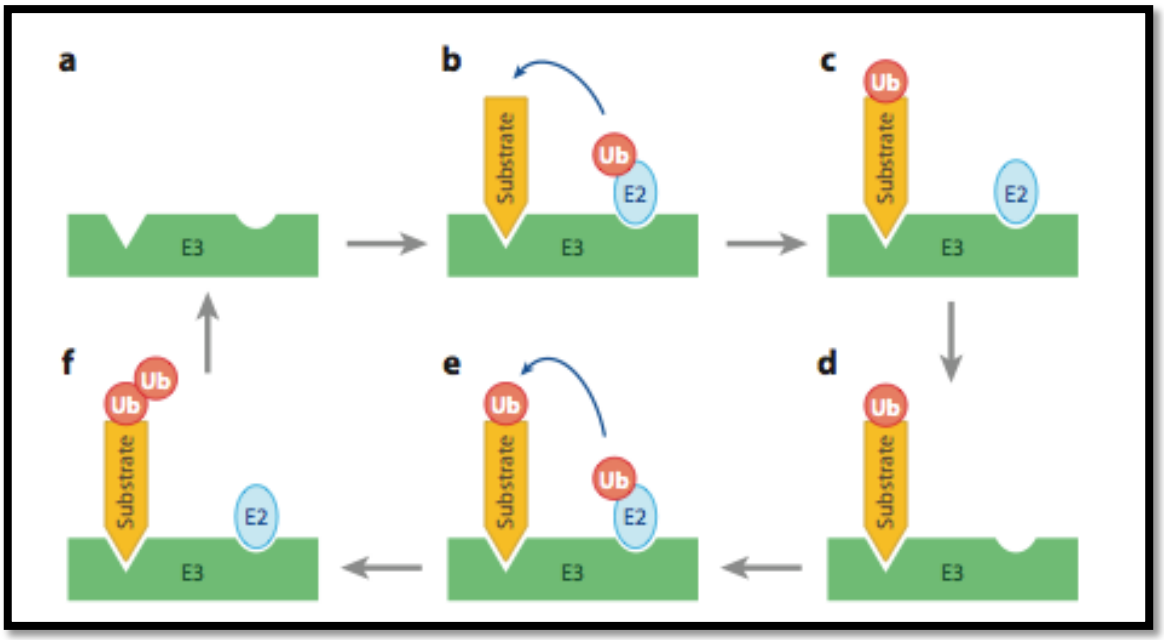

Figure 1.2.5: The reaction cycle of RING E3, association between E2 and E3. (a) Unliganded E3. (b) The E3 bind to the substrate and E2~Ub. The order in which they bind is not predetermined. (c) Ubiquitin is transferred from E2~Ub to the substrate, which becomes monoubiquitinated. (d) To initiate further ubiquitination, the E2 must dissociate to allow a fresh molecule of E2~Ub to bind. (e) The newly recruited E2~Ub attaches to E3. (f) The E2 transfers its Ub to the substrate, which becomes diubiquitinated (116).

After the ubiquitin molecule has been transferred to the target protein, a sequential reaction can take place where more ubiquitin molecules can be transferred to the same substrate resulting in the formation of a polyubiquitinated chain (Figure 1.2.5) (116, 118). Therefore, the RING E2-E3 complexes can monobiquitinate a substrate lysine or synthesise polyubiquitin assembled through different lysine residues of ubiquitin. These modifications have a wide range of effects including protein function, structure, and assembly as well as proteasome-dependent proteolysis (116, 119).

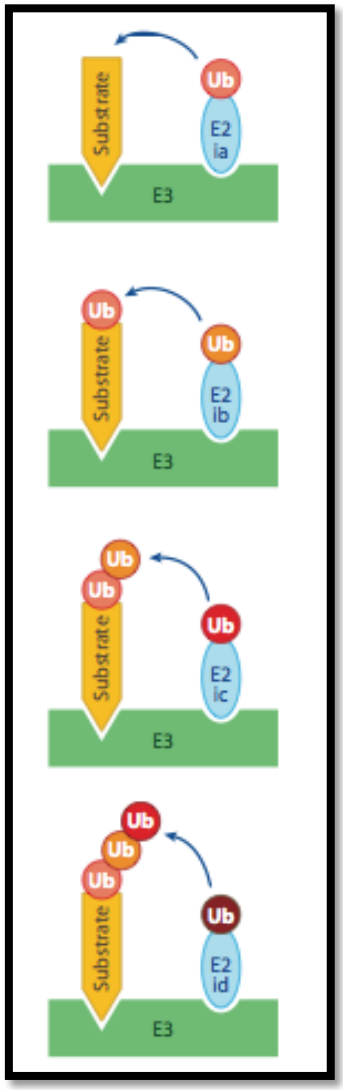

Figure 1.2.6: Polyubiquitination of the substrate. Addition of Ub to the substrate by different E2s (ia, ib, ic, id) resulting in a polyubiquitin chain (116)**.**

After the E2 has transferred the ubiquitin molecule to E3, it must be recharged with ubiquitin from E1 (Figure 1.2.6) (116).

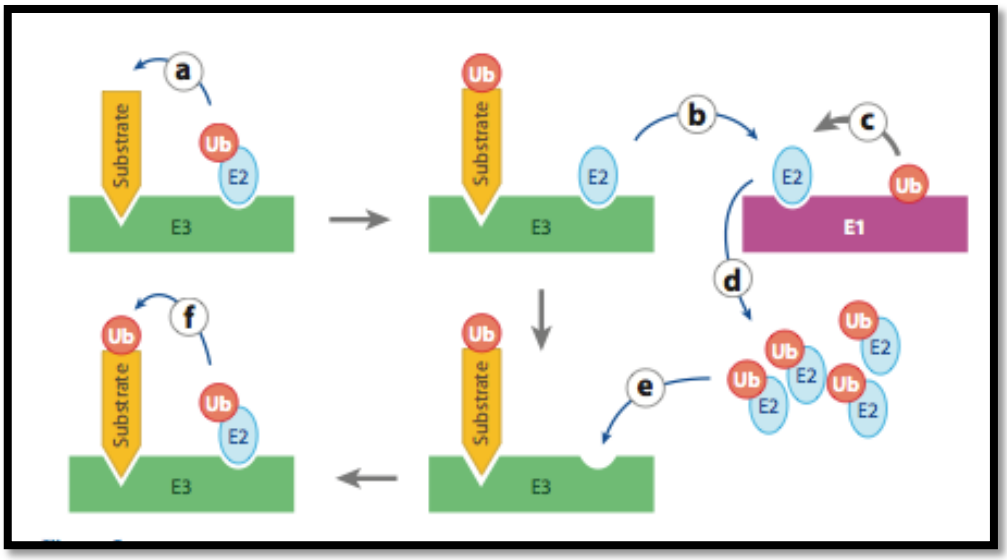

Figure 1.2.7: The process by which E2 is used and recycled. (a) The E2 transfers Ub to the substrate. (b) E2 has to dissociate from RING E3. (c) E2 binds to E1 to gain another ubiquitin molecule. (d) The E2 returns to the cellular pool of E2~Ub. (e) The spent E2 makes way for a fresh molecule from this cellular pool. (f) The second cycle of ubiquitin transfer begins (116).

RING fingers are unique in terms of their action in comparison to other big groups of E3 ligase such as Homologous to the E6-AP Carboxyl Terminus (HECT). RING E3 ligases effect the direct transfer of ubiquitin from E2~Ub to substrate (Figure 1.2.8) (116).

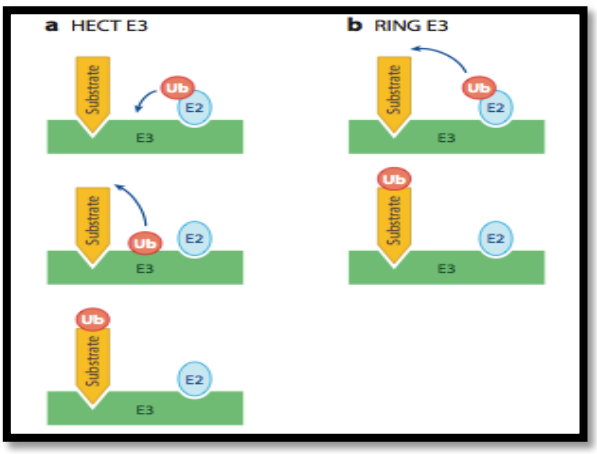

Figure 1.2.8: Comparison between HECT (a) and RING (b) E3s (a) HECT E3s have a conserved cysteine residue, which accepts ubiquitin from E2~Ub forming an E3~Ub thioester. Ubiquitin is transferred from this covalent E3 intermediate to substrate. (b) In comparison, RING E3s affect the direct transfer of ubiquitin from E2~Ub to substrate (116)

The protein RNF168 belongs to the RING finger family of E3 ubiquitin ligase (120). There is evidence to suggest that RNF168 plays a role in the intrinsic antiviral defence of cells from herpes simplex type1 viral infection (HSV-1). It is important to understand the structure and function of RING E3 ligases and specifically RNF168 as this could provide useful information about how RNF168 could play similar role against RSV infection (116, 121-123).

1.4.1.3 RNF168 Background

RNF168 is a 571 long amino acid long protein containing a RING finger motif, two Motifs Interacting with Ub (MIU) domains and three putative nuclear localisation signals (109). The two MIU domains are responsible for binding to ubiquitinated proteins. This is shown in recent studies where inactivation of two MIU domains resulted in a reduced binding of RNF168 to ubiquitinated proteins. The basic structure of the RNF168 depicting the two MIU domains is shown below (Figure 1.2.9) (109, 124-126).

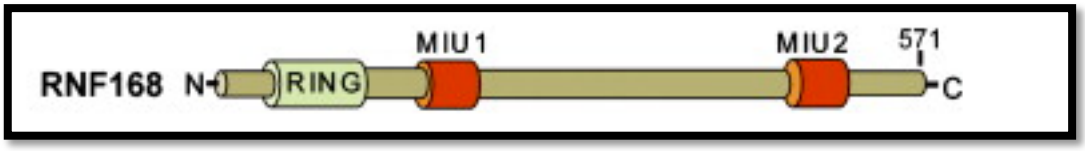

Figure 1.2.9: RNF168 structure showing the two MIU domains (126).

The RING finger protein RNF168 is a relatively new ubiquitin E3 ligase that has a role as a chromatin modifier through ubiquitination of histones H2A and H2AX. This process of post-translational histone modifications is important in increasing chromatin accessibility to a number of regulatory factors. Histone ubiquitination is relevant in nuclear process which govern gene silencing through activating or inhibiting transcription and maintaining genome stability, acting as a scaffold to organise DNA damage response (DDR) (109, 127, 128).

DNA repair and signalling must occur to maintain cell viability and homeostasis. The most harmful type of DNA lesion is DNA double strand breaks (DSBs). A fault in DSB

repair can be associated with accelerated ageing, infertility, exhaustion of stem cell pools and impaired development of nervous and immune systems (126, 129, 130).

RIDDLE (radiosensitivity, immunodeficiency, dysmorphic features, and learning difficulties) syndrome is a human immunodeficiency disorder associated with defective DSB repair. RNF168 E3 ligase initiates a DNA damage response (DDR) to DSBs by ubiquitination of histones H2A and H2AX. The targeting of histones is specifically monoubiquitination of K13-15 lysines (131, 132). RNF8 is the first E3 ligase recruited to the DSB damage site and initiates H2A or H2AX ubiquitination with K63-linked ubiquitin chains. RNF168 is also involved in catalysing RNF8–dependent histone ubiquitination. RNF168-dependent chromatin modifications coordinate the recruitment of 53BP1 and BRCA1 proteins, which are involved in DNA repair to DNA lesions. The mutated gene causing RIDDLE syndrome is RNF168. The inability of RNF168 to function normally, results in failure of 53BP1 and BRCA1 DNA repair factors to localise at the DNA damage site due to loss of histone ubiquitination (131, 133).

RIDDLE syndrome presents with clinical features of increased radiosensitivity, mild motor control, immunodeficiency, learning difficulties and dysmorphic features. A illustration of 2 predicted products of mutated RNF168 alleles is shown (Figure 1.3.1) (124, 133).

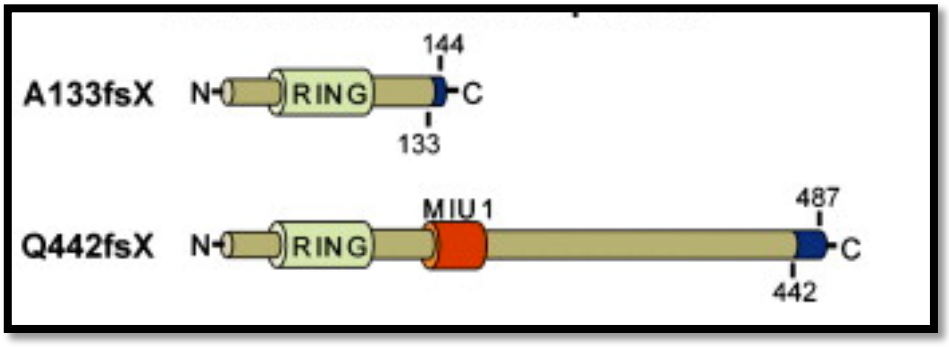

Figure 1.3.1: A depiction of the two predicted products of the mutated RNF168 alleles derived from a RIDDLE syndrome patient A133fsx and Q44fsX (126).

RNF168 has been found to play a role in the intrinsic antiviral defense against herpes simplex virus type 1 (HSV-1) through histone ubiquitination (121).

1.4.1.4 RNF168 and Herpes Simplex Virus Type 1

Research has shown that when HeLa cells are infected with Herpes Simplex Type 1 (HSV-1), a RING finger E3 ligase ICP0 modulates a cellular response to DNA damage. ICP0 is one of the first viral proteins that are expressed during HSV-1 infection. The deletion of ICP0 significantly impairs viral replication. The targets for ICP0 degradation are RNF8 and RNF168 cellular DNA damage ubiquitin ligases, which were responsible for ubiquitinating histones resulting in the anchoring repair factors at sites of damage (121, 122, 134). Chaurushiya et al suggest that ICP0 mimics a cellular phosphosite leading to degradation of RNF8(135). Through targeting these ligases, ICP0 expression results in the loss of ubiquitinated forms of histones H2A and H2AX. This stops the recruitment mediator proteins Mdc1 and 53BP1, preventing the accumulation of repair factors at cellular damage sites. This pathway was identified as a key way in which HSV-1 overcame a host cell intrinsic antiviral defence. The basic outline of the pathway in which RNF168 contributes to intrinsic antiviral defence is shown below (Figure 1.3.2) (121, 122, 134).

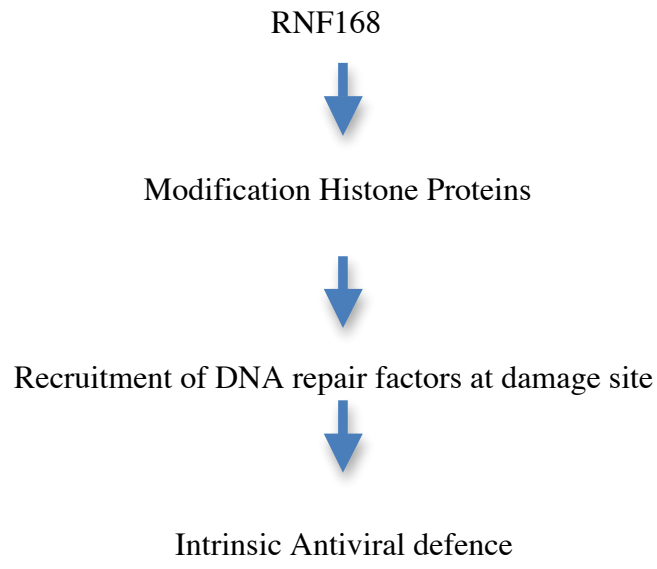

Figure 1.3.2: Basic pathway of how RNF168 contributes to antiviral defence based on research of HeLa cells infected with HSV-1.

A study found that when the HSV-1 wild type (WT) infected HeLa cells at a multiplicity of infection (MOI) 5:1 there was decrease in RNF168 expression 2 hours post-infection. To provide evidence to support the theory that HSV-1 infection led to the degradation of histones by ubiquitination, the same infected samples were probed for ubiquitinated H2A. This showed a decrease uH2A expression at 2 hours post infection**.** These finding were shown as a western blot (Figure 1.3.3) (121).

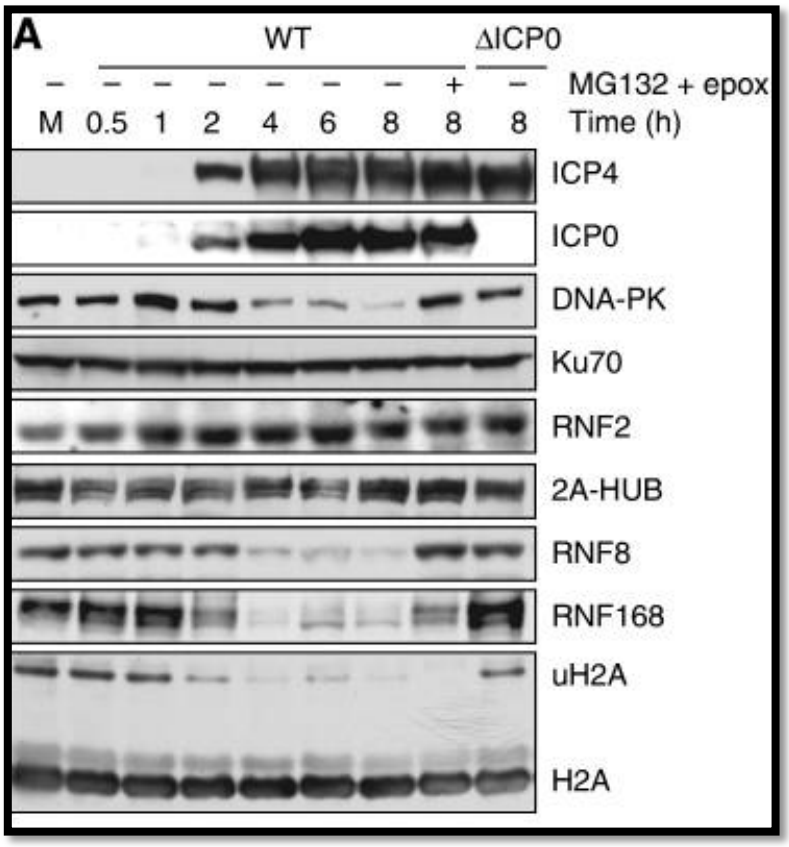

Figure 1.3.3: ICP0 induces a decrease in RNF168 expression and loss of ubiquitinated H2A first seen at 2 hours post-infection (121).

Both the changes seen with RNF168 and uH2A expression with WT did not occur for ICP0 null-virus (Figure 1.3.2). To confirm that ubiquitination was linked to the decrease in RNF168 expression seen, proteasome inhibitor was added, which rescued RNF168 from degradation (121).

When applying this knowledge towards carrying out investigation into RNF168 it is clear that RSV and HSV-1 are two different viruses. The HSV-1 genomes enters the nucleus during replication whereas RSV replicates in the cytoplasm of cells (136, 137). Furthermore, RSV may not possess a protein equivalent to ICP0 that causes degradation of RNF168(121). This suggests that any mechanism by which RNF168 is affected by RSV infection would be different to HSV-1. Therefore, one of the main aims of this investigation will be to determine the mechanistic way in which RSV affects RNF168 expression. At present there is very limited knowledge of the effect of RSV on RNF168 expression in airways epithelial cells with evidence of any association gathered by our team.

1.4.1.5 Evidence Supporting an Investigation into RNF168 and RSV

Professor Ralph Tripp supplied a list of potential epithelial innate resistance genes. The graph below shows a list of these genes and the level of RSV N gene expression when these genes are knocked down by small interfering RNA (siRNA) (Apperley, Flanagan, McNamara and Tripp unpublished). Despite RSV N gene expression after RFFL, TRIM2 or RNF168 knockdown showing great variation, the level expression was considerably greater than the control. The graph below show the RSV N gene expression for all genes investigated (Figure 1.3.4) (Apperley, Flanagan, McNamara and Tripp unpublished).

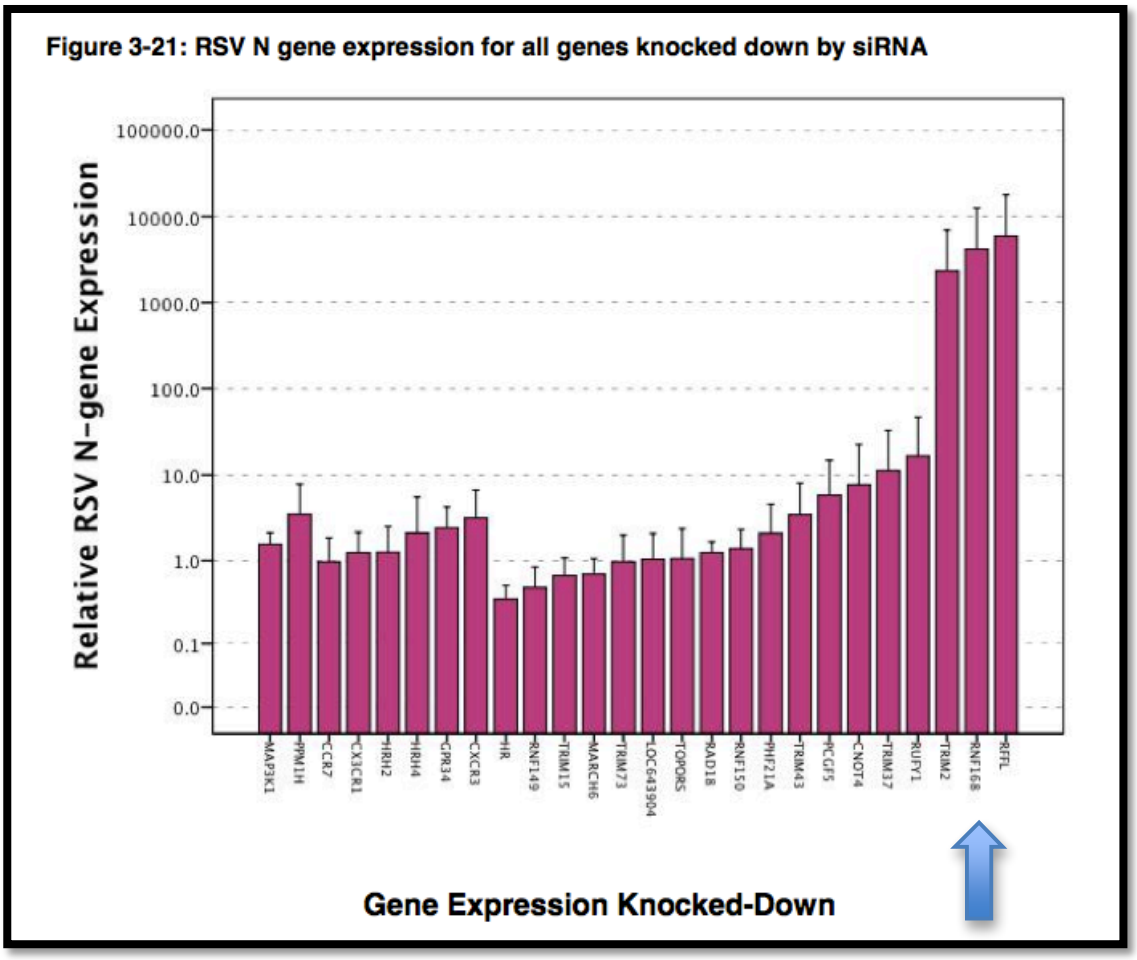

Figure 1.3.4: RSV N gene expression for all genes knocked down by siRNA (RNF168 shown by arrow) (Apperley, Flanagan and McNamara unpublished).

Another experiment involving the knockdown of RNF168, UBE2G2 and RFFL was carried out. A mean of 6 repeat experiments was calculated. There was little variation seen between experiments, making the data more reliable (Figure 1.3.5) (Apperley, Flanagan and McNamara unpublished). However, in comparison to the previous experiment (Figure 1.3.4), the levels of RSV N gene expression were not as high. Knockdown of RNF168 induced an increase in RSV N gene expression. However, the level of expression was less than 2 times greater than the level of the control (Figure 1.3.4) (Apperley, Flanagan and McNamara unpublished).

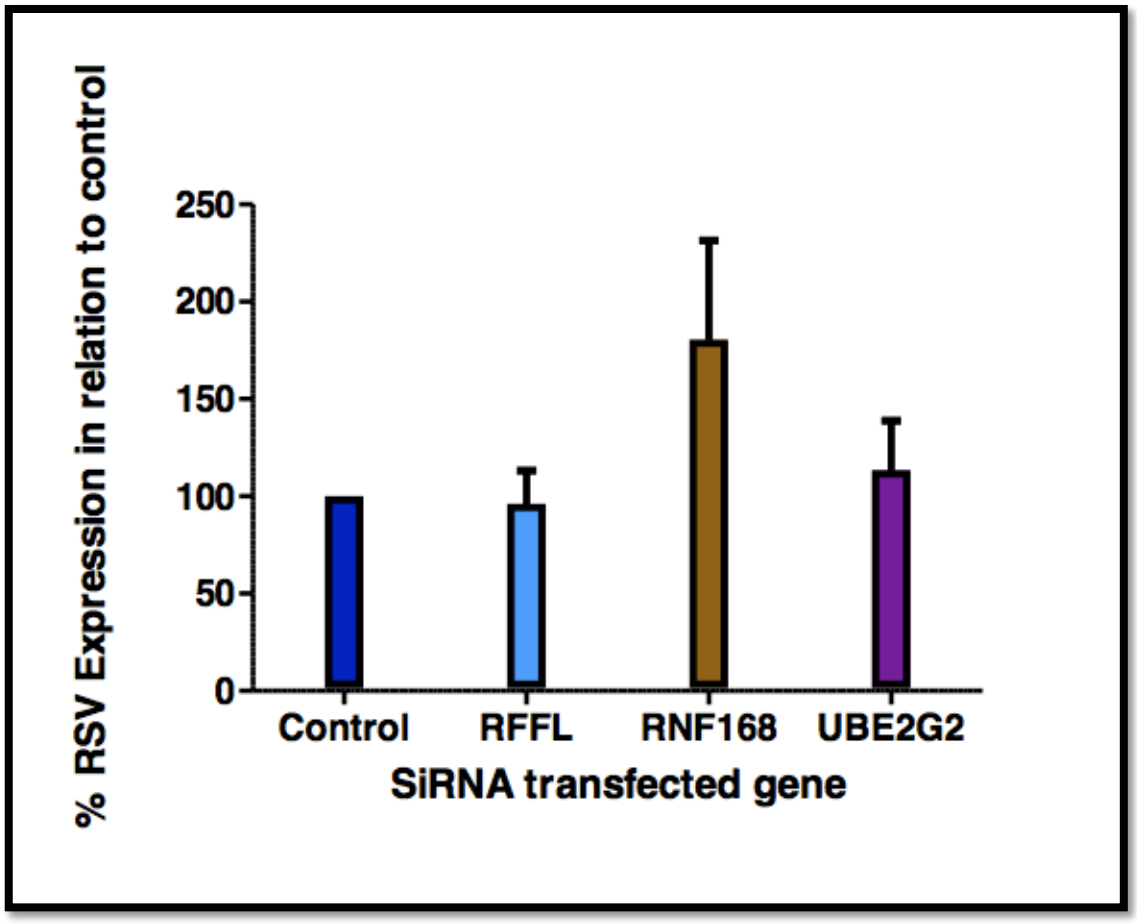

Figure 1.3.5: Graph showing the percentage of RSV expression in relation to control for RFFL, UBE2G2 and RNF168 (Apperley, Flanagan, McNamara and Tripp unpublished).

1.4.1.6 RNF168 Investigation Summary

It was found previously that when the gene RNF168 was knockdown by siRNA, RSV N gene expression increased more than most of the other genes selected for knockdown (Apperley, Flanagan, McNamara and Tripp unpublished). The E3 ubiquitin ligase RNF168 has a role in antiviral defence when HeLa cells are infected with herpes simplex virus type 1 (HSV-1). RNF168 E3 ubiquitin ligase has been demonstrated to have a potential role for intrinsic antiviral defence to HSV-1 infection(121). It has been shown that RNF168 is responsible for modifying histone proteins by ubiquitination, which causes the recruitment of repair factors to double strand break sites (DSBs). A protein in HSV-1, ICP0, functions as an E3 ubiquitin ligase causing the degradation of RNF168(121). Given the role this protein plays in intrinsic antiviral defence, it is hypothesised that RSV affects the expression of RNF168 when overcoming the intrinsic antiviral defence of the target cell.

Therefore, due to this background knowledge, an investigation into RNF168 expression in RSV infected A549 cells were carried out. This was to determine the effect RSV had on the RNF168 and as a consequence how it could be implicated in the antiviral defence of a cell from RSV. RSV time-course experiments were carried out to establish whether there was a relationship between duration of RSV infection and RNF168 expression. Titration experiments were carried out to determine if there was a relationship between the multiplicity of infection (MOI) of RSV and RNF168 expression. Experiments were also carried out with interferon beta stimulation of A549 cells to see if interferon affected RNF168. This was because interferon is released from cells as part of the cell's innate immune response and could have an effect on RNF168 expression. Polyinosinic:polycytidylic acid (PolyI:C) is an immunostimulant which is known to interact with TLR3. It is considered to be a synthetic analogue of double-stranded RNA like a virus and is recognised by TLR3. An investigation into the effects of polyI:C on RNF168 expression was carried out to see whether TLR3 had a mechanistic role in RNF168 expression (138).

To provide supporting evidence that the experiment had been carried out effectively by infecting cells at the correct MOI and duration of infection, PCR of samples was carried out for RSV N gene expression. Interleukin-8 (IL-8) and interleukin-6 (IL-6) are proinflammatory cytokines produced by respiratory epithelial cells in response to RSV infection (48, 95).

To provide additional evidence that the experiment had been carried out effectively by infecting cells at the correct MOI and duration of infection, Sandwich Enzyme enzyme-linked immunosorbent assay (ELISA) for IL-8 and IL-6 were carried out on the supernatants taken from infected cells. To visibly establish the effect of RSV, polyI:C and interferon beta on RNF168, Western Blotting was used to measure RNF168 expression.

1.4.2 CXCL5 Investigation

1.4.2.1 Background

Chemokines are grouped into 4 subfamilies, which are CXC, CC, CX3C and C on the basis of structural cysteine motif found near the amino acid terminus (139). CXCL5 belong to the CXC chemokines family, which is predominantly implicated in the chemotaxis of inflammatory cells through the generation of local concentration gradients (140). Human CXCL5, is also referred to as epithelial cell-derived neutrophil-activating peptide-78 (ENA-78), is involved in a variety of human inflammatory diseases (141). It has been shown that this chemokine is involved in neutrophil activation and recruitment. CXCL5 has been implicated in pulmonary disease, lung cancer, arthritis and other cancers. This CXC chemokine is also produced from adipose tissue when stimulated by cytokine TNF-alpha. This leads to the involvement of CXCL5 in inflammatory obesity-related diseases as shown in Figure 19 (139, 140).

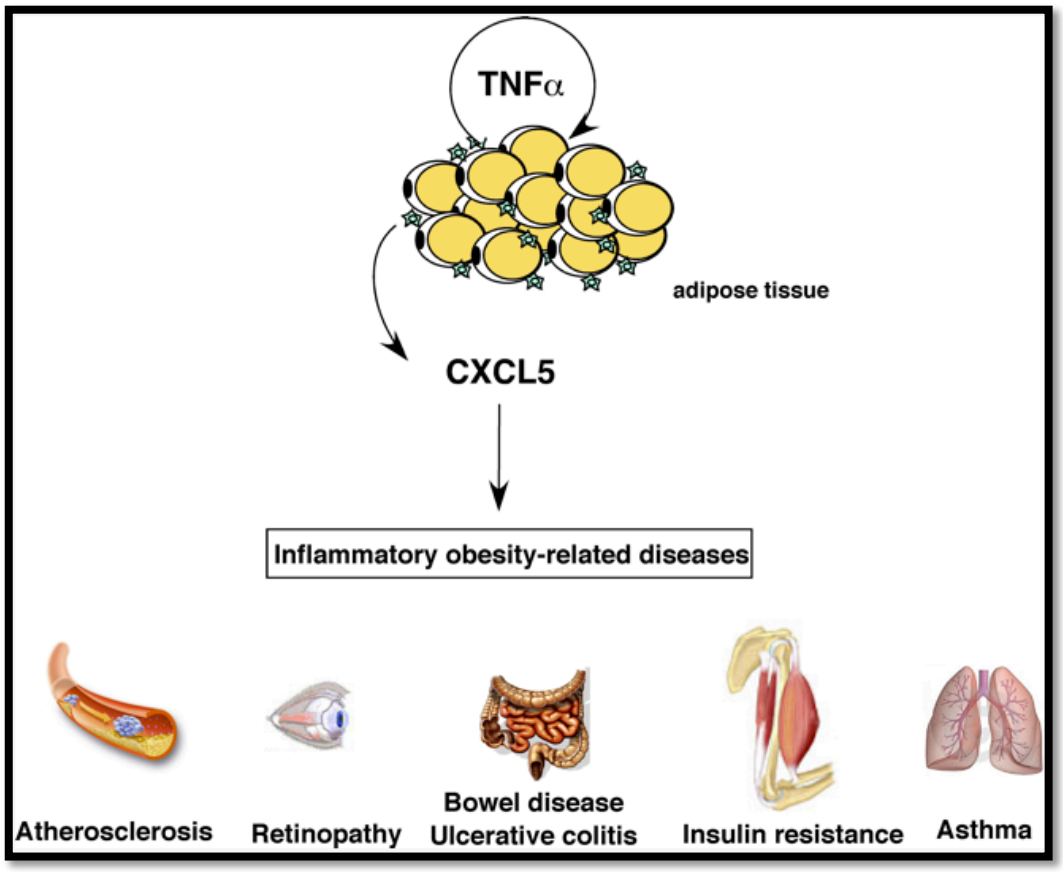

Figure 1.3.6: CXCL5 inflammatory obesity-related diseases (140).

1.4.2.2 Reasoning behind CXCL5 Investigation

CXCL5 is a small cytokine belonging to the CXC chemokine family and has a role as a neutrophil chemoattractant. To understand the early event of RSV infection with regards to neutrophil activation and recruitment, proteomic analysis of a change in protein expression was carried out (Flanagan et al). A comparison was made between infected and control cells. This comparison was made by analysing samples using mass spectrometry coupled to nanoflow chromatography. Taqman PCR further measured expression of the neutrophil chemoattractant CXCL5 for samples infected at time points 0, 2, 4, 6, 24 and 48 hours. The results suggest CXCL5 expression is transient peaking at 6 hours but only measured mRNA and not protein expression (Flanagan et al). If protein expression can be confirmed, it would suggest that CXCL5 might play a role in early neutrophil recruitment. To provide supporting evidence to the data obtained a CXCL5 enzyme-linked immunosorbent assay (ELISA) was carried out on supernatants collected from RSV infected A549 cells at 0, 2, 4, 6, 24, 48 hours.

1.5 Aims

The main aims of an investigation into RNF168 are:

- To determine if RSV infection of A549 cells has an effect on RNF168 expression
- To gain a better understanding about how mechanistically this change in RNF168 expression occurs.

The aims of an investigation into CXCL5 (additional topic) are:

- To determine how CXCL5 levels are affected by RSV infection of A549 cells over various timepoints.

2. Materials and Methods

2.1 Tissue Culture of A549 cells Splitting Cells into T75 flask and 24-well plates

D.J Giard developed the A549 cell line in 1972 through the removal and culturing of cancerous lung tissue present in a 58 year-old male (142). A549 cells were grown in T75 flasks (Thermo Scientific) until confluent. The growth medium was Dulbecco Modified Eagle Medium (DMEM) (Sigma-Aldrich) with 10% Fetal Calf Serum (FCS) also known as fetal bovine serum (FBS) Gibco by Life Technologies) and gentamicin (Sigma-Aldrich, 50 mg/ml). Confluence was observed by microscope (Leica DFC420). The media was removed and cells were washed twice in 10ml of Phosphate Buffered Saline (PBS) (Sigma-Aldrich) to remove remaining dead cells. The PBS was removed and 3ml of trypsin (Sigma-Aldrich) added. The flask was incubated at 37 °C in 5% CO_2 for 1 minute before the trypsin was deactivated by adding 5ml of full media (DMEM with 10% FCS and gentamicin, 50mg/ml) to the flask. The contents of the flask were then transferred to a 10ml tube. The tube was spun in a centrifuge for 10 minutes at 1500 revolutions per minute (rpm) (550G).

The supernatant was discarded and pellet resuspended in 1ml of full media. A volume of approximately 200µl of this suspension was added to a T75 flask containing 15ml of media. This volume varied according to the number of cells required for the flask to reach confluence at a specific time. This was calculated by using a haemocytometer to do a cell count of the confluent flask before splitting. The remaining volume of suspended cells was used for seeding cells in a 24-well plate (Thermo Scientific) or discarded. Again the volume used depended on how fast the plate was required to reach confluence as well as the number of plates to be seeded.

This was frequently 100µl in 10ml of full media (DMEM with 10% FCS and gentamicin). Cell counts were made using haemocytometer to estimate the number of cells, which should be seeded into each well. To each well of the 24-well plate, 1ml of full media (DMEM with 10% FCS and gentamicin) containing approximately 100,000 cells was added. The cells were usually split so that wells would be fully confluent in 2 days time. The 24-well plates and the newly split flask were left in an incubator at 37° C in 5% CO_2 until required for use. Confluence was checked daily.

2.2 Harvesting RSV from T75 Flask

It should be noted that RSV is most stable when within cells. Unbound virus degrades quickly so it was important to work quickly when thawing and freezing the virus containing cryovials.

2.2.1 RSV Propagation

30,000 Hep-2 cells/cm^2 were seeded into a volume of 15ml full media (DMEM with 10% FCS and gentamicin) in a T75cm^2 flask and left to grow to approximately 50-70% confluence overnight at 37°C in 5% CO_2. Media was then removed and the flask washed twice with PBS to remove cell debris and dead cells. A cryovial of rapidly thawed RSV was added to the flask along with 4ml of serum free media (DMEM with gentamicin but no FCS). For thawing, the cryovial was agitated in a water bath set to 37°C. When the pellet is almost completely thawed the cryovial was taken to the hood where the contents were gently pipetted up and down to thaw remaining virus for quick use.

The RSV was gently dispersed over the whole flask. The flask was left to rock gently for 2 hours in the incubator at 37°C in 5% CO_2. After 2 hours 11ml of full media was added and the flask left for 24 hours. After 24 hours 11ml of the media in the flask was removed and replaced with serum free media making the percentage of FCS present in the flask 2%. The flask was assessed daily for cytopathic effect (dead cells floating in media). The flask was viewed under the microscope for the presence of syncytia (Figure 2.1.1).

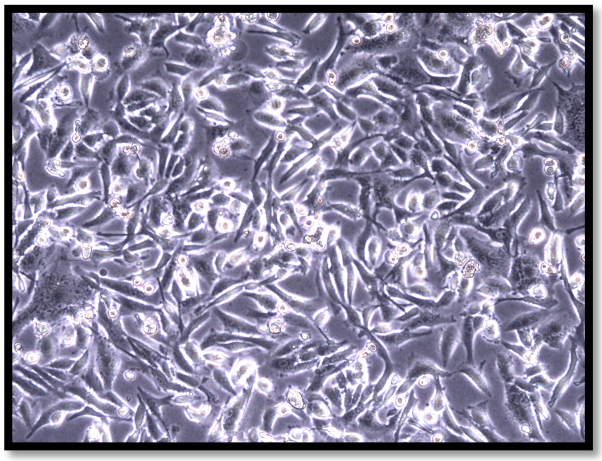

Figure 2.1.1: Infected Hep-2 cells after 48 hours with syncytia present.

2.2.2 Harvesting RSV

RSV was harvested at 48 hours. Most of the media was removed from the flask until 4.5ml was remaining. Cells were harvested using a cell scraper and were placed in a 10ml tube on ice and using a 2ml syringe with an orange needle (25 gauge) the cells were lysed by passing the cells through the syringe 10 times. The cells were spun down in a centrifuge at 1500 rpm (550G) for 5 minutes at 4°C.

The pellet containing Hep2 cells debris was discarded and the supernatant retained. The supernatant (500µl per aliquot) was quickly transferred to pre-labelled cryovials and snap frozen in liquid nitrogen. The cryovials were transferred to the -80°C freezer. The batch number, date and location were noted in the stock folder.

2.2.3 Plaque Assay for RSV

The plaque forming units of RSV were measured using the following protocol:

2.2.3.1 First Day

Into a 96-well plate (flat-bottomed plate) $1x10^4$ A549 cells/well were transferred with full media (DMEM with 10% FCS and gentamicin, 50mg/ml) and left overnight at 37°C in an incubator.

2.2.3.2 Second Day

In a separate plate, the virus stock was titrated out to be tested using dilutions starting at 1/100. A minimum of 8 dilutions was done quickly with FCS free medium (DMEM and gentamicin 50mg/ml). The 96-well plate was removed from the incubator and the A549 cells were washed with PBS. To the plate 50µl of the dilutions of virus stock per well was added. The plate was left for 2 hours at 37°C. To the plate 150µl of full media was added and left overnight at 37°C

2.2.3.3 Third Day

The cells were washed with PBS (100µl/well) and fixed for 20 minutes (at room temperature) with 100% methanol containing 2% hydrogen peroxide (Sigma-Aldrich, Sigma). They were then washed with PBS again (100µl/well). Biotinylated anti-RSV antibody (Serotech Biotin, Goat) (1/200 dilution with PBS/1%BSA) was added, 100µl per well to the plate. The plate was left to incubate for 1 hour at room temperature before being washed with PBS/BSA twice. Afterwards 100µl of 1/500 dilution (in PBS) of extravidin peroxidase was added and left for 30 minutes at room temperature. The plate was washed with PBS/BSA twice and 50µl of 3 amino-ethylcarbazole substrate per well was added and left for 20 minutes to 24 hours. The 3 amino-ethylcarbazole (OPD (0-phenylenediamine) peroxidase substrate supplied by Sigma-Aldrich) was in tablet form and made up of the following:

- 0.3ml of 3.3 mg/ml AEC in DMSO
- 10µl hydrogen peroxide
- 1.25ml, 24.3 mM citric acid
- 2.6ml, 100 mM Na_2HPO_4
- 1.15ml distilled water

When plaques appeared and have acquired the desired coloration, PBS was added to the cells to stop reaction. The number of plaques was counted in the whole well. The dilutions of the virus were chosen so that there were 100-200 plaques per well and all replicates of that dilution were counted. From this an mean number of plaques were calculated. The plaque forming units are calculated by: Mean number of plaques x dilution x 20. An example of the plaque formation is shown (Figure 2.1.2).

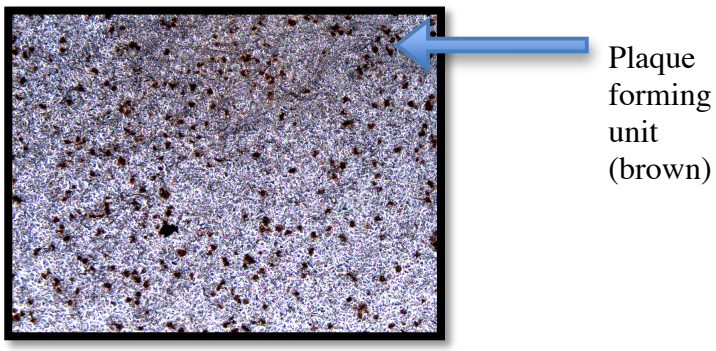

Figure 2.1.2: Image taken from microscope showing plaque formation (Brown areas).

2.3 Calculation of the appropriate level of Multiplicity of Infection (MOI)

When setting up experiments it was important to know beforehand the specific multiplicity of infection (MOI) or range of multiplicity of infection to use. This was calculated by getting a ratio between the number of RSV particles and the number of cells in the well of a confluent 24-well plate. The number of cells in a confluent 24-well plate was calculated using a haemocytometer. The calculations from the plaque-forming assay gave an indication of the number of RSV particles. Based on this data, the volume of RSV to be used for an experiment was calculated.

The reasoning behind RSV MOI calculation is as follows: if there is 100,000 cells to be infected at a 1:1 MOI with the number of viral particles $1x10^6$ per ml. For there to be one particle for one virus, the number of particles would have to be divided by 10. Therefore, $1x10^6$ / 10 give 1 $x10^5$ virus particles for $1x10^5$ cells giving a 1:1MOI. This means the volume to be added to cells must be divided by 10 i.e. per ml means 1ml divided by 10 to give 100µl of virus that must be added to cells.

Range of MOIs used was from 0.025:1 to 1:1. An explanation of these MOIs is given in the table below.

Table 2.1: Interpretation of RSV Multiplicity of Infection

Multiplicity of Infection (MOI)	Interpretation
NI	Control: A549 cells, which were not infected with RSV.
0.025:1	For every 40 A549 cells there is one RSV virus particle
0.25:1	For every 4 A549 cells there is one RSV virus particle
0.5:1	For every 2 A549 cells there is one RSV virus particle
1:1	For every 1 A549 cell there is one RSV virus particle

2.4 Cell count calculation of 24 wells plate

The 1ml media from the well of the 24-well plate was removed and cells washed with 500µl of PBS to remove any dead cells or cell debris. Trypsin (100µl) was added to the well of A549 cells to dislodge bound cells and the plate placed in the incubator for 1 minute. The role of trypsin was to suspend the cells stuck down on the plate. The cells were then checked under a microscope to see how many cells were still stuck down. Full media (500µl) was added to the well. The cells were then scrapped from the well. The contents were then mixed up and down with a pipette. All of the 600µl in the well was transferred to a microcentrifuge tube and 10µl was taken for the haemocytometer.

The number of cells was counted in each of the 4 quadrants of the haemocytometer. For example, if the values in the 4 quadrants were 24, 34, 40 and 37 then the mean is 33.75. The cell count calculation would be 33.75 x 10^4x0.6 (as the total volume was 600µl), which gives 202,500 cells per well.

2.5 Infecting Cells

When the cells in the 24-well plate had reached maximum confluence the media from wells was removed and replaced with 1ml FCS free media (DMEM that did not contain FCS only gentamicin, 50mg/ml). FCS free media was used because it encouraged the virus to attach to the cells. The RSV cryovial was taken from the freezer and left to thaw in the water bath until only a small piece of ice was visible in the cryovial. According to the multiplicity of infection (MOI) calculations that had been carried out before hand, a specific amount of RSV was added to selected wells quickly. The cells were then incubated at 37°C at 5% CO_2. After 2 hours 1ml of full media was added to each well to give optimum conditions for the growth of A549 cells. The plate was placed back into the incubator at 37°C at 5% CO_2 for a specific time period before harvesting.

There were 2 types of RSV infection experiments carried out. One was a MOI titration where cells underwent infection with different MOIs ranging from 0.025:1 to 1:1 either over 4 or 24 hours. All titration experiments had a control (NI) where a well of A549 cells was not infected with RSV. The other experiment was a RSV time-course experiment where cells underwent infection with RSV over 0, 2, 4, 6, 24 and 48 hours. 0 hours was where no RSV had been added and was used as a starting control. The 0 hours samples were harvested immediately after all other samples had been infected with RSV. All time-course experiments had paired controls for each time point. When recording data controls were labeled as NI.

2.6 Stimulating A549 Cells with Interferon-Beta, PolyI:C and Palivizumab.

The range of concentrations of interferon-β (IFN-β) used was 1 to 100ng/ml. The concentration of IFN-β used was 100μg/ml and the volume was 2μl in a microcentrifuge tube. The microcentrifuge tube was spun down for 10 seconds and placed on ice. The 2μl of IFN-β was taken and added to 198μl of full media in a new microcentrifuge tube to dilute the IFN-β to give a 1/100 dilution. The contents of this tube were used to stimulate A549 cells. The 24-well plate containing confluent A549 a cell was taken out of the incubator and the media removed from all wells to which IFN-β was to be added.

To stimulate A549 cells with 1ng/ml of IFN-β (Invivogen), 1μl of IFN-β (1/100 dilution) was added to 999μl of media. If one sample was to be stimulated with 5ng/ml of IFN-β, 995μl of full media was added to the well with 5μl of the 1 in 100 dilution of IFN-β. If one sample was to be stimulated with 10ng/ml of IFN-β, 990μl of full media was added to the well with 10μl of the 1 in 100 dilution of IFN-β. If one sample was to be stimulated with 50ng/ml of IFN-β, 950μl of full media was added to the well with 50μl of the 1 in 100 dilution of IFN-β. If one sample was to be stimulated with 100ng/ml of IFN-β, 900μl of full media was added to the well with 100μl of the 1 in 100 dilution of IFN-β. After stimulation the 24-well plate was placed back in the incubator at 37°C at 5% CO_2 and left there until it was time to harvest the cells.

The media was removed from all wells where cells were to be stimulated with polyI:C. To each well 1ml of full media was added. Only a preliminary time course experiment was done, where 50ng/ml of polyI:C (Invivogen) was added to each well. The 24-well plate was placed back in the incubator at 37°C at 5% CO_2 until it was time for each sample to be harvested.

To show that changes in RNF168 expression were affected by RSV and not another factor, cells were infected with RSV MOI 1:1, which had been mixed with 5µl palivizumab (Synagis, MedImmune). The normal infection protocol and harvesting this sample for real-time PCR and Western blotting was carried out (See Sections 2.5 and 2.7).

2.7 Harvesting Cells for Enzyme-Linked Immunosorbent Assay (ELISA) and Western Blot

Culture supernatants were removed and transferred to a labelled microcentrifuge tube. The tubes were stored in a -20°C freezer until they were required for analysis by the Enzyme-Linked Immunosorbent Assay (ELISA). After the supernatant had been taken, the cells were harvested for the Western Blot.

Firstly, 1ml of Phosphate Buffered Saline (PBS) was added to the wells and cells were scraped using a cell scraper from the bottom of the well so that they were suspended in the PBS. This suspension was transferred to a labelled 10ml tube. The well was then washed with 1ml of PBS again and the contents transferred to the same 10ml tube. This was done so that any protein left in the well would not be lost. This process was repeated for all samples. All of the 10 ml tubes containing each sample were then spun in a centrifuge for 10 minutes at 1500 rpm (550G).

Afterwards, the supernatant was discarded and pellets resuspended in 500µl of PBS and transferred to a labelled microcentrifuge tube. Tubes were placed in a mini-centrifuge and spun at maximum speed for 3 minutes at 13.3 x 10^4 rpm. The supernatant was then removed from the microcentrifuge tubes to leave dry pellets, which were placed in the -20°C freezer. The pellets were then used to run a western blot the day after or were put in Sodium Dodecyl Sulfate (SDS) (with protease inhibitor and dithiothreitol) and stored at -30°C until required for further use.

2.8 Western Blotting, ELISA and Real-time PCR

2.8.1 Background and Theory of Western Blotting (primary source: Advansta Protein Analysis: Electrophoresis, Blotting and Immunodetection)

Western blotting, an analytical technique used for the study of proteins allows detection of a single protein among a mixture of proteins from a biological sample, allowing an estimation of molecular weight and relative amount. This protein mixture is separated using a polyacrylamide gel then electrically transferred to a PVDF membrane (143).

The membrane is a replica of protein composition and pattern making it possible to detect target proteins due to antibody-antigen interaction. The specificity of this technique is attributed to the antibody, which recognises and binds to an epitope unique to the protein of interest. This technique consists of sample preparation, electrophoresis, separation of proteins, transfer of proteins, membrane staining and developing (143).

A brief overview of the process of Western Blotting with diagrammatic representation is shown below (Figures 2.3, 2.4 ad 2.5) (143):

1) **Sample preparation**: Proteins from A549 cells are harvested as explained in the previous section. To the microcentrifuge tube containing the protein pellet, Sodium Dodecyl Sulphate (SDS) is added. This causes the proteins to be coated with a negative charge so that they will separate when run on the gel based on size. Bromophenol blue a blue dye, is added to samples to aid in loading. The dye will migrate ahead of proteins on the gel so that the progress of the gel can be monitored. Protease inhibitor is added to prevent the degradation of the protein of interest. Dithiothreitol (DTT) is added to the samples as a reducing agent. DTT prevents the oxidation of cysteines and will complete protein unfolding by breaking disulphide bonds between cysteine residues.

2) **Polyacrylamide electrophoresis:** The polyacrylamide gel is placed in an electrophoresis tank, filled with buffer. Samples are loaded with a tip into the wells of the polyacrylamide gel (Figure 2.3). The electrophoresis supply is attached to a power supply, which provides the voltage. When the power supply is turned on, the negatively charged proteins migrate away from the anode. The protein is separated according to size by electrophoresis.

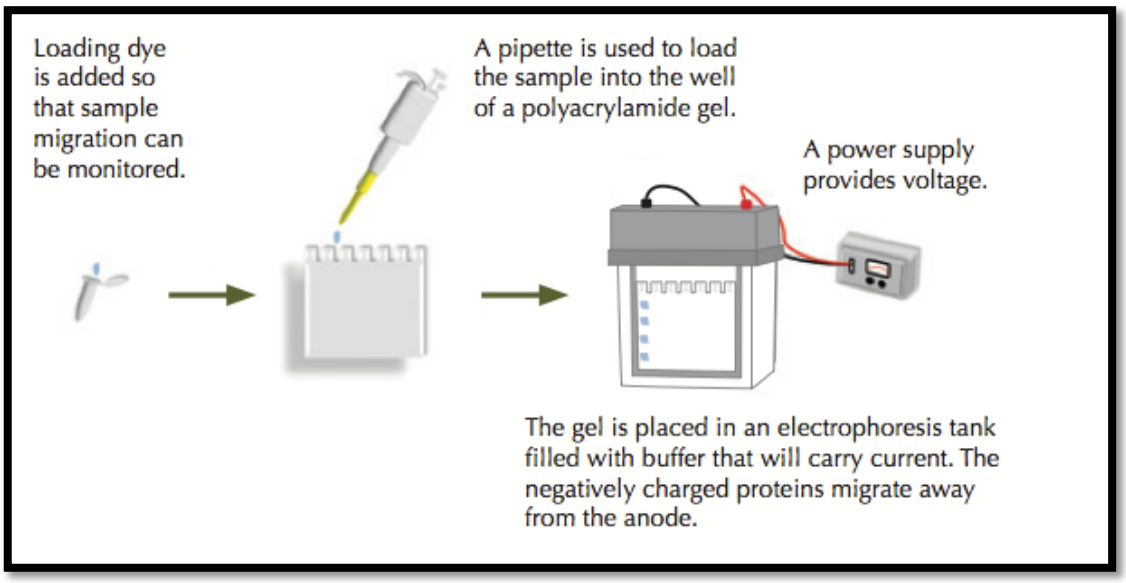

Figure 2.1.3: Sample loading and setting up of the polyacrylamide gel for electrophoresis(143).

3) **Electrophoretic transfer to membrane support**: The proteins are transferred electrophoretically to a membrane where they are immobilised. The membrane is a solid support, which binds and immobilises the protein allowing for detection by antibody hybridisation. Systems for transfer use an electric current to drive the negative charged protein towards the positive electrode. The membrane used for transfer is polyvinylidene difluoride (PVDF). Membranes can also be made of nitrocellulose. The advantages of PVDF membranes are that they offer mechanical strength and a higher bonding strength than nitrocellulose.

4) **Blocking and Antibody hybridisation:** The membrane is blocked to prevent non-specific binding of the antibodies (Figure 2.1.3). The protein-based blocking agent used is non-fat dry milk. This is preferred to BSA because it is cost effective. The blocking agent is diluted in Tris-buffered Saline (TBS) with Tween 20 detergent added. The membrane was then incubated with primary antibody directed against specific epitope present on target protein.

5) **Information and background about antibodies:** The antibodies used in this investigation were monoclonal antibodies. The production of monoclonal antibodies involves synthesising cells, which are isolated from the spleen of an immunised animal and fused with myeloma cells. This forms hybridomas, which secrete antibodies into their culture media. These antibodies are tested for their affinity to antigen. Hybridomas having the most stable production of antibodies are selected and grown in culture indefinitely. After several washes to remove unbound antibody, the secondary antibody is added and binds to the primary antibody, providing a means of detection.

   The primary antibody is diluted in the blocking agent and applied so that it covers the entire membrane (Figure 2.1.4). The antibody manufacturer may recommend the starting dilution but the concentration of antibody required for the best image must be determined empirically. Factors that were taken into account when selecting the antibody concentration were, abundance of target protein in the sample, the affinity of the antibody for the protein of interest and the sensitivity of the detection system used.

   The primary antibody is usually kept on overnight at 4°C. The time that the primary antibody should be left on is recommended in the manufacturer guide. After incubation the primary antibody is washed away using wash buffer. The secondary antibody is added to the membrane (Figure 2.1.4). Selection of the secondary antibody depends on the species in which the primary antibody was made. For example if the primary antibody was made in rabbit, then the secondary antibody will be anti-rabbit (a secondary raised in a species other than rabbit).

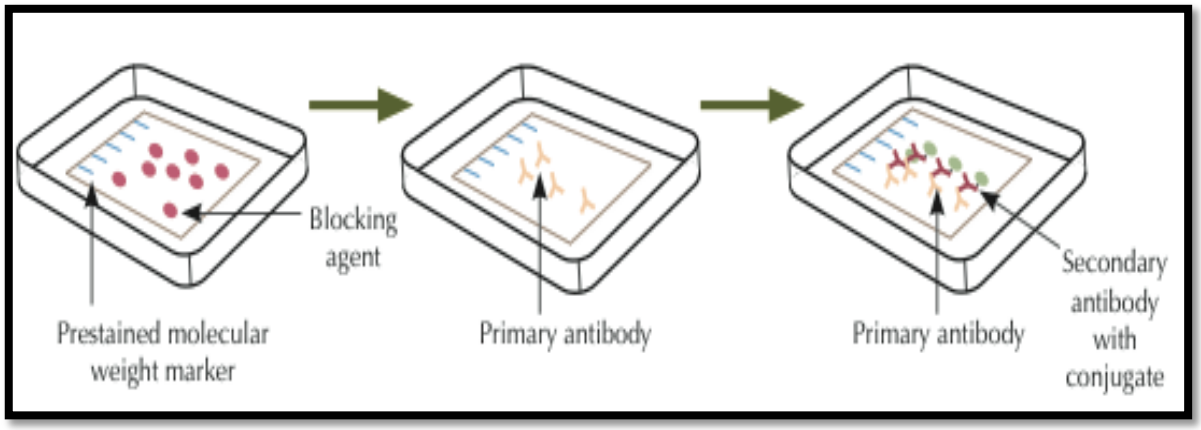

Figure 2.1.4: Blocking membrane. Process of adding primary and secondary antibodies (143).

6) **Detection:** Detection of the protein can be achieved through chemiluminescence, fluorescence and colorimetric techniques. In this investigation chemiluminescence was used to detect the protein of interest. Chemiluminescence methods commonly use horseradish peroxidase enzyme (HRP)-conjugated secondary antibodies (Figure 2.1.5). The reaction between the horseradish peroxidase enzyme and substrate produces light, which can be detected by exposing the blot to an x-ray film (Figure 2.15). The advantages of chemiluminescence are that the membrane can be stripped and reprobed, multiple exposures can be done with x-ray films, the results can be easily documented and this technique is highly sensitive.

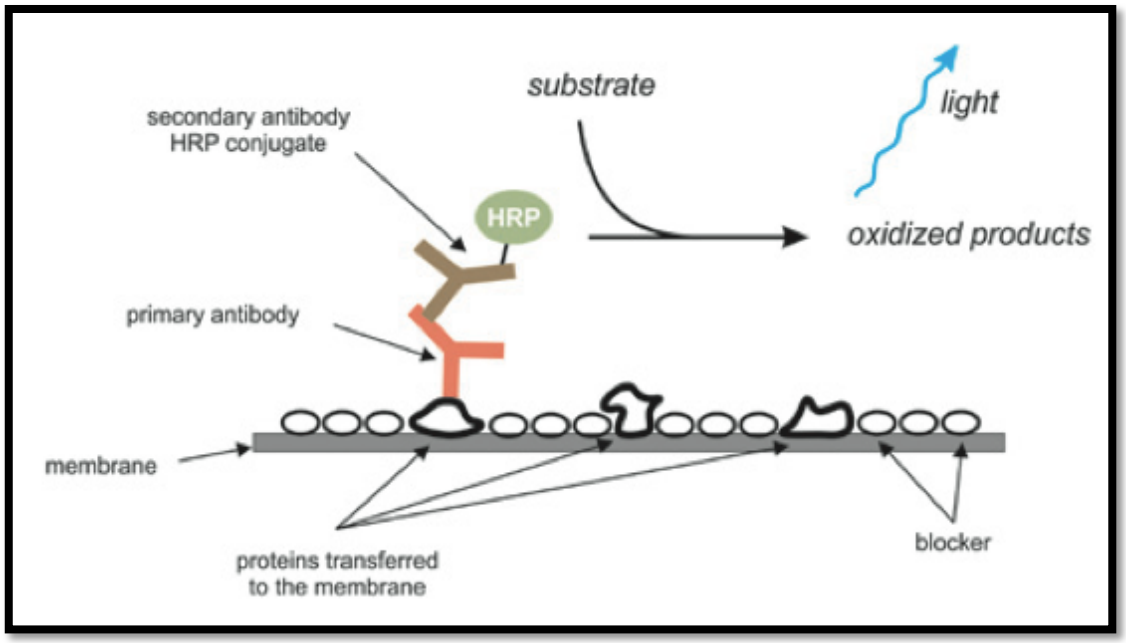

Figure 2.1.5: Diagrammatic representation of the binding of primary and secondary antibody to membrane (143).

2.8.2Western Blotting Protocol

This is more specific detail about how the technique of Western Blotting was applied in this project.

2.8.2.1 Sample Preparation

Samples were taken from the -30 degrees freezer and thawed on ice. The pellet was dissolved at 100°C for 3 minutes in denaturing and reducing buffer consisting of anionic denaturing detergent Sodium Dodecyl Sulphate (SDS), 10% Dithiothreitol (Sigma-Aldrich, Sigma) and a 1 in a 100 dilution of Protease Inhibitor (PI) (Thermo Scientific). The tubes were then placed on ice ready to load onto the gel. Of each sample, 5µl was loaded into each well of the Bio-Rad Miniprotein precast gel (12% Tris/ glycine buffer), which was run in the Bio-Rad Western Blot System (electrophoresis tank) using running buffer at 140 volts.

To make up running buffer the following was added and mixed in a 1 litre bottle:

- 3.03 grams Tris Base (Fisher Chemical)
- 14.4 grams Glycine (Fisher Chemical)
- 1 gram SDS (Bio-Rad Electrophoresis)
- 1 litre of double-distilled water

Precision Plus Protein Standards All Blue (also known as ladder) (Bio-Rad) was loaded into the first well to enable the size of the detected bands to be measured. The ladder gave an indication of where precisely to cut the gel to select the proteins of interest for analysis. The ladder showing where the proteins of interest are located has been shown (Figure 2.1.6).

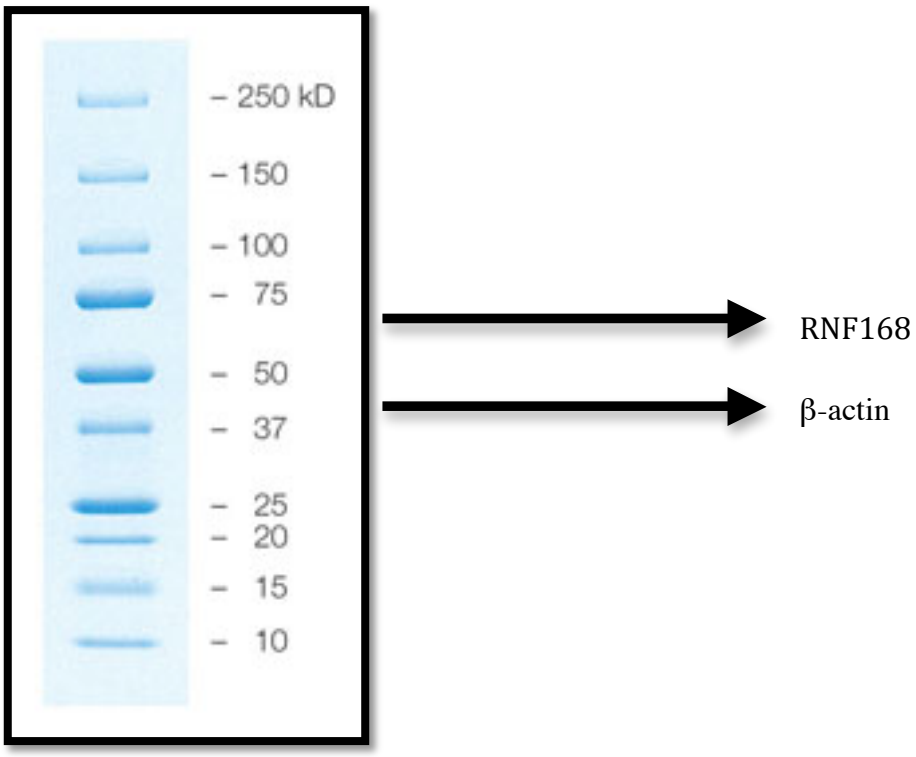

Figure 2.1.6: Precision Plus Protein All Blue Standards.The arrows indicate the rough location of proteins of interest.

The gel was run for 1 hour. Afterwards the gel was removed from the electrophoresis tank and the plastic cassette enclosing the gel removed. Using the relative positions of the protein ladder, the gel was cut to select an area where the proteins (RNF168 and β-actin) of interest were located.

2.8.2.2 Protein Transfer

The gel was placed on top of a PVDF membrane (Transblot-Turbo Transfer Pack 0.2μM PVDF, Bio-Rad USA) and sandwiched between papers pre-wetted with transfer buffer. An electric field (positive to negative) (Trans-Blot® Turbo™ Transfer System, Bio-Rad) at mixed molecular weight setting was applied for 7 minutes to the transfer the proteins from gel to the membrane. The membrane containing the gel samples was then cut out and left to block in 5% skimmed milk solution (1g Marvel milk in 20ml 1xTris Buffer Saline (Sigma-Aldrich, Sigma) with 0.5% Tween (1xTBST)) for 30 minutes. Blocking the membrane prevents non-specific binding of primary and secondary antibodies to the membrane.

2.8.2.3 Immunostaining

While the membrane was left to block, the primary antibody was diluted in 5% skimmed milk solution (1g of milk in 20ml 1xTBST) as a 1/1000 dilution. After blocking, the milk was removed and the primary antibody RNF168 (Abcam) was added to the membrane and incubated overnight at 4°C with agitation. This is an example given of probing the membrane for RNF168.

The next day the membrane was washed in 1x TBST in 5 separate washes lasting 1, 3, 10, 5 and 5 minutes. The secondary antibody, anti-mouse (Mouse) was added as a 1/1000 dilution and left on the rocker for 1 hour at room temperature with agitation. The washes with 1x TBST were repeated again.

2.8.2.4 Developing Blot

ECL Prime Western Blotting Detection Reagent (GE Healthcare life Sciences, Amersham) was made up using equal volumes of solution A and solution B. This volume was frequently 500µl of each solution. After washes, the membrane was placed on cling film and covered with ECL for 5 minutes. After 5 minutes the membrane was wrapped up in another piece of cling film and transferred to a cassette.

In the dark room the ECL High Performance chemiluminescence film (Amersham Hyperfilm) was placed down over the membrane for 10 seconds. The film was then developed for 1 minute in 400 ml of developer G153 (Agfa Healthcare Inv, Belgium), rinsed in 400ml distilled water, then 1 minute in 400ml of Fixer G354 (Agfa Healthcare Inv, Belgium) and rinsed in 400ml water again.

The instructions for making developer and fixer are:

- Developer (400ml): 50ml solution B (G153, part B, Agfa Healthcare Inv, Belgium) + 150ml solution A (G153, part A, Agfa Healthcare Inv, Belgium) + 200ml water
- Fixer (400ml): 100ml fixer (G354 Agfa Healthcare Inv, Belgium) + 300ml water

The film was then hung to dry. Afterwards the film was lined up with the membrane, which was still taped to the cassette. This was to see whether the bands that had developed were in fact the protein of interest by measuring the number of Kilodaltons of protein against the ladder and comparing this estimate with number of Kilodaltons that the protein is stated to be according to the manufacturer.

2.8.2.5 Probing for Actin

To check that protein had been loaded evenly and in order to get a ratio of the level of expression of the protein of interest, beta-actin (β-actin) (Mouse) was probed. This involved taking the membrane out of the cassette and leaving it to the block in 5% skimmed milk solution for 30 minutes. The primary antibody β-actin was diluted in 5% skimmed milk solution as 1/1000 dilution and added to the membrane. The milk was removed and the primary β-actin antibody added to the membrane.

The membrane was then left for 1 hour on a rocker. The primary antibody was removed and the membrane washed with 1x TBST in 5 separate washes for 1, 3, 10, 5 and 5 minutes. The secondary antibody, anti-mouse (Goat) was diluted in 5% skimmed milk solution as a 1/1000 dilution, was added. The membrane was agitated for 1 hour at room temperature. The antibody was removed and washed again in 1xTBST. The steps for developing the blot were repeated.

Tables 2.2 and 2.3 provide the details for the antibodies used throughout this investigation.

Table 2.2: Conditions Required for Each Antibody

Antibody	Duration and Conditions of Antibody left on Membrane
Anti-RNF168	Overnight at 4°C with agitation
β-Actin	1 hour at room temperature with agitation
Anti-Mouse	1 hour at room temperature with agitation

Table 2.3: Primary and Secondary Antibodies

Primary Antibody	Manufacturer and Catalogue Number	Kilodaltons (kDa)	Secondary Antibody	Manufacturer and Catalogue Number
Anti-RNF168 (Mouse)	ABCAM Catalogue number: ab58063	65	**Anti-Mouse IgG HRP (Goat)**	R&D Systems Catalogue: HAF007
β-Actin (Mouse)	ABCAM Catalogue Number: ab8226	42	**Anti-Mouse IgG HRP (Goat)**	R&D Systems Catalogue: HAF007

2.8.2.6 Measuring RNF168 Expression

Western blotting is an analytic technique, providing one of the most effective visual representations of protein expression. This technique was used to investigate how the expression of RNF168 was affected by different stimuli. The β-actin expression for the same sample was measured as a loading control to determine the amount of protein loaded for each sample. As a result, the level of RNF168 expression relative to β-actin could be measured. This made the densitometry values acquired more reliable as it would show the true level of RNF168 in each sample accounting for uneven protein loading. Densitometry of the RNF168 and β-actin were carried out using ImageJ software. The densitometry values for the protein of interest were divided by the densitometry values for β-actin to give the level of expression relative to β-actin.

Densitometry analysis is measuring the intensity of band of a protein. The darker the band the greater the expression of the protein. An example of this is shown below with RNF168 (Figure 3.2).

Densitometry value for RNF168 = 603
Densitometry value for β-actin = 9473
Level of RNF168 expression relative to β-actin = 603/9473=0.06.

Figure 2.1.7: Calculating the level of RNF168 expression relative to β-actin. The density of both bands for RNF168 and β-actin were measured and the level of RNF168 expression relative to β-actin calculated. The values were plotted in a graph where the level of RNF168 expression relative to β-actin was the y-axis and the stimuli (specific to concentration/MOI) were plotted on x-axis (where NI= control).

2.8.3 Enzyme-Linked Immunosorbent Assay (ELISA) Background and Protocol

2.8.3.1 ELISA Background

The purpose of an enzyme linked immunosorbent assay (ELISA) is to quantify how much protein there is (144). Before the development of ELISA, radioimmunoassays were used. This involved using radioactive labelled antibodies and antigens. However, due to health threats of this technique, safer options were required. As a result, Swedish scientists Eva Engvall and Peter Perlmann primarily developed the ELISA technique in 1971(144, 145).

An ELISA is carried out using a 96-well plate because they give high throughput results. The type of ELISA being used here is a Sandwich ELISA where a sample antigen is detected and quantified between two layers of antibodies (capture and detection). The advantage of a Sandwich ELISA is that the sample does not need to be purified. Furthermore, the ELISA is very sensitive and potentially can be 2-5 times more sensitive than an indirect and direct ELISA. Sandwich enzyme-linked immunosorbent assays use antibodies and colour change to identify a substance as well as how much of that substance there is. The ELISAs were performed using the materials provided by the Duoset ELISA Development kit (R&D Systems) to measure natural and recombinant interleukin-8 (IL-8), interleukin-6 (IL-6) and CXCL5 (also known as ENA-78) (144, 146).

When cells undergo infection they proinflammatory cytokines as a response. These proinflammatory cytokines include interluekin-8 (IL-8) and interleukin-6 (IL-6). A549 cells produce increasing levels of IL-8 and IL-6 in response to RSV infection (147, 148). If the MOI of infection increases then there will be more virus particles to stimulate more cells to release these cytokines. Thus, to provide supporting evidence that A549 cells undergo infection by RSV and that the RSV MOI titration experiments have been carried out accurately, the supernatant from each sample was taken for IL-8 and IL-6 Sandwich ELISAs (148)

Taqman PCR measured expression of the neutrophil chemoattractant CXCL5 for samples RSV infected at time points 0, 2, 4, 6, 24 and 48 hours. The results suggest CXCL5 expression is transient peaking at 6 hours. To provide supporting evidence to the data obtained CXCL5 Sandwich ELISA was carried out on supernatants collected from RSV infected A549 cells at 0, 2, 4, 6, 24, 48 hours with controls at each time point.

2.8.3.2 Interleukin-8 (IL-8), Materials Required for ELISA by R&D Systems (149)

The following materials were used and brought to room temperature before use (149):

- **Capture antibody (1 vial):** 720µg/ml of mouse anti-human IL-8/CXCL5 when reconstituted with 1.0ml of PBS. After reconstitution, it was aliquoted and stored at -70° C in a manual defrost freezer for up to 6 months. The capture antibody was then diluted to a working concentration of 4.0µg/ml in PBS, without carrier protein.
- **Detection antibody (1 vial):** 3.6µg/ml of biotinylated goat anti-human IL-8/CXCL5 when reconstituted with 1.0ml of Reagent Diluent (see Solutions Required section). After reconstitution, the detection antibody was stored at -70°C in a manual defrost freezer for up to 6 months. The detection antibody was diluted to a working concentration of 20ng/ml in Reagent Diluent.
- **Standard (3 vials):** 100ng/ml of recombinant human IL-8/CXCL5 when reconstituted with 0.5ml of distilled water. The standard was allowed to sit for a minimum of 15 minutes with gentle agitation prior to making dilutions. The reconstituted standard was aliquoted and stored at -70°C for up to 6 months. A seven-point standard curve using 2-fold serial dilutions in Reagent Diluent, and a high standard of 2000 pg/ml was recommended.
- **Streptavidin- horseradish peroxidase (HRP) (1 vial):** 1.0ml of Streptavidin conjugated to horseradish-peroxidase. Streptavidin-HRP was stored at 2-8°C for up to 6 months after initial use. It was diluted to a 1/200 working concentration using Reagent Diluent.

2.8.3.3Interleukin-6 (IL-6) Materials Required for ELISA provided by R&D Systems (150)

The following materials were used and brought to room temperature before use:

- **Capture Antibody (1 vial)** - 360 mg/ml of mouse anti-human IL-6 when reconstituted with 1.0 ml of PBS. After reconstitution, capture antibody was stored at -70° C in a manual defrost freezer for up to 6 months. Capture antibody was diluted to a working concentration of 2.0 mg/ml in PBS4, without carrier protein.
- **Detection Antibody (1 vial)** - 9 mg/ml of biotinylated goat anti-human IL-6 when reconstituted with 1.0 ml of Reagent Diluent (see Solutions Required section). After reconstitution, detection antibody was aliquoted and store at -20° C to -70°C in a manual defrost freezer for up to 6 months. Detection antibody was dilute to a working concentration of 50ng/ml in Reagent Diluent.
- **Standard (1 vial**) - 120ng/ml of recombinant human IL-6 when reconstituted with 0.5ml of distilled water. Allow the standard to sit for a minimum of 15 minutes with gentle agitation prior to making dilutions. The reconstituted standard was aliquoted and stored at -70° C for up to 6 months. A seven-point standard curve using 2-fold serial dilutions in Reagent Diluent, and a high standard of 600pg/ml was recommended.
- **Streptavidin-HRP (1 vial)** - 1.0mL of streptavidin conjugated to horseradish-peroxidase. Streptavidin-HRP was stored at 2-8° C for up to 6 months after initial use. Streptavidin was diluted to the working concentration specified on the vial label (1 in 200 dilution) using Reagent Diluent.

2.8.3.4 CXCL5 Materials Required for ELISA provided by R&D Systems (151)

The following materials were used and brought to room temperature before use:

- **Capture Antibody**- 360 mg/ml of mouse anti-human ENA-78 when reconstituted with 1.0 ml of PBS. After reconstitution, capture antibody was aliquoted and stored at -70° C in a manual defrost freezer for up to 6 months. Capture antibody was diluted to a working concentration of 2.0 mg/ml in PBS, without carrier protein.
- **Detection Antibody**- 18 mg/ml of biotinylated goat anti-human ENA-78 when reconstituted with 1.0 ml of Reagent Diluent (see Solutions Required section). After reconstitution, detection antibody was stored at -70° C in a manual defrost freezer for up to 6 months. Detection antibody was diluted to a working concentration of 100ng/ml in Reagent Diluent.
- **Standard**- Each vial contains 90 ng/ml of recombinant human ENA-78 when reconstituted with 0.5 ml of Reagent Diluent (see Solutions Required section). The standard was allowed to sit for a minimum of 15 minutes with gentle agitation prior to making dilutions. The reconstituted standard was aliquoted and stored at -70° C for up to 2 months. A seven-point standard curve using 2-fold serial dilutions in Reagent Diluent, and a high standard of 1000 pg/ml is recommended.
- **Streptavidin-HRP**- 1.0ml of streptavidin conjugated to horseradish-peroxidase. Streptavidin-HRP was stored at 2-8°C for up to 6 months after initial use. It was diluted to the working concentration specified on the vial label (1 in 200 dilution) using Reagent Diluent.

2.8.3.5 Solutions Required for IL-8, IL-6 and CXCL5 ELISA

The Bovine Serum Albumin (98% (BSA) used to make block buffer and Reagent Diluent must be good quality as this is critical towards the quality of results obtained. This is so that impurities such as proteases, binding proteins, soluble receptors or other substances, which interfere with the detection of certain analytes, are reduced.

The solutions required for ELISA include:

- **Phosphate buffered saline (PBS)**- 137 mM NaCl, 2.7 mM KCl, 8.1 mM Na_2HPO_4, 1.5 mM KH_2PO_4, pH 7.2-7.4, 0.2 μm filtered.
- **Wash buffer**- 0.05% Tween 20 in PBS, pH 7.2-7.4. (R&D Systems Cat # WA126)
- **Block buffer- For CXCL5 and IL-8**: 1% BSA in PBS with 0.05% NaN_3. **For IL-6:** 1% BSA in PBS, pH 7.2-7.4
- **Reagent diluents-** For IL-8: 1% BSA, 0.05% Tween 20 in Tris-buffered Saline (20 mM Trizma base, 150 mM NaCl), pH 7.2-7.4, 0.2 μm filtered. **For CXCL5 and IL-6**: 1% BSA in PBS, pH 7.2-7.4, 0.2 mm filtered.
- **Substrate solution**- 1:1 mixture of Colour Reagent A (H_2O_2) and Colour Reagent B (Tetramethylbenzidine).(R&D Systems Catalog # DY999).
- **Stop solution**- 2 NH_2SO_4 (R&D Systems Catalog #DY994).

2.8.3.6 Interleukin-8, Interleukin-6 and CXCL5 (ENA-78) Plate Preparation(149-151)

Plate Preparation

1. The Capture Antibody was diluted to the working concentration in PBS (Sigma-Aldrich, Sigma pH 7.4) without a carrier protein. The 96-well plate (Thermo Scientific) was then immediately coated with 100µl per well of diluted Capture Antibody. The plate was sealed and incubated overnight at room temperature. For all steps in this protocol fresh reagent reservoir container and pipette tips were used.
2. Each well was aspirated and washed with Wash Buffer. The washes were repeated 2 further times for a total of 3 washes. Washes were carried out with 400µl per well of Wash Buffer using an autowasher (Bio-tek). For good performance complete removal of liquid at each step is essential. After the final wash, the plate was inverted and blotted against paper towels to remove any remaining Wash Buffer.
3. Plates were blocked by adding 300µl of Block Buffer to each well. The plates were then incubated at room temperature for a minimum of 1 hour.
4. Washes were repeated as in step 2. The plate was now ready for sample addition.

2.8.3.7 Assay Procedure (149-151)

1. To each well a 1 in 10 dilution of sample in Reagent Diluent (total volume 100µl) was added. Dilutions were judged empirically. Samples were diluted in reagent diluent so that values could be read and were within the standard curve as the cells produce high levels of IL-8. The levels of IL-6 produced tend to be less so the sample was added directly to the ELISA plate without dilution. For CXCL5 the dilution was 1 in 50. The plate was covered with an adhesive strip and incubated at 1 hour at 37°C with agitation. All samples were done in duplicate and a plate layout recorded.
2. Washes were repeated as in step 2 of the Plate Preparation.
3. Detection Antibody (100µl) diluted in Reagent Diluent was added to each well. The plate was covered with an adhesive strip and incubated for 1 hour at 37°C with agitation.
4. Washes were repeated as in step 2 of the Plate Preparation.
5. A working dilution of Streptavidin-HRP (100µl) was added to each well. The plate was covered and incubated at room temperature for 20 minutes. Avoid placing the plate in direct light.
6. Washes were repeated as in step 2 of the Plate Preparation.
7. Substrate solution (Ultra TMS ELISA, Thermo Scientific) (100µl) was added to each well. The plate was incubated for 20 minutes at room temperature in a drawer so that it was not in contact with direct light.
8. Stop solution (BDH AmalaR)(50µl) was added to each well. The plate was tapped to ensure thorough mixing. The optical density of each well was determined using a microplate reader (Bio-tek) set to 450nm.

The ELISA software, KC Junior was used to record the concentration level of IL-6, IL-8 and CXCL5. The duplicate values for each sample were meand and plotted as a graph.

2.9 RNA Extraction, Reverse Transcription and Real-time PCR

In order for RSV infected samples of A549 cells to be run for real- time PCR, samples must first undergo RNA extraction (isolation) and reverse transcription. The processes leading to real-time PCR are shown in the figure below (Figure 2.1.8).

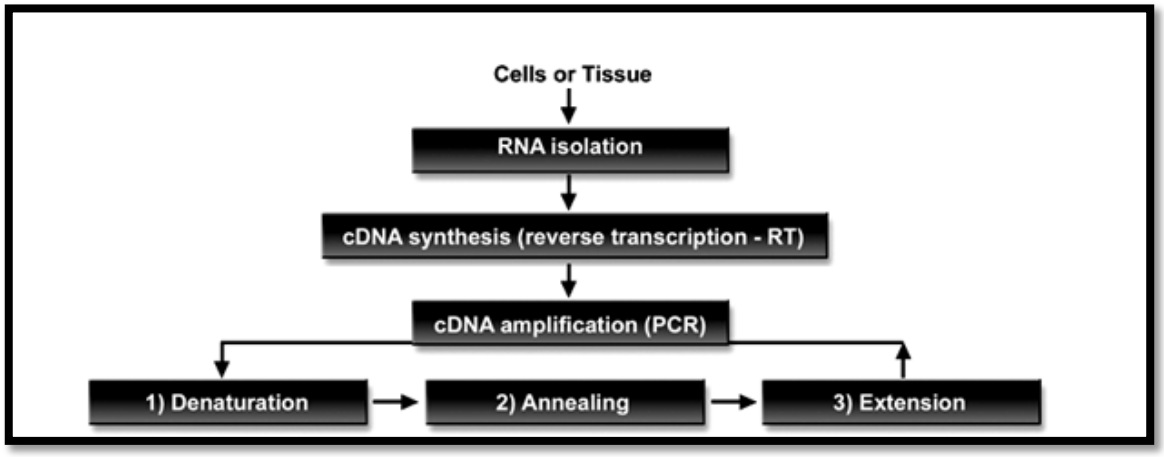

Figure 2.1.8: Summary of steps that lead to PCR (152).

2.9.1 RNA Extraction Protocol

The RNA from RSV infected A549 cells in a 24-well plate were extracted using the Qiagen QIA shredder and RNeasy mini kit. This protocol was modified from Qiagen RNA mini kit (153, 154).

For a 24-well plate containing infected A549 cells (153, 154) :

1. The supernatant was removed from wells.
2. 350µl buffer RLT (guanidine-thiocyanate–containing buffer) (Qiagen)/2-mercaptoethanol (β-ME) (Sigma-Aldrich, Sigma) (10µl β-ME to every 1ml RLT buffer) per well was added to a microcentrifuge tube. (At this point the microcentrifuge tube can be placed in a -70°C fridge and further steps carried out at a later time). This was to remove RNA from the cells. The purpose of RLT buffer was to lyse cells before RNA isolation from cells. The addition of buffer RLT also causes the inactivation of ribonuclease (RNase), ensuring purification of intact RNA. 2-mercaptoethanol is used to eliminate ribonuclease released during cell lysis. Ribonuclease is made up of several disulfide bonds, which make the enzyme very stable, and it is these bonds which 2-

mercaptoethanol reduce and denature irreversibly. This is so that ribonuclease does not digest the RNA during the extraction procedure.

3. All of the 350µl was added to the QIA shredder spin column (Qiagen). The spin column was placed in a 2ml collection tube and spun for 2 minutes at full speed ($13.3x\ 10^4$ rpm or 15,821G). The QIA shredder is a unique biopolymer shredding system in microcentrifuge spin-column format. It homogenises cell or tissue lysate to reduce viscosity. Homogenisation shears the high molecular-weight cellular components to create a homogenous lysate. The QIA shredder is chemically inert and does not bind nucleic acids.
4. The QIA shredder was then discarded. To the sample in the 2ml collecting tube, 350µl of 70% ethanol was added and mixed well by pipetting.
5. All of the contents of the 2 ml collection tube (700µl) were added to the RNeasy spin column (Qiagen) placed in a new 2ml collection tube. This makes up part of the RNeasy procedure where RNA is purified. This technology combines the microspin technology with the selective binding properties of a silica –based membrane. The specialised high salt buffer systems enables up to 100µg of RNA longer than 200 bases to bind to the RNeasy silica membrane. The addition of ethanol was to provide the appropriate binding conditions. When the sample is added to the RNeasy spin column, total RNA binds to the membrane and contaminants are washed away.
6. The contents were then spun at full speed for 15 seconds in the mini-centrifuge at full speed. The flow through was then discarded.
7. Buffer RW1 (700µl)(Qiagen) was then added to the column and the contents spun for 15 seconds at full speed. The flow through was discarded. Buffer RW1 is added to wash the membrane bound RNA.
8. To the column 500µl of RPE (Qiagen) was added to the column. The column was spun for 15 seconds at full speed. The flow through was discarded.
9. Another 500µl of RPE was added to the column. The column was spun for 2 minutes at full speed. Buffer RPE is a concentrated wash buffer for washing membrane bound RNA.
10. The RNeasy spin column was carefully removed from the collection tube, ensuring that it does not contact the flow through. The spin column was placed

in a new 2ml collection tube (the old collection tube containing flow through was discarded). The contents were spun for 1 minute at full speed.

11. The RNeasy spin column was placed in new 1.5ml microcentrifuge tube.
12. RNAse free water (40µl) (Fisher) was added directly to the membrane and left for 2 minutes. The contents were spun at full speed to elute RNA.
13. The RNA was placed immediately on ice and transferred to the -70°C freezer or measured for the quality of RNA using nanometry. When it was time for reverse transcription the samples were placed on ice. A summary diagram of the process of RNA extraction has been provided (Figure 2.1.9)

2.9.2 Quantification of RNA Purification

Nucleic acid is quantified using a spectrophotometer. Analysis of RNA purity is by the NanoDrop ND-1000.RNA has an absorption maximum of at 260 nanometres (nm). The ratio of absorption at 260 and 280nm is used to assess RNA purity of RNA preparation. Pure RNA has a ratio of absorption between 1.8 and 2.0. An A260 reading of 1.0 is equivalent to 40µg/ml of RNA. The optical density at 260 nm is used to determine the RNA concentration in a solution (155).

After RNA had been obtained, the quality of the RNA was measured by nanodrop by carrying out the following(155):

1. The computer and nanodrop was turned on.
2. The nanodrop software was opened and nucleic acid selected.
3. When prompted 1µl RNAse free water (Fisher) and OK button selected.
4. The sample type was changed to RNA 40
5. 1µl RNAse free water was added and the blank button selected.
6. The water was wiped from the nanometer and with tissue paper
7. 1µl of the sample was added to the nanometer and measure button selected.
8. Afterward 1µl RNAse free water was added and the lid closed.
9. Wipe between samples.
10. When all of the samples have been measured select ‘show report’ then ‘reports-save reports’ and finally select ‘export table.’

Values taken from a set of samples measured by the nanometer are shown in the table below (Table 2.3). This set of samples was from an RSV time-course experiment.

Table 2.3: Nanometry Values

Duration of RSV Infection	Ratio of Absorption
0 Hours	1.94
2 Hours	2.13
4 Hours	2.13
6 Hours	2.12
24 Hours	2.15
48 Hours	2.15

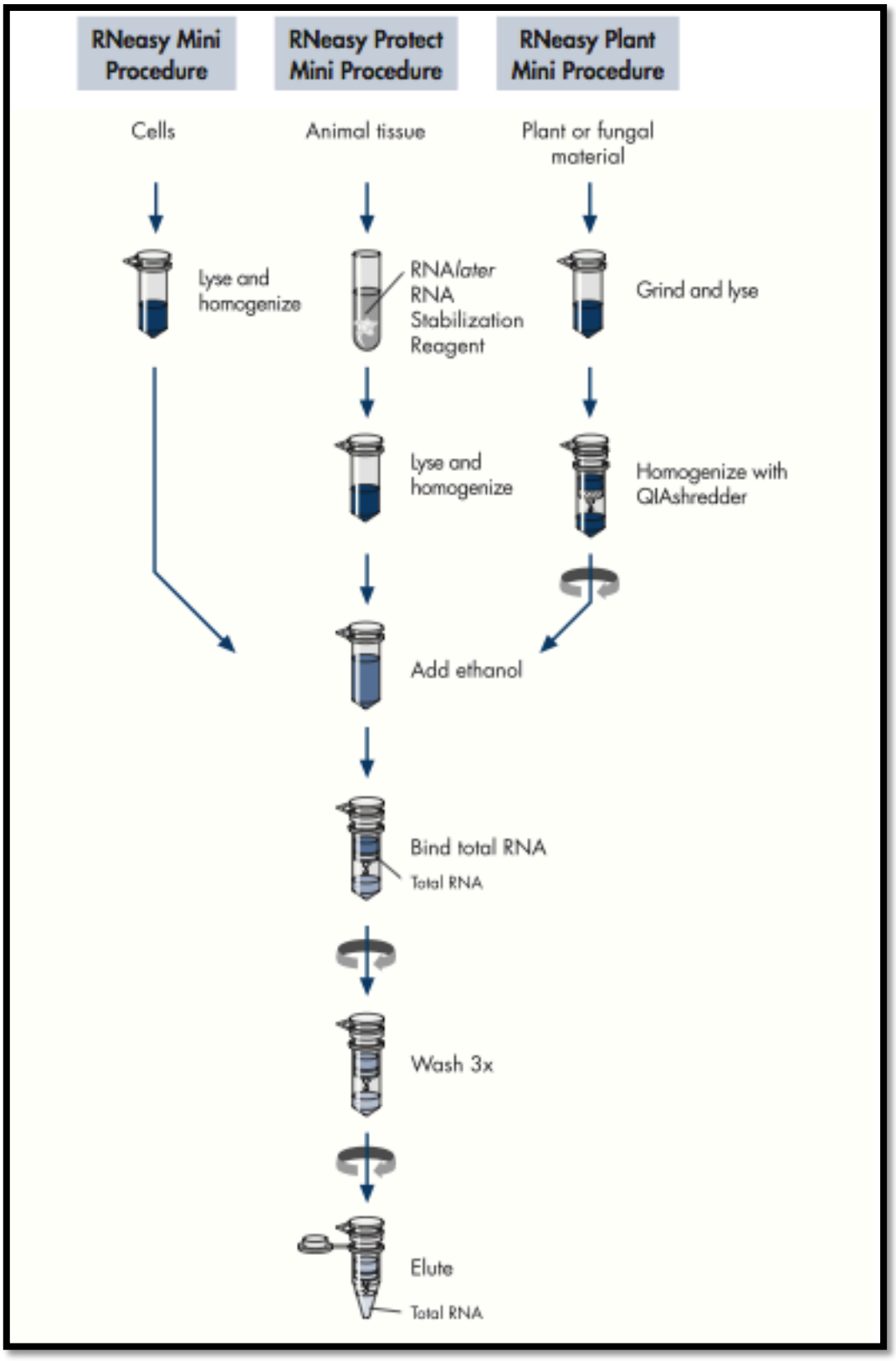

Figure 2.1.9: RNA extraction basic outline. The method applied here is the 'RNeasy Mini Procedure (154).' Taken from Qiagen RNeasy Mini Handbook.

2.9.3 Reverse Transcription

The Reverse Transcriptase buffer (10xRT buffer), Random Primer, Deoxyribonucleotide Triphosphates (dNTP) and Reverse Transcriptase (RT) were provided in a 'High Capacity cDNA Reverse Transcription Kit' supplied by Applied Biosystems. To each microcentrifuge tube the following was added in this order:

1. 10xRT buffer (2μl) for ensuring that the mixture is at the correct pH for reverse transcription to take place.
2. Random Primer (2μl) used in real-time PCR for preparing the first strand of cDNA.
3. Deoxyribonucleotide triphosphates (dNTP (1μl) are used to generate cDNA during PCR. Highly purified dNTP is required to achieve accurate results with real-time PCR.
4. RNA (10μl), which is the sample RNA, obtained using the Qiagen RNA extraction protocol.
5. Water (4.5μl) (Sigma-Aldrich, Sigma Molecular Biology Reagent)
6. The contents of the tubes were the spun down in a microcentrifuge tube for 10 seconds at 13.3x 10^4 rpm.
7. The reverse transcriptase was added directly to the mixture with efficient mixing. This enzyme should be kept in the freezer just before use to prevent denaturing. All other materials that have been used for reverse transcription were kept on ice.
8. To provide the ideal conditions for the reaction to occur, the microcentrifuge tubes were placed in heat blocks at 37°C.

2.9.4 Making up the RSV and L32 probe

Ribosomal protein L32 (RL32) is a human protein coded by the RPL32 gene. It is present in all cells and was the housekeeping gene in this experiment. The other probe used was the RSV probe, which measured the level of human RSV N gene expression.

A figure is provided for the primers used for RSV N gene detection (Figure 2.2.1) (156).

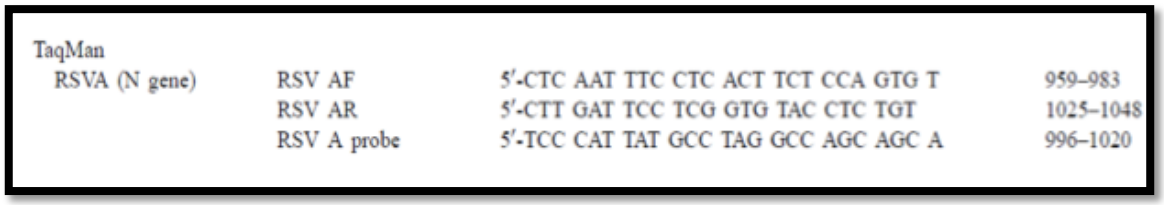

TaqMan			
RSVA (N gene)	RSV AF	5′-CTC AAT TTC CTC ACT TCT CCA GTG T	959–983
	RSV AR	5′-CTT GAT TCC TCG GTG TAC CTC TGT	1025–1048
	RSV A probe	5′-TCC CAT TAT GCC TAG GCC AGC AGC A	996–1020

Figure 2.2.1: The primers used for PCR RSV N gene expression. These are the primer sequences that are used for detection of RSV N gene expression by real-time PCR. It shows the primer and probe names, sequences and nucleotide position for each (156).

The RSV and L32 (bought from Life Technologies as pre-developed assay) probes were provide by Sigma chemical company and are custom synthesised. The RSV probe was designed by Dewhurst-Maridor and made by Sigma (156). The RSV probe was labelled with FAM and TAMRA dyes. The RSV primers were synthesised by Sigma. The L32 probe was already made ready for addition to the Taqman® Gene Expression Master Mix. To make the RSV probe, the following was added to a microcentrifuge tube:

- 10μl of RSV AF (forward)
- 10μl of RSV AR (reverse)
- 40μl of RSV FAM
- 40μl of RNAse free water (Fisher)

Both the L32 and RSV probes were mixed with Taqman® Gene Expression Master Mix (Life Technologies). The Taqman® Gene Expression Master Mix contains buffers, dNTPs, internal reference dye (dye that provides an internal reference to which the reporter dye signal can be normalized during data analysis) and hot-start DNA polymerase that is essential for powering real-time PCR(157).

In one tube the RSV probe was mixed with Taqman® Gene Expression Master Mix. In the other microcentrifuge tube the L32 probe was mixed with Taqman master mix. For example if the probes were made for 6 samples then in each microcentrifuge tube there would be 160 Taqman® Gene Expression Master Mix and 16 of RSV or L32 probe. These volumes chosen were in surplus to ensure that there was enough Taqman master mix and probes for each sample, accounting for any pippetting errors.

2.9.5 Polymerase Chain Reaction (PCR)

2.9.5.1 Background

Polymerase Chain Reaction (PCR) was developed by Kary Mullis in 1983 and is used to amplify copies of a chain of DNA in order to produce thousands of copies of a particular DNA sequence (158). The technique that was applied in this project was real-time PCR. This technique is also referred to as quantitative real-time PCR (qPCR), which was first made commercially available to Applied Biosystems in 1996 (159).

2.4.5.2 Real-Time PCR

Real-time PCR (is used for a broad range of applications including genotyping, pathogen detection, single nucleopeptide (SNP) analysis, pathogen detection, and quantitative gene expression analysis. The combination of real-time polymerase chain reaction with reverse transcription enables quantification of messenger RNA (mRNA) and microRNA (miRNA)(156).

Real-time PCR measures amplification of DNA strands in real-time without the need to process products using gel-based analysis after PCR has taken place, as seen in traditional PCR. Real-time PCR is more precise than traditional PCR and includes ultra-rapid cycling, which takes 30 minutes to 2 hours. Another benefit of real-time PCR is that it allows the researcher to better determine the amount of DNA in the sample before the amplification by PCR (160).

A summary of the advantages of real-time PCR are (161):

1. Increased dynamic range of detection.
2. No post-PCR processing.
3. Detection is capable down to a 2-fold change.
4. Collects data in the exponential growth phase of PCR.
5. An increase in reporter fluorescent signal is directly proportional to the number of amplicons generated.
6. The cleaved probe provides a permanent record amplification of an amplicon.

During a PCR reaction the sample DNA made from RNA taken from sample cells undergoes amplification. Amplification occurs in cycles during which the original DNA serves as a template for new copies of DNA to made. In real-time PCR there is a maximum of 40 amplification cycles (Figure 3.1). Amplification is exponential because for each cycle, the DNA made in previous cycle acts as a template. Real-time PCR reactions are characterised by the point in time during cycling when amplification of a target is first detected than the amount of target accumulated. The higher the starting copy of nucleic acid, the sooner the significant fluorescence increase is observed(162).

Real-time PCR can be used to detect the level of RSV N gene expression from samples that have had RSV added. Samples, which have a greater RSV MOI, would be expected to have greater levels of RSV N gene expression, as more RSV particles would have been added to a set number of cells. All samples analysed by PCR were done in duplicate. After the data was collected these values were meand. The purpose of carrying out PCR is to provide evidence consistent with RSV infection of A549 cells indicating that experiments had been carried out accurately.

2.4.5.3 The Principles of the Polymerase Chain Reaction

There are four phases in total throughout the PCR amplification(159):

1. **Baseline** – during this stage exponential amplification is taking place despite no signal being released. The amplification levels are below those that can be detected by the Real-Time PCR.
2. **Exponential** –the product should double exactly per cycle to produce a number of amplicons assuming that the asay is a 100% efficient. During this phase the real-time PCR quantifies the amplicons.
3. **Linear**–as the reaction substances are consumed the efficiency of amplification is reduced.
4. **Plateau** – reaction ceases and no more products synthesised for remaining cycles.

There are three components to the Real-Time PCR instrument (159):

1. **Light source** – establishes receptor dye range detected by instrument.
2. **Detection system**– determines the spectral range and sensitivity of assay.
3. **Thermocycling mechanism** – monitors speed that assay is run and temperature changes between each well.

The threshold level is the point at which the fluorescent signal is detected, above the background. The threshold level line is set during the exponential phase. Once the sample reaches this level, the cycle number is quantified and this is the result obtained from the real-time PCR – Cycle Threshold (Ct) (159).

2.4.5.4 Loading PCR plate

The microcentrifuge tubes were taken out of the heat block and placed temporarily on ice. Water (50µl) (Sigma pure water, molecular biology reagent) was added to each sample so that there would be enough of each sample to load into each well of the 96-well PCR plate (Starlab).

In each PCR well the following was added:

- 1.25µl of probe (RSV or L32).
- 12.5µl of Taqman® Gene Expression Master Mix.
- 11.25µl of sample diluted in RNase free water.

The first 2 rows of L32 were allocated for the L32 probe and the next 2 for the RSV probe. Therefore, both samples for each probe were done in duplicate.

An example diagram of the layout of PCR plate is shown below where the 3 RNA samples were taken from control (non-infected/NI) A59 cells sample, RSV infected cells (RSV) and RSV infected cell treated with Palivizumab (P) (Figure 2.2.2).

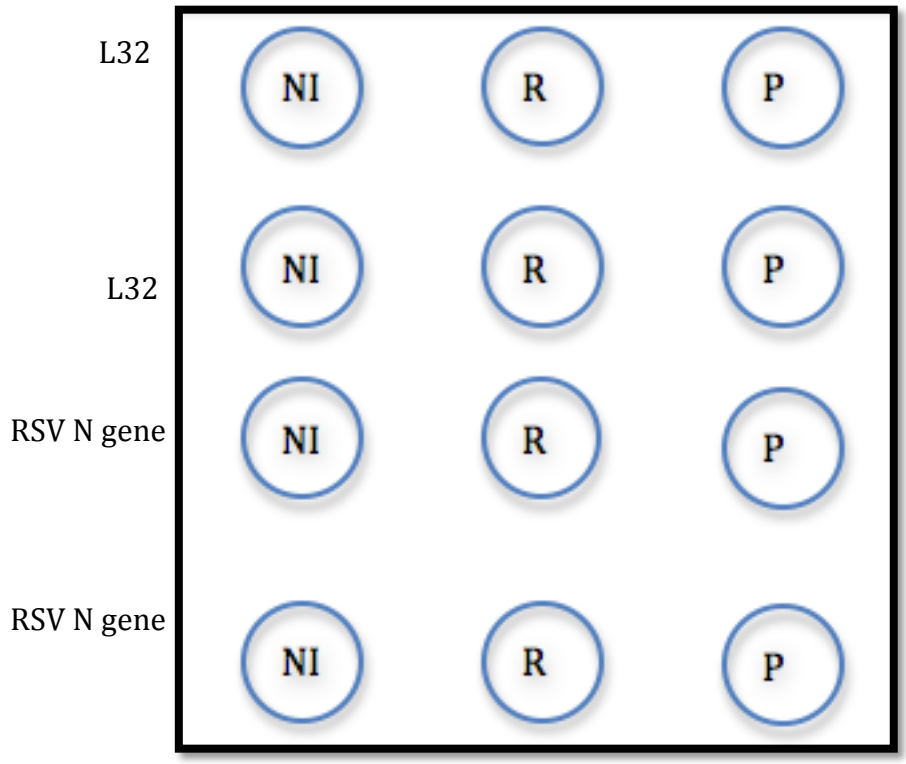

Figure 2.2.2: Example layout of PCR plate where NI= control, R= RSV infected, P = palivizumab added to RSV.

The PCR plate was covered with a film and the plate was spun to ensure that all of the contents were at the bottom of the w ells. The plate was put into an Applied Biosystems 7300 Real-Time PCR reader. Real-time PCR computer software provided a plate layout where each sample and the corresponding probe added was labelled. The correct temperature cycle for the PCR to work efficiently was set. This depended on the TaqMan® Gene Expression Master Mix used which was from Applied Biosystems. The real-time PCR was run for 40 cycles, for approximately 2-3 hours. The amplification curves were monitored every 30 minutes. An example, of the amplification curves obtained from real-time PCR is shown (Figure 2.2.3).

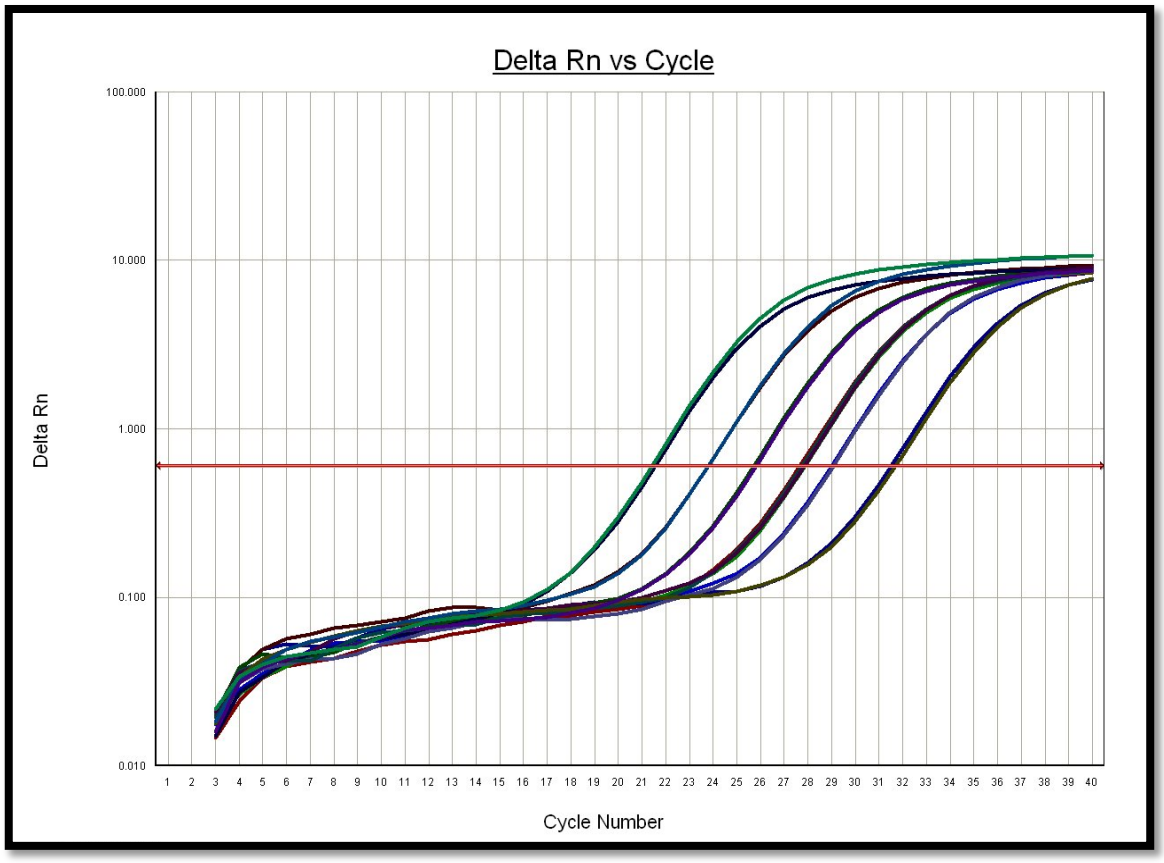

Figure 2.2.3 Measurement of RSV N gene expression by real-time PCR. Explanation provided by Life Technologies (163). Each line represents a samples amplification curve. The x-axis shows the number of amplification cycles that each sample has undergone. The y-axis, delta Rn is the magnitude of the signal generated by a given set of PCR conditions. The horizontal red line is the threshold. The threshold line can be set arbitrarily but must be set in a region associated with exponential growth of PCR product. This region should be where the precision of the replicates is highest, which is usually the middle of the exponential phase as shown. Once the threshold line has been set, then the Ct (threshold cycle) value can be obtained for each sample. The Ct is the intersection between the amplification curve and threshold line to give a cycle number. It is the Ct values that are used to calculate the level of RSV N gene expression (163, 164).

2.4.5.5 PCR RSV N Gene Data Analysis

The RSV N gene expression based on RSV ct values was calculated in 2 steps:

1) The mean Ct value for L32 expression of the sample minus the mean ct value for RSV expression of the same sample.

This was done to normalise the PCR data. This calculation allowed correction for some of the samples potentially having more mRNA and therefore cDNA within them.

2) 2 to the power of n, where n = value obtained from step 1.

This is the conversion from Ct values to fold differences. This particular calculation is because every cycle is a 2-fold change.

3. Results

3.1 Overview of Experiments Carried Out

The initial aim of this investigation was to determine whether RNF168 expression was affected by RSV infection of A549 cells. A preliminary RSV MOI titration experiment was carried out at 4 hours post RSV infection to determine if RSV was affecting RNF168 expression. Changes in expression were noted resulting in this experiment being repeated 2 further times. To provide supporting evidence that A549 cells had been productively infected with RSV, the samples in each experiment were analysed for RSV N gene expression by real-time PCR. Further evidence to support infection was provided by measuring the concentration levels of IL-6 and IL-8 in samples by Sandwich ELISA. To show that IL-8 was being released from cells in response to RSV infection, the concentration of IL-8 was compared to the IL-8 concentration of the RSV prep added to A549 cells.

RSV MOI titration experiments were then carried out at 24 hours to see what effect a comparatively longer duration of infection would have on RNF168 expression. 24 hours RSV experiments were repeated 3 times. To provide supporting evidence that A549 cells had been correctly infected with RSV, the samples in each experiment were analysed for RSV N gene expression by real-time PCR. Further evidence to support infection was provided by measuring the concentration levels of IL-6 and IL-8 in samples. The RNF168 expression values for the three experiments were meand and standard error of the mean calculated. The RNF168 expression values for all 3 experiments were then calculated relative to the control. The primary purpose of 4 and 24 hours experiments were to determine whether there was a relationship between RSV MOI and RNF168 expression at these time points.

To provide supporting evidence for both 4 and 24 hours titration experiments a RSV infection time-course was done. This was primarily to identify if there was a relationship between duration of RSV infection and RNF168 expression. Changes in RNF168 expression had been seen at both 4 and 24 hours for cells with a RSV MOI of 1:1. As a result, cells were infected with RSV at MOI 1:1 and protein samples harvested at time points of 0, 2, 4, 6, 24 and 48 hours of RSV infection. 0 hour was a starting control where the cells had not been infected with RSV and was harvested immediately after all other samples of A549 cell had been infected. There was a paired control for all other time points of RSV infection.

As changes in RNF168 expression were seen in RSV infected cells further investigations were carried out with IFN-β and polyI:C. This was to gain an understanding of the mechanism by which RNF168 expression was affected by RSV. Two titration experiments involving IFN-β stimulation at varying concentrations for 4 and 24 hours were carried out 3 times each. The concentration of IFN-β used ranged from 1-100ng. This was to see whether RNF168 expression was affected by the time and concentration of IFN-β stimulation. Furthermore, any change in RNF168 expression may suggest a relationship between IFN-β and RSV infection at the same time points. To provide further supporting evidence for a possible relationship between duration of IFN-β stimulation and RNF168 expression an IFN-β time-course experiment was done. In this experiment cells stimulated with IFN-β were harvested at 0, 2, 4, 6, 24 and 48 hours. 0 hours was taken to be a starting control where the cells were not stimulated with IFN-β and harvested immediately after all other sample cells had undergone IFN-β stimulation. Every other time point had a paired control. Samples were used to run a Western Blot. Therefore, evidence from these experiments could implicate IFN-β in the RNF168 expression pathway.

A time-course experiment was carried out with polyI:C. A549 cells were stimulated with 50ng/ml polyI:C and harvested at 0, 2, 4, 6, 24 and 48 hours. Again 0 hours was taken to be a starting control where the cells were not stimulated with polyI:C and harvested immediately after all other sample cells had undergone polyI:C stimulation. This experiment time point had paired control. Samples were used to run a Western Blot to measure RNF168 expression. This experiment involving polyI:C was carried out to see if TLR3 was implicated in the RNF168 pathway when cells are infected with RSV.

To show that RSV was responsible for affecting RNF168 expression directly and not any other factor, A549 cells were treated with palivizumab and RSV (MOI 1:1) for 24 hours. This sample was compared to a sample infected with RSV MOI 1:1 for 24 hours and a 24 hours control sample through measuring RSV N gene expression and Western Blot analysis for RNF168 expression.

It should be noted that when measuring RNF168 expression in all experiments in this investigation, the values recorded were relative to the loading control β-actin. The values for RNF168 expression from experiments that had been carried out 3 times were meand to given an overall interpretation of how RSV or IFN-β affected RNF168 expression. The standard error of the mean was calculated to establish the precision of values obtained. For all experiments, which measured RNF168 expression that had been carried out 3 times, RNF168, expression values were calculated relative to the control. As a result, the control value becomes 1, which in this case was taken to be 100%. The percentage increase or decrease in RNF168 expression could then be determined relative to the control.

The samples from the same experiment for 4 hours post RSV infection were analysed for IL-8 and IL-6 concentrations in addition to RSV N gene expression and RNF168 expression (Table 3.1.1). One set of samples from the same experiment for 24 hours post RSV infection was measured for IL-8 and IL-6 concentrations in addition to RSV N gene expression and RNF168 expression. The same samples in RSV time-course experiment was analysed for IL-8 concentration, RSV N gene expression and RNF168 expression.

A CXCL5 Sandwich ELISA was carried out for supernatants taken from A549 cells that had RSV time-course infection for time point 0, 2, 4, 6, 24 and 48 hours. Again time 0 hours was a starting control and was harvested immediately after all other samples had undergone RSV infection. Each time point had a paired control to see whether time itself was influencing the amount of CXCL5 released from A549 cells.

Statistical analysis was done by Student T Test (two-tailed) to determine whether there were any statistically significant differences between the control and infected or stimulated samples. Statistical analysis was carried out on experiment that had been carried out 3 times, which were:

- 4 hours RSV titration data
- 4 hours IFN-β data
- 4 hours real-time PCR data
- 4 hours IL-6 data
- 4 hours IL-8 data
- 24 hours RSV data
- 24 hours IFN-β data

3.2 Measurement of RNF168 at 4 hours Post Infection

A total of 3 experiments were carried out where the same samples in each experiment underwent real-time PCR, Sandwich ELISA and Western blot analysis. The table below links the data obtained for each experiment with regards to these techniques.

Table 3.1.1: Real-time PCR, Sandwich ELISA and Western Blot Experiments for each Sample

Experiment	PCR	Sandwich Elisa (IL-6)	Sandwich ELISA (IL8)	Western Blot for RNF168 Expression	RNF168 Expression Relative to Control
1	Figure (a)	Figure (a)	Figure (a)	Figure (a)	Figure (a)
2	Figure (b)	Figure (b)	Figure (b)	Figure (b)	Figure (b)
3	Figure (c)	Figure (c)	Figure (c)	Figure (c)	Figure (c)

When comparing the data from all of the different techniques applied it was clear that the cells were being infected with productively for all 3 experiments. This was exhibited by high levels concentration of Il-8 and IL-6 as well as high levels of RSV N gene expression for samples infected with high RSV MOI in comparison to controls in each experiment.

3.2.1. The Effect of RSV Infection of A594 cells for 4 hours on RSV N Gene Expression

RNA harvested from samples that had undergone a 4 hours RSV MOI titration were run on real-time PCR in duplicate for RSV N gene and L32 a housekeeping gene. The Ct values derived from each sample duplicate are shown in the table below (Tables 3.3 and 3.4).

Table 3.1.2: Step 1 Calculate the Mean L32 Ct values for 4 hours RSV MOI Titration Experiment

Multiplicity of Infection of RSV particles to A549 cell (MOI) where NI=non-infected control	1-L32 Ct Values	2-L32 Ct Values	Mean L32 Ct values
NI	22.93	21.79	22.36
0.025	22.94	22.62	22.79
0.25	22.17	21.42	21.80
0.5	22.78	20.57	21.68
1	21.92	19.44	20.68

Table 3.1.3: Step 2 Calculate the Mean RSV N gene Ct values for 4 hours RSV MOI Titration Experiment

Multiplicity of Infection of RSV particles to A549 cell (MOI) where NI= non-infected control	1-RSV N gene Ct Value	2-RSV N gene Ct Value	Mean RSV N gene Ct Value
NI	0	0	0
0.025	36.28	27.45	31.86
0.25	30.63	23.59	27.11
0.5	26.40	21.68	24.04
1	24.25	19.89	22.07

The RSV values are subtracted from the L32 Ct mean values. This was to determine the level of true RSV N gene expression for each sample. These values were then inputted as the n value when calculating 2^n. This was done to account for the exponential growth of the sample every amplification cycle (Table 3.5).

Table 3.1.4: Calculations for the Relative Expression of RSV N Gene to L32 for 4 hours RSV MOI Titration Experiment 1 (Figure 3.1.1 (c))

Multiplicity of Infection (MOI) where NI=Non-infected	Step 1: Mean RSV	Step 2: Mean L32	Step 3: L32-RSV (n value)	2^n
NI	0	22.36	-22.36	1.85×10^{-7}
0.025	31.86	22.78	-9.07	1.84×10^{-3}
0.25	27.11	21.80	-5.31	0.03
0.5	24.04	21.68	-2.36	0.19
1	22.07	20.68	-1.38	0.38

The 2^n values obtained from the table above there plotted (Figure 3.1.1 (c)). The 2^n values were plotted on graphs (3.1.1).

(a)

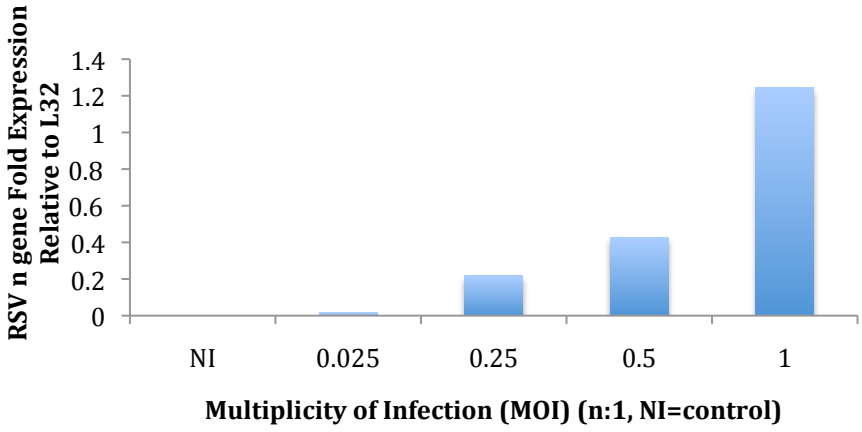

(b)

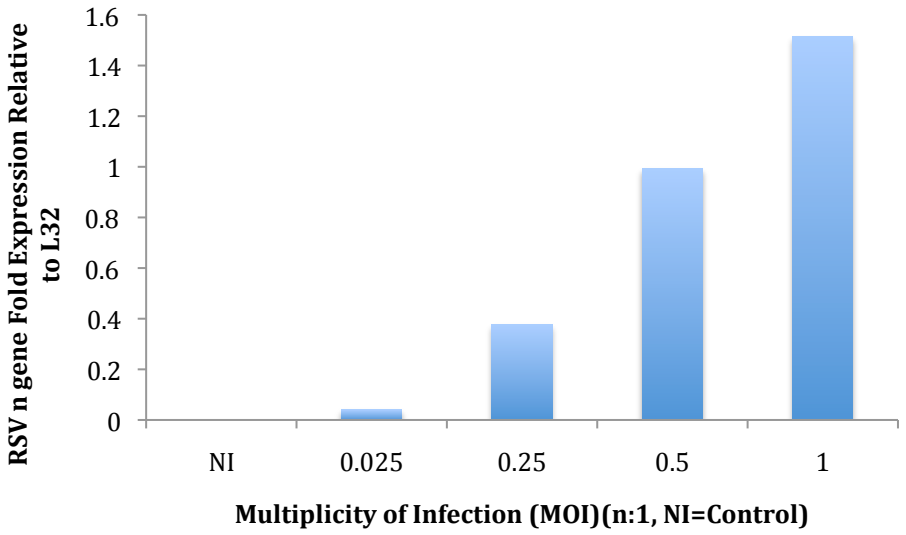

(c)

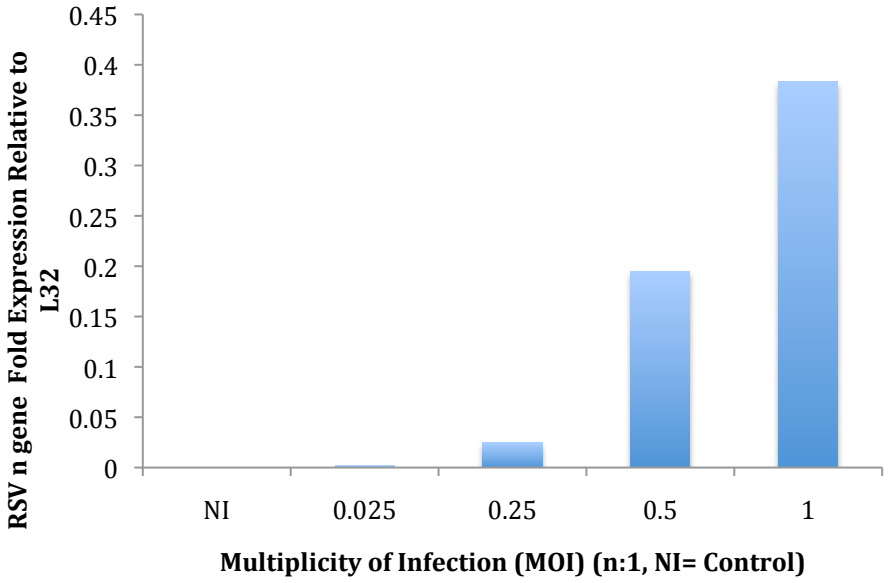

Figure 3.1.1: RSV N gene expression in A549 cells undergoing RSV infection for 4 hours. A549 cells were infected with RSV of increasing MOI for 4 hours. The RNA was harvested from these samples and real-time PCR carried out. This experiment was carried out 3 times.

All 3 experiments have shown increasing RSV infection with increasing MOI. Controls (NI) gave the lowest level of RSV N gene expression in all 3 experiments (Figure 3.1.1). An MOI of 1:1 gave the highest value of RSV N gene expression in all 3 experiments (Figure 3.1.1). However, the range of values varied between experiments with the highest values ranging from a 0.38 in one experiment (Figure 3.1.1 (c)) to 1.52 in another (Figure 3.1.1 (b)).

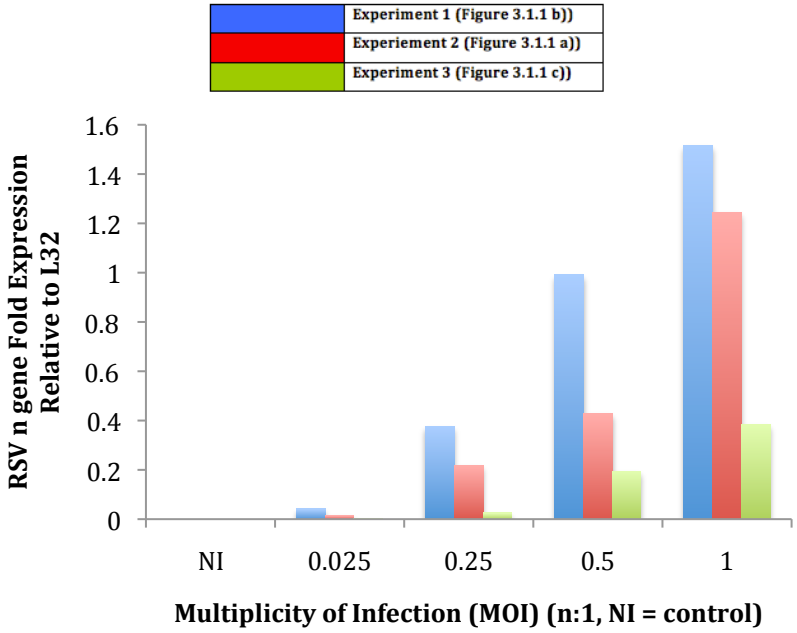

Figure 3.1.2: Combined graph of all three experiments (Figure 3.1.1) of RSV infection of A549 cells for 4 hours. The results of the 3 experiments were combined into a graph to showing a clear comparison between the values obtained.

Experiment 1 recorded the highest level of RSV N gene expression whereas experiment 3 had the lowest levels across all samples (Figure 3.1.2). The control gave the lowest level of RSV N gene expression in all 3 experiments (Figure 3.1.2). An MOI of 1:1 gave the highest value of RSV N gene expression in all three experiments (Figure 3.1.2). At MOI 1:1 the range of values varied between experiments with the highest values ranging from a 0.38 in experiment 3 to 1.51 in experiment 1.

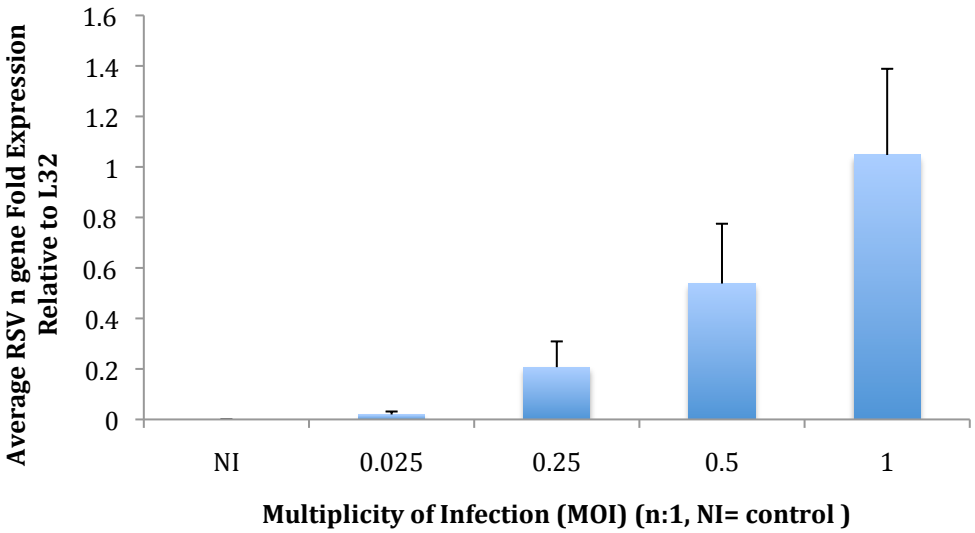

Figure 3.1.3: **PCR data showing mean of 3 experiments of RSV N gene expression for A549 cells infected with RSV for 4 hours.** An mean of all three experiments was calculated with precision noted by standard error of the mean error bars.

Table 3.1.5: P-values for 4 Hours RSV infections to determine whether there was any statistical significant ($p<0.05$) difference between samples and the control for RSV N gene expression

RSV MOI (n:1)	P Value
0.025:1	0.24
0.25:1	0.18
0.5:1	0.15
1:1	0.09

Mean values show that as the MOI increases the level of RSV N gene expression increases. The lowest level of RSV N gene expression is in the control at 7.9×10^{-5}. The highest value was at MOI 1:1 at 1.04. The level of accuracy of experiments decreases with MOI as shown by the standard error bars increasing in size (Figure 3.1.3). Therefore, the MOI of 1:1 value is the least precise given that it has the largest standard error of the mean value. The difference in RSV N gene expression for the control in comparison to infected samples is not statistically significant ($p<0.05$) (Table 3.1.5). The greatest difference amongst infected samples for RSV N gene expression in comparison to the control was RSV MOI 1:1 ($p=0.09$) (Table 3.1.5).

3.2.2 Effect of 4 Hours Post RSV Infection on Interleukin- 6 (IL-6) Concentration Levels

The following table shows the numerical values IL-6 concentration (pg/ml) taken from a Sandwich ELISA of A549 cells infected at 4 hours (table 3.6).

Table 3.1.6: Example of Sandwich ELISA IL-6 Concentration Values for 4 hours RSV Infection

Multiplicity of Infection (1:n) (Where NI is non-infected cells)	Result 1 IL-6 Concentration (pg/ml)	Result 2 IL-6 Concentration (pg/ml)	Mean (pg/ml)
NI	16.60	11.26	13.93
0.025	78.90	64.55	71.73
0.25	500.89	486.79	493.84
0.5	930.43	937.50	933.97
1	1341.13	1494.45	1417.79

Values such as these are plotted on graphs (Figure 3.1.7).

(a)

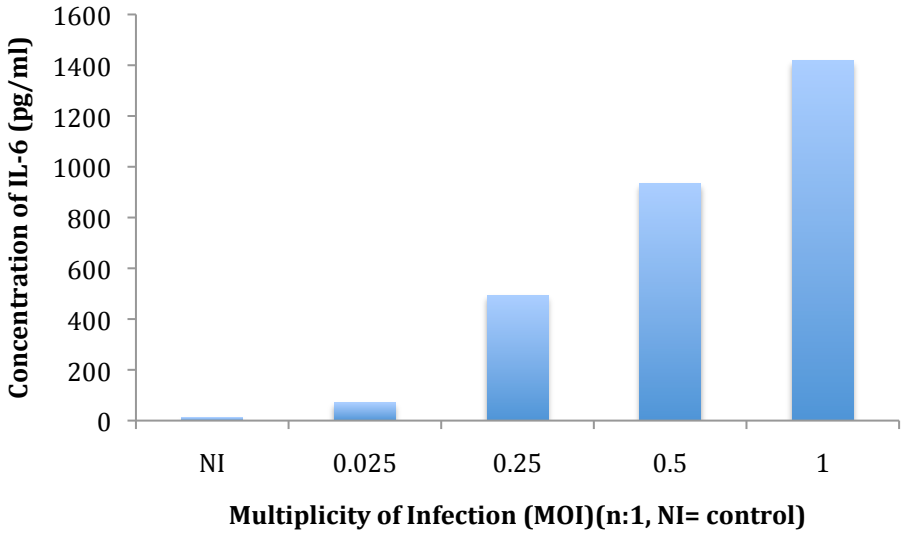

(b)

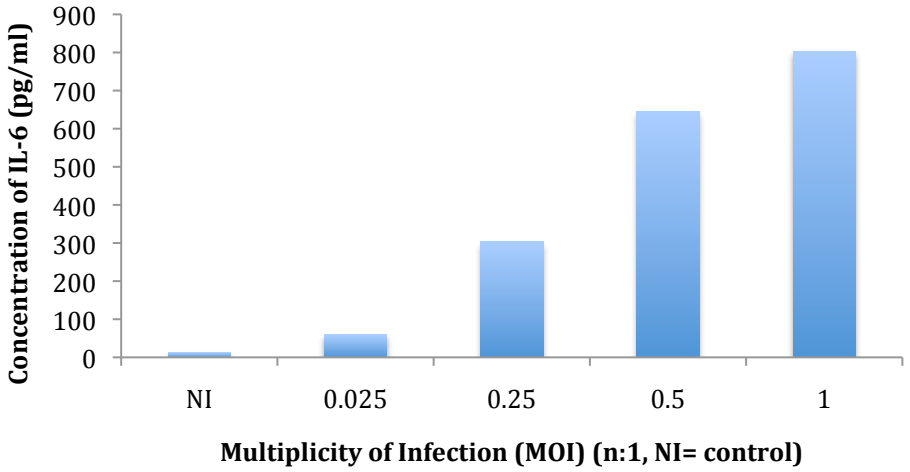

(c)

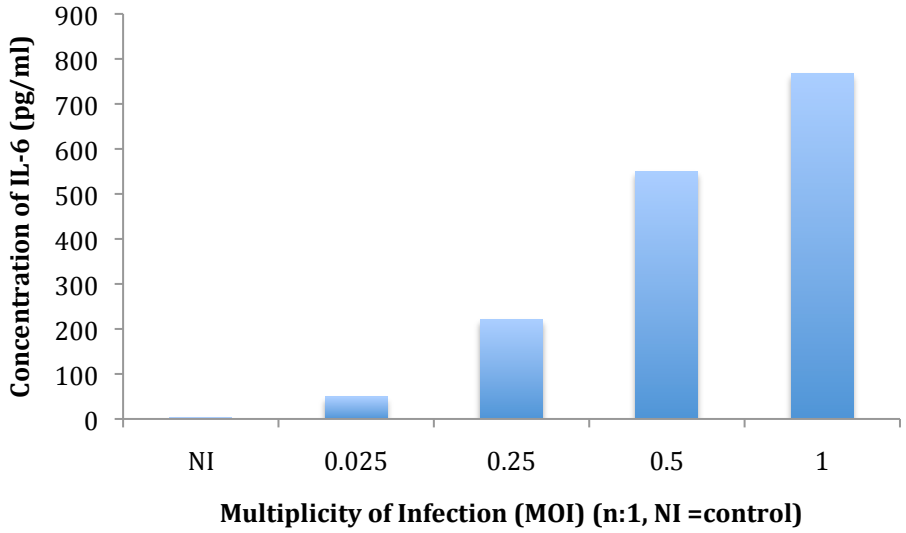

Figure 3.1.4: The concentration levels of IL-6 produced from 4 hours RSV infected A549 cells. A549 cells were grown in 24-well plates and infected with RSV at MOI titration experiment for 4 hours duration. This experiment was carried out 3 times. The supernatant from these samples was taken and used to run a Sandwich ELISA.

In all 3 experiments as the MOI increases, the concentration of IL-6 increases (Figure 3.1.4). The lowest concentration of IL-6 was present in the control in all 3 experiments (Figure 3.1.4). The concentration of IL-6 is greater in all RSV infected samples in comparison to the controls (Figure 3.1.4). The highest concentration of IL-6 is seen in at MOI 1:1 ranging from 766.55 (Figure 3.1.4 (c)) to 1417.79 pg/ml (Figure 3.1.4 (a)).

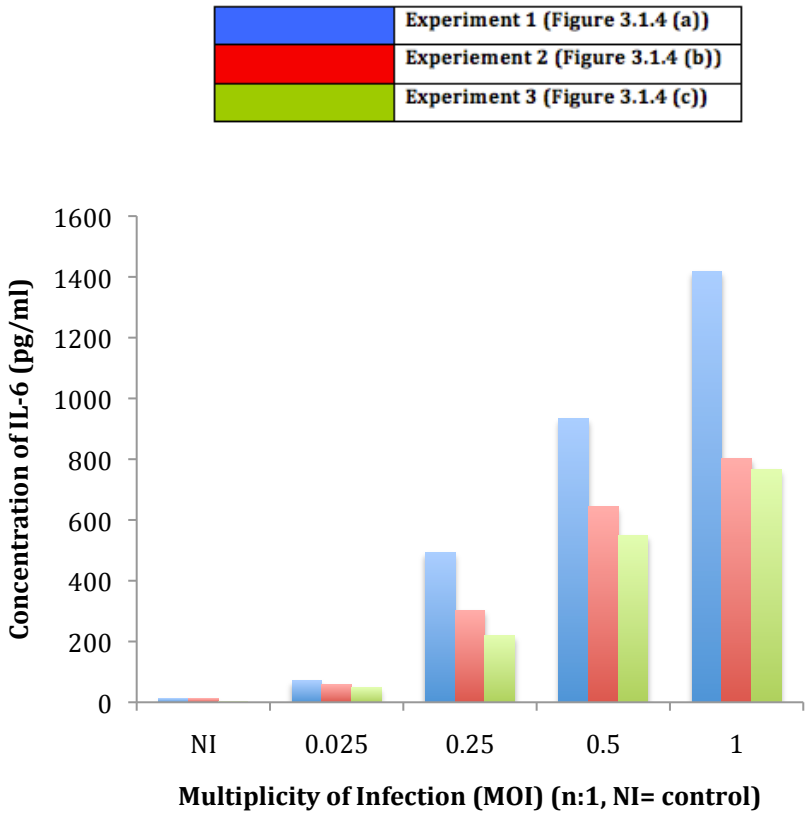

Figure 3.1.5: Combined graph of 3 identical experiments (Figure 3.1.4) showing the levels of IL-6 produced from 4 hours RSV infected A549 cells. Values of the 3 experiments were combined together to provide a clear comparison between data obtained.

When comparing experiments to one another the range of IL-6 concentrations vary across experiments (Figure 3.1.5). The highest values were in experiment 1 whereas the lowest values were in experiment 3 across all samples (Figure 3.1.5).

The highest value in all 3 experiments is recorded at MOI 1:1,ranging from 1417.79pg/ml (experiment 1) to 766.54pg/ml (experiment 3) (Figure 3.1.5). The lowest values across all 3 experiments are recorded for the control (Figure 3.1.5).

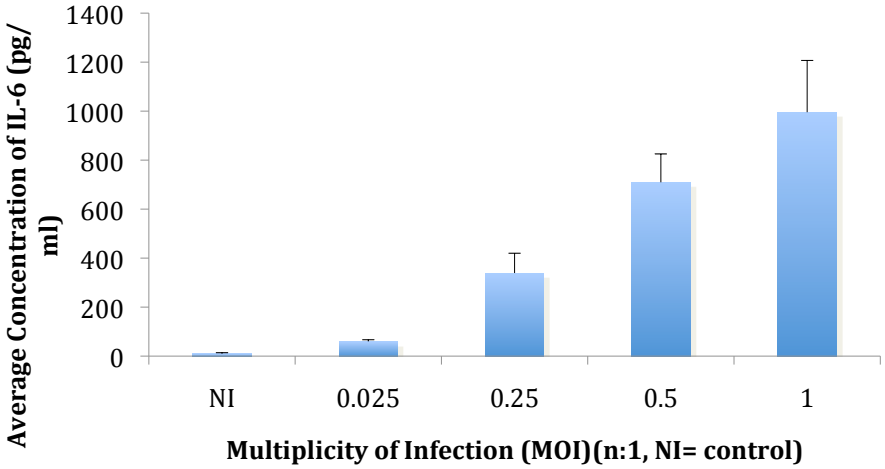

Figure 3.1.6: Mean IL-6 values taken for all three experiments (Figure 3.1.4.) where A549 cells undergo 4 hours RSV infection with standard error bars. An mean of the experiments was taken with standard error calculated to determine the accuracy of the experiments carried out.

Table 3.1.7: P-values for IL-6 to determine whether there was any statistical significant ($p<0.05$) difference between samples and the control

RSV MOI (n:1)	P Value
0.025:1	0.006
0.25:1	0.052
0.5:1	0.025
1:1	0.042

As RSV MOI increases, the concentration of IL-6 increases (Figure 3.1.6). All RSV infected samples have a greater concentration of IL-6 than the control, which had the lowest levels (Figure 3.1.6). The lowest level for the control is 10.35 and the highest value at MOI 1:1 995.64 (Figure 3.1.6). The precision of the values obtained decreases as MOI increases as shown by the size of the standard error bars which were the largest at MOI 1:1 and the least accurate value (Figure 3.1.6).

In comparison to the control, the IL-6 concentration levels are significantly greater ($p<0.05$) at RSV MOIs 0.025:1 ($p=0.006$), 0.5:1($p=0.025$) and 1:1 ($p=0.042$) (Table 3.1.7).

3.2.3 Effect of 4 Hours Post RSV Infection on Interleukin- 8 (IL-8) Concentration Levels

Table 3.1.8: Example of Sandwich ELISA IL-8 Concentration Values for 4 hours RSV MOI titration experiment

Multiplicity of Infection (1:NI) Where NI is non-infected cells	Result 1: IL-8 Concentration (pg/ml)	Result 2: IL-8 Concentration (pg/ml)	Mean: IL-8 Concentration (pg/ml) ((Result 1 +Result 2)/2)
NI	183.22	391.56	287.39
0.025	417.09	365.96	391.53
0.25	391.56	822.34	606.95
0.5	645.16	763.19	704.17
1	805.43	839.26	822.35

Values such as these are plotted on graphs (Figure 3.1.7).

(a)

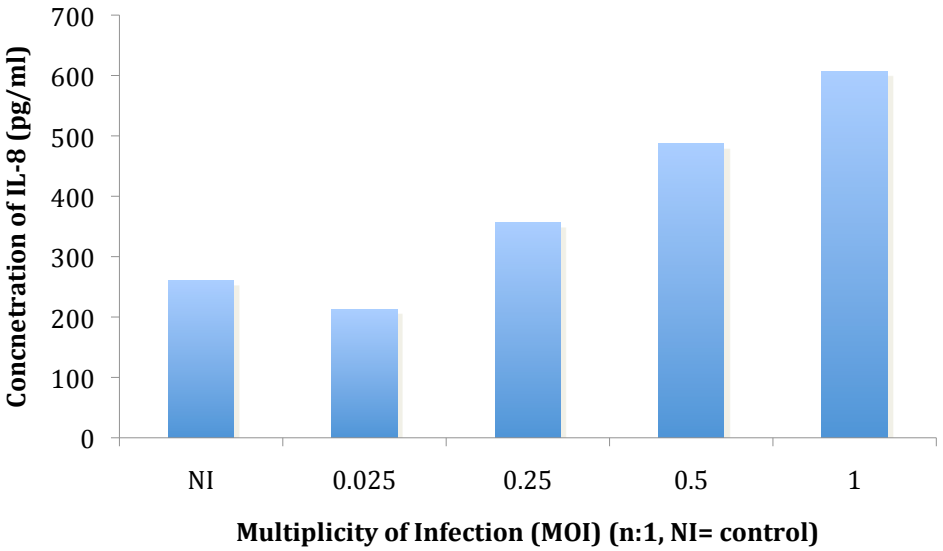
700
600
500
400
300
200
100
0
Concnetration of IL-8 (pg/ml)
NI
0.025
0.25
0.5
1
Multiplicity of Infection (MOI) (n:1, NI= control)

(b)

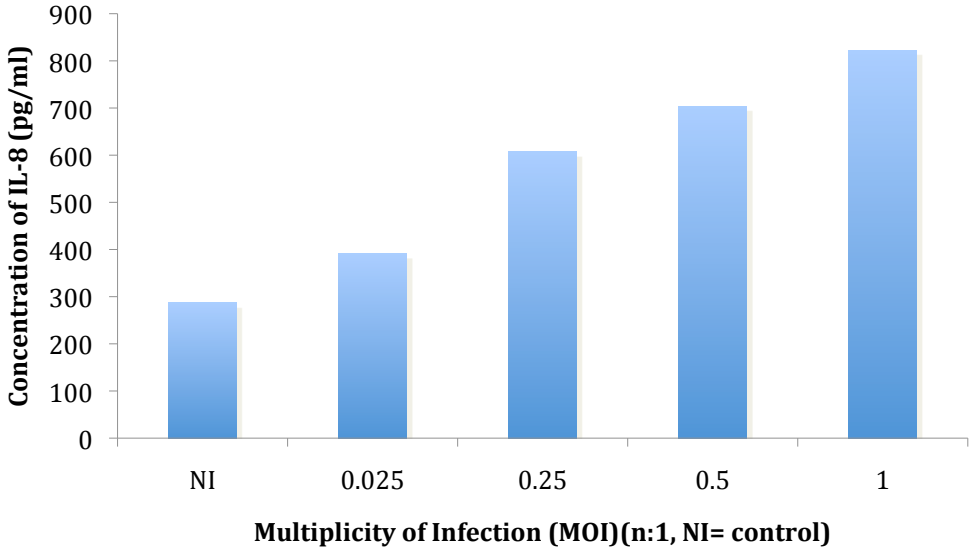
900
800
700
600
500
400
300
200
100
0
Concentration of IL-8 (pg/ml)
NI
0.025
0.25
0.5
1
Multiplicity of Infection (MOI)(n:1, NI= control)

(c)

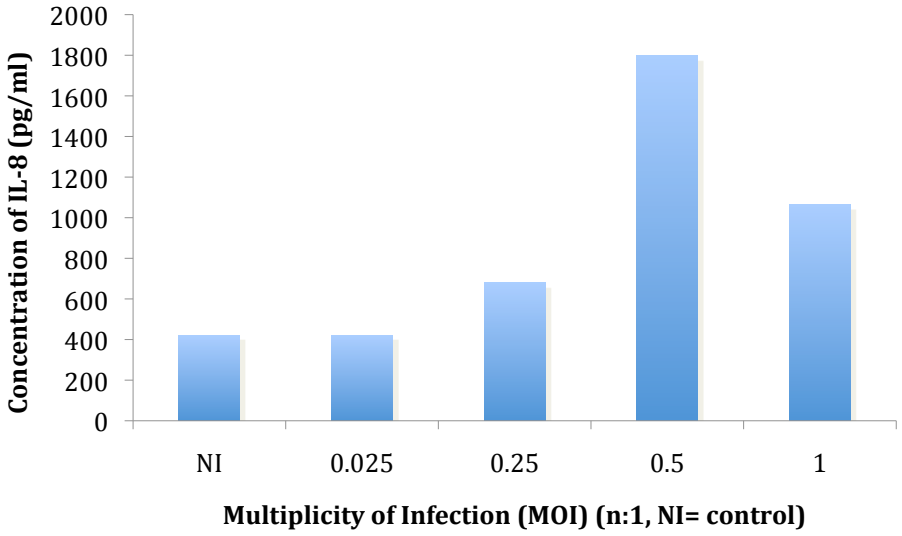

Figure 3.1.7: The effect of a 4 hours RSV infection on the levels of IL-8 released from A549 cells. A549 cells were infected with RSV at 4 hours as an MOI titration experiment. The supernatant was taken of these samples and run for an IL-8 Sandwich ELISA. This experiment was carried out 3 times.

All RSV infected samples had higher concentrations of IL-8 than the control across two experiments (Figure 3.1.7). However, in one experiment the control had IL-8 concentration of 261.12 pg/ml, which was greater than RSV MOI 0.025:1 sample, which had an IL-8 concentration 212.8pg/ml (Figure 317 (a)). In another experiment the concentration levels for the control and MOI 0.025:1 were almost identical (Figure 3.1.7 (c)). As the MOI of RSV increases, the concentration of IL-8 increases in two experiments (Figure 3.1.7 (a) and (b)). However, this is not true in one experiment where the highest IL-8 concentration value is at 0.5:1 after which the IL-8 concentration decreases (Figure 3.1.7 (c)).

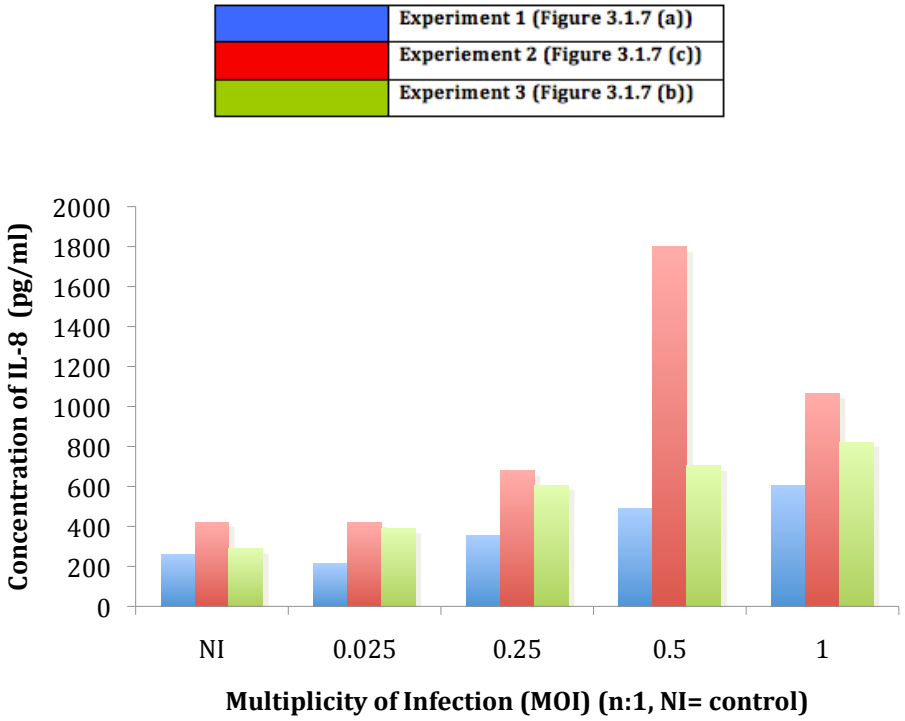

Figure 3.1.8: Combined graph of 3 experiments (Figure 3.1.7) measuring IL-8 concentrations for 4 hours RSV infection of A549 cells. The data was combined so that there could be a clear comparison between experiments.

Across all samples the highest concentration levels IL-8 are in experiment 2 whereas experiment 1 had the lowest (Figure 3.1.8). In two of the experiments the highest concentration level of IL-8 was at a MOI of 1:1, which was 607.05pg/ml for experiment 1 and 822.34pg/ml for experiment 3 (Figure 3.1.8). Experiment 3 had the highest concentration levels of IL-8 recorded at RSV MOI 0.5:1, as 1798.53pg/ml (Figure 3.1.8). This was the highest IL-8 concentration recorded across all three experiments (Figure 3.1.8).

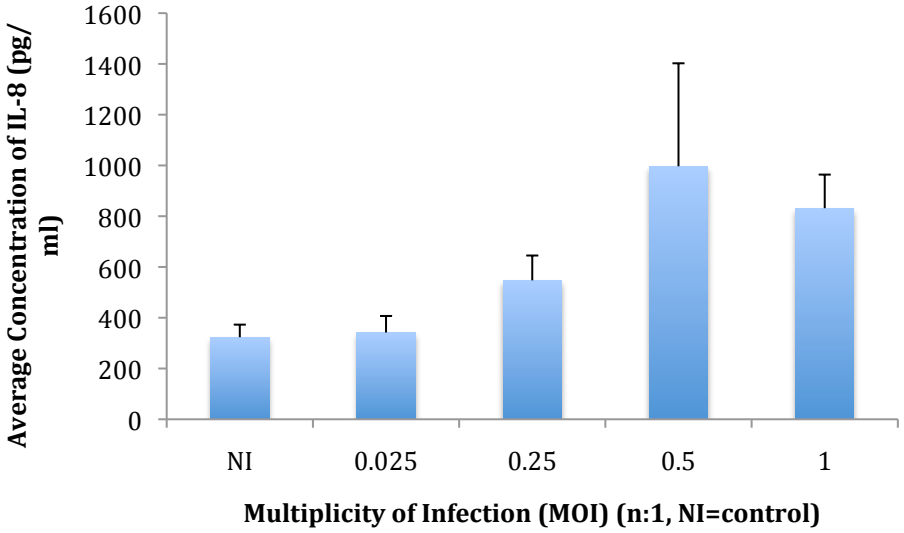

Figure 3.1.9: Mean IL-8 concentration for 4 hours RSV infection of A549 cells with standard error bars. A mean value of all 3 experiments (Figure 3.1.7) was calculated with standard error bars to determine the accuracy of values.

Table 3.1.9: P-values for IL-8 to determine whether there was any statistical significant ($p<0.05$) difference between samples and the control

RSV MOI (n:1)	P Value
0.025:1	0.72
0.25:1	0.08
0.5:1	0.20
1:1	0.03

All infected samples have a greater concentration of IL-8 in comparison to the control (Figure 3.1.9). From the means calculated higher RSV MOIs given greater concentrations of IL-8 (Figure 3.1.9). The highest concentration levels of IL-8 are recorded at 0.5:1 as 996.7 pg/ml (Figure 3.1.9). This value has the greatest standard error of the mean error bar suggesting that this value is the least accurate (Figure 3.1.9). The IL-8 concentration was significantly greater than the control at MOI 1:1 ($P=0.03$, where $p<0.05$ is statistically significant).

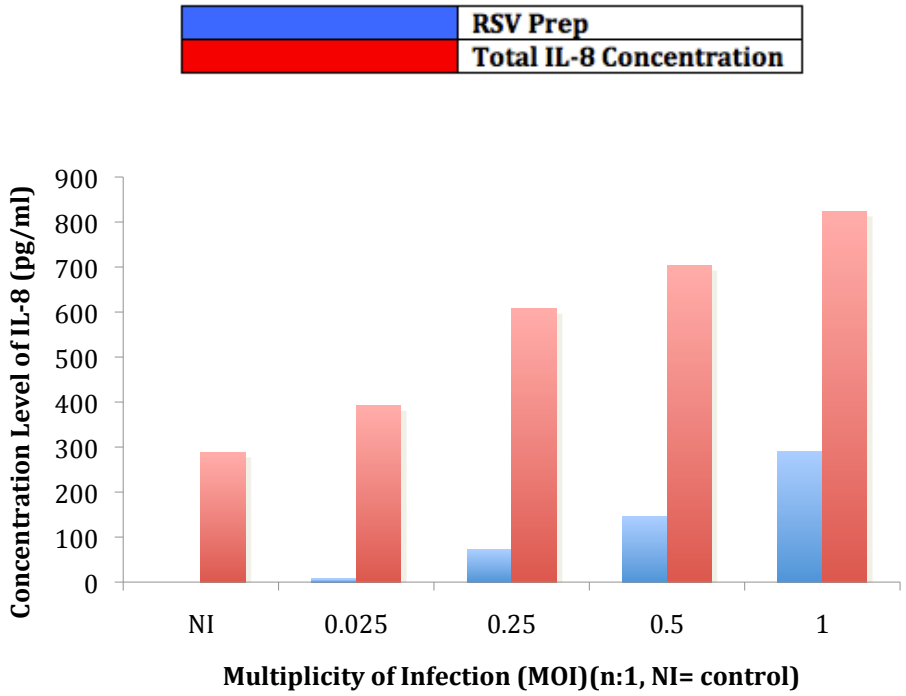

Figure 3.2.1: Comparison between the total concentrations levels of IL-8 and amount of IL-8 in the RSV prep. The purpose of this experiment was to show that RSV infection leads to production of IL-8 from A549 cells accounting for IL-8 concentrations recorded instead of the IL-8 present in the RSV prep. In addition to A549 cells that had been infected with RSV as a MOI titration experiment, RSV prep (MOI 1:1) was added to a well in the 24-well plate that did not contain A549 cells. This well was kept under the same condition as all other sample. The supernatant was taken from all of these wells after 4 hours and used to run an IL-8 Sandwich ELISA. Once the IL-8 concentration for the RSV prep only sample had been measured, this value was divided to show the IL-8 concentration for RSV prep added to samples that were infected at a lower MOI.

For all samples the concentration of IL-8 in the RSV prep added to A549 cells was lower than the total IL-8 concentration that the same sample produced (Figure 3.2.1). For MOI 1:1 the concentration of IL-8 was 532pg/ml greater for MOI 1:1 than the RSV prep. The biggest difference in IL-8 concentration between RSV prep and total IL-8 concentration was for MOI 0.5:1, which was 559pg/ml.

3.2.4 Western Blot data: The Effect of 4 Hours RSV infection on RNF168 Expression

The table below shows the values taken from densitometry carried out on western blot images of RNF168 for samples of A549 cells, which had undergone 4 hours RSV infection (Table 3.8).

Table 3.2.1: Example Densitometry values of Western Blot Image for RNF168 and Actin for 4 Hours RSV MOI Titration of A549 Cells

Multiplicity of Infection (1:NI) Where NI is non- infected cells	RNF168	Actin	RNF168/Actin	Divided by Control (0.32)
NI	2198.04	6931.43	0.32	1
0.025	2565.87	7123.43	0.36	1.13
0.25	2775.28	6822.13	0.41	1.28
0.5	3420.58	6883.01	0.50	1.56
1	3104.34	5646.11	0.55	1.72

Values such as these were plotted in graphs (Figure 3.2.1).

(a)

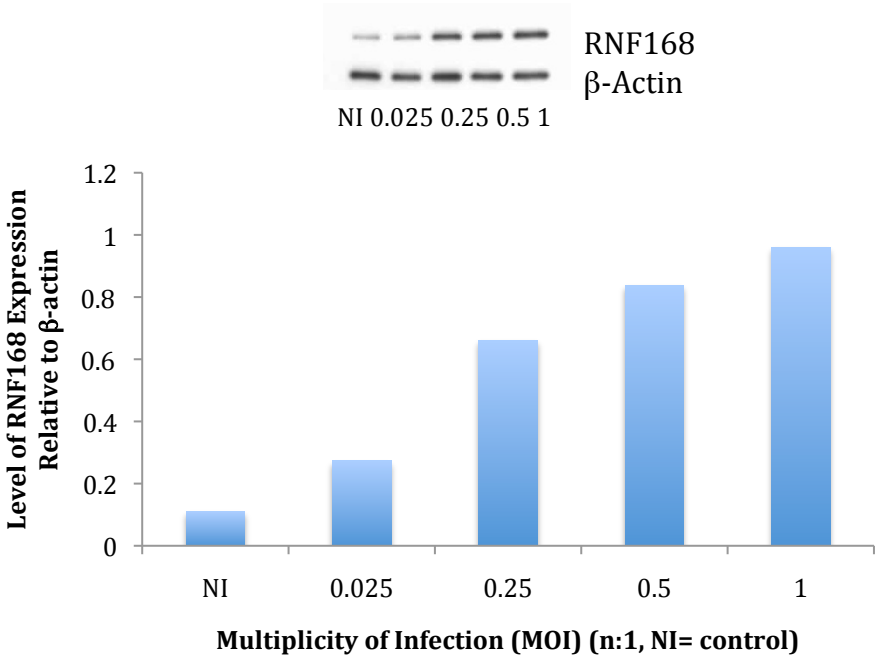
RNF168
β-Actin
NI 0.025 0.25 0.5 1
Level of RNF168 Expression Relative to β-actin
1.2
1
0.8
0.6
0.4
0.2
0
NI
0.025
0.25
0.5
1
Multiplicity of Infection (MOI) (n:1, NI= control)

(b)

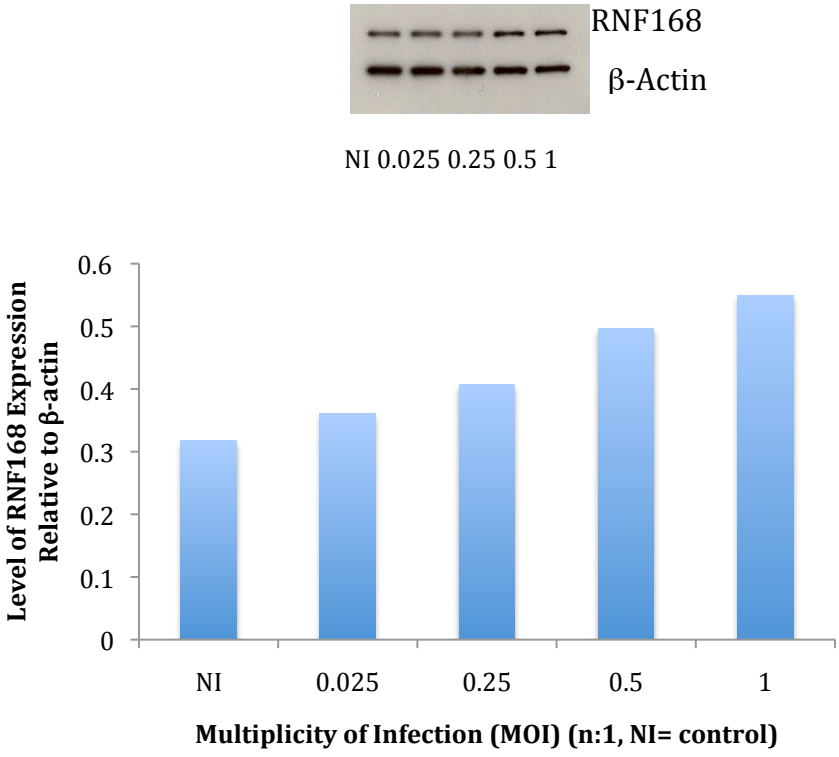
RNF168
β-Actin
NI 0.025 0.25 0.5 1
Level of RNF168 Expression Relative to β-actin
0.6
0.5
0.4
0.3
0.2
0.1
0
NI
0.025
0.25
0.5
1
Multiplicity of Infection (MOI) (n:1, NI= control)

(c)

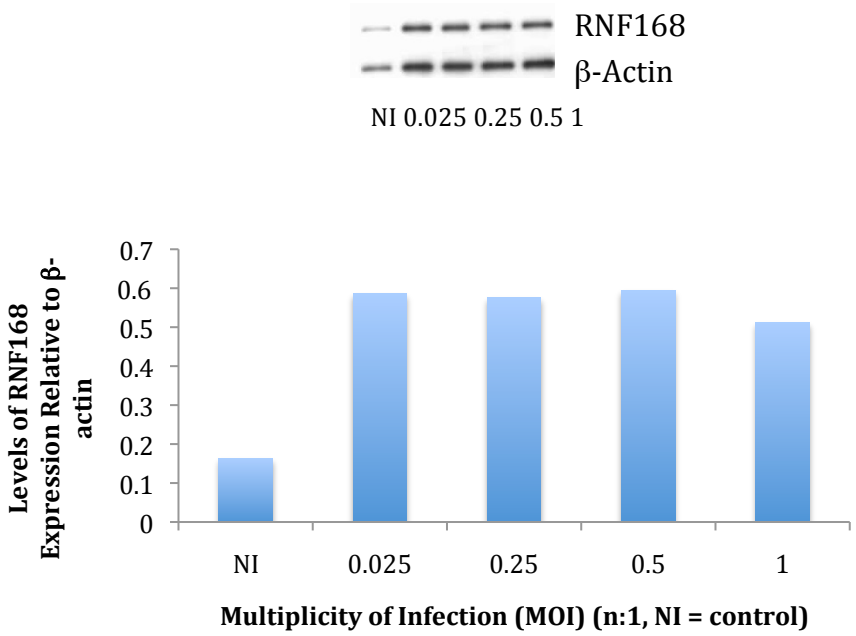

Figure 3.2.2. Level of RN168 expression for A549 cells that have undergone 4 hours RSV infection. A549 cells were infected with RSV for 4 hours as MOI titration experiment. This experiment was carried out 3 times. The proteins from these cells were harvested and used to run a Western Blot. The images underwent densitometry analysis using ImageJ software.

In comparison to the control all RSV samples have shown an increase in RNF168 expression (Figure 3.2.2). In two experiments as the MOI of RSV increases, the level of RNF168 expression also increases (Figure 3.2.2. (a) and (b)). However in one experiment, the level of RNF168 expression increases from control to MOI 0.025:1 and stays at a relatively similar level as MOI increases (Figure 3.2.2. (c)).

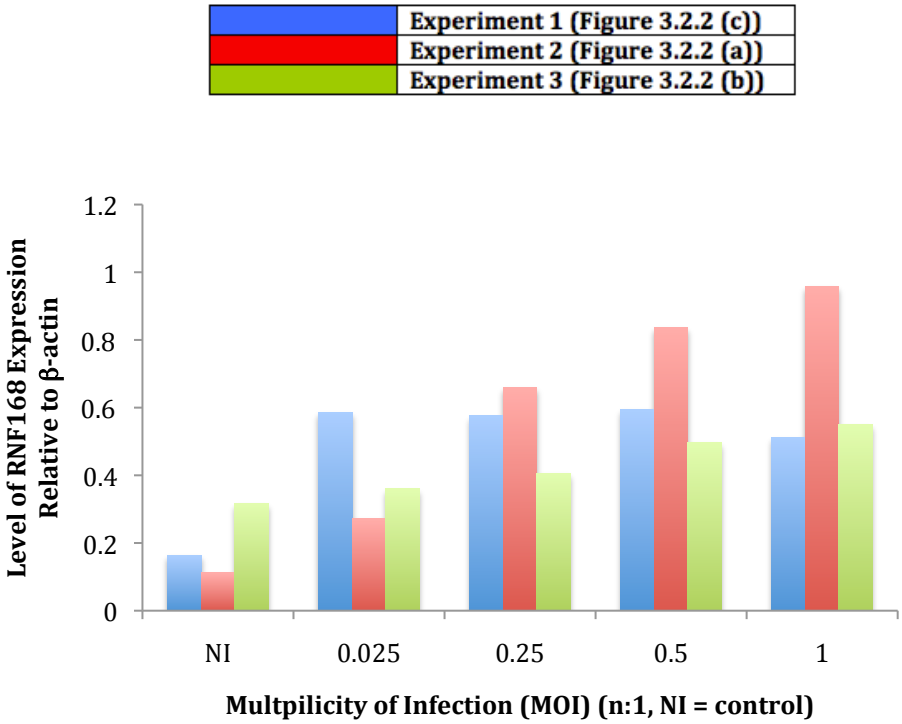

Figure 3.2.3: Combined graph of 3 replicate experiments (Figure 3.2.2) measuring the level of RNF168 expression from A549 cells infected with RSV for 4 hours. The data from 3 experiments (Figure 3.2.2) was combined so that there could be a clear comparison between experiments.

The highest level of RNF168 expression was at an MOI of 1:1 in experiment 2, which was 0.96. In two of the experiments the highest level of RNF168 was at MOI 1:1 at 0.96 and 0.55 for experiments 2 and 3 respectively (Figure 3.2.3). For experiment 1 the highest level of RNF168 expression was at MOI 0.025:1 at 0.59 (Figure 3.2.3). Only experiment 2 and 3 show an increasing concentration of IL-8 with increasing MOI. The lowest IL-8 concentration for all 3 experiments was the control (Figure 3.2.3).

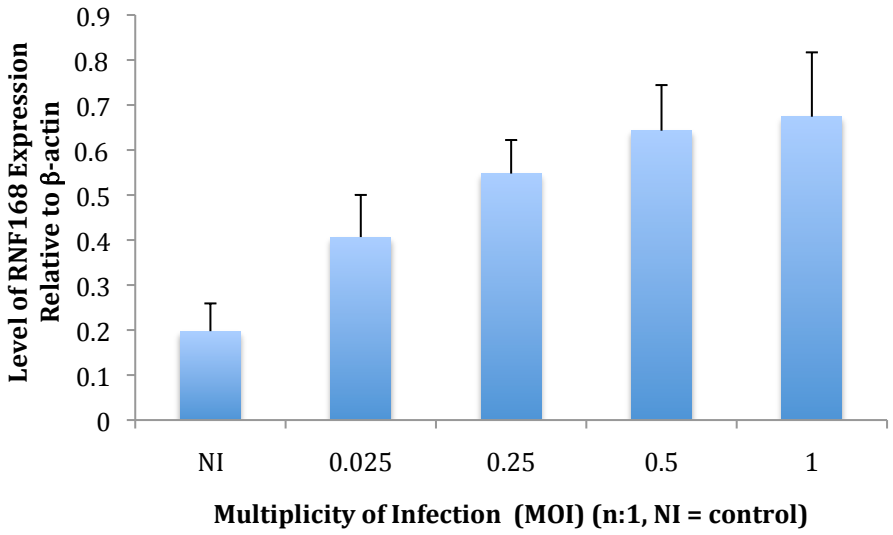

Figure 3.2.4: Graph showing mean values of RNF168 expression from 3 replicate experiments (Figure 3.2.2) where A549 cells have undergone RSV infection for 4 hours. Mean values were calculated to give an overall impression of the relationship between RSV and RNF168 expression for 4 hours RSV infection.

Table 3.2.2: P-values for 4 Hours RSV to determine whether there was any statistical significant (p<0.05) difference between infected samples and the control in terms of RNF168 expression

RSV MOI (n:1)	P Value
0.025:1	0.20
0.25:1	0.12
0.5:1	0.11
1:1	0.13

The mean values calculated from the 3 experiments shows that as RSV MOI increases, the level of RNF168 expression also increases (Figure 3.2.4). The highest value was at MOI 1:1 at 0.67 and the lowest was the control at 0.2 (Figure 3.2.4). The value at MOI was 1:1 as this has the largest standard error bar and was thus the least precise (Figure 3.2.4). In comparison to the control there was no statistically significant difference ($p<0.05$) between the control and RSV infected samples (Table 3.2.1). The increase in RNF168 expression for 0.5:1 RSV in comparison to the control was more significant ($p=0.11$) when compared to other RSV infected samples (Table 3.2.1).

3.2.5. Western Blot data: The Effect of 4 Hours RSV infection on RNF168 Expression Relative to Control

(a)

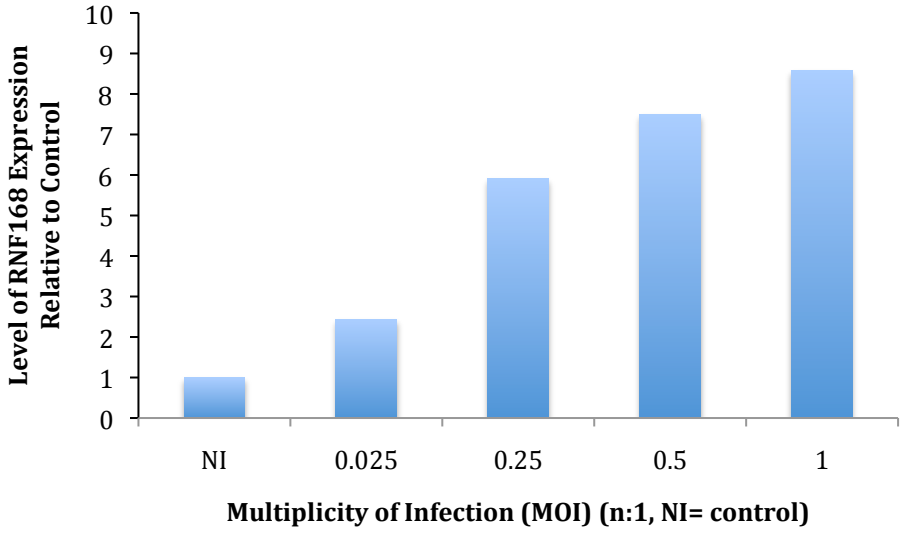

(b)

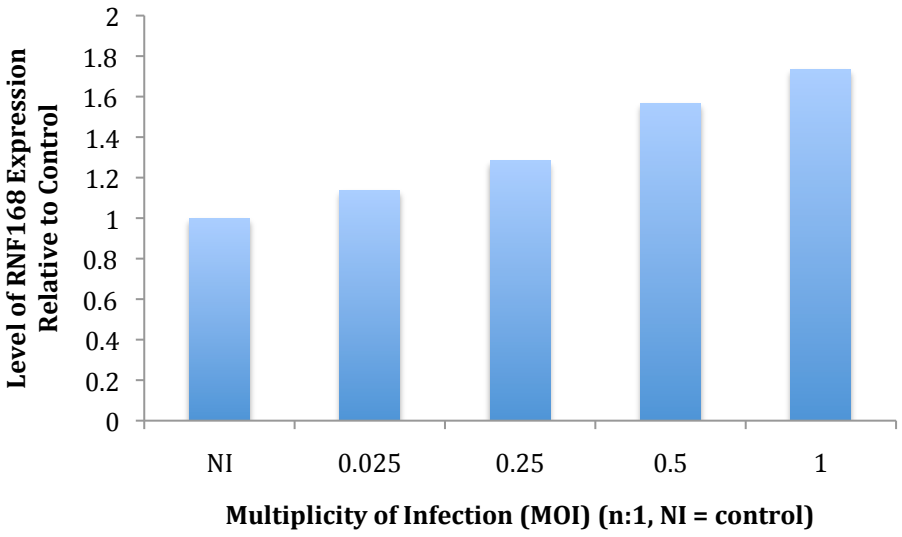

(c)

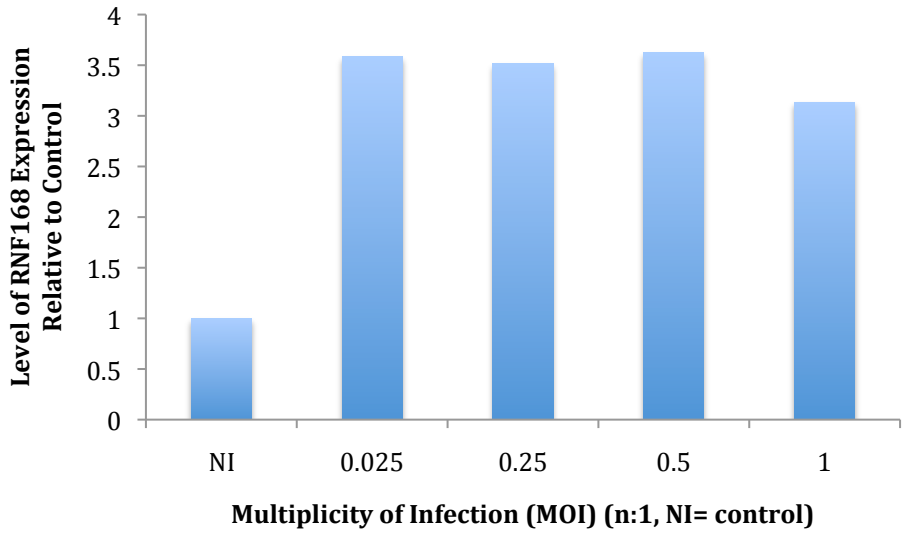

Figure 3.2.5: Level of RNF168 expression relative to control for A549 cells infected with RSV for 4 hours. The values for all three experiments were calculated relative to the control. This was to standardise for the yield and the number of cells in each sample.

In comparison to the control all RSV samples have shown an increase in RNF168 expression (Figure 3.2.5). The control had the lowest level of RNF168 expression in all three experiments (Figure 3.2.5). In two experiments as the MOI of RSV increases, the level of RNF168 expression also increases (Figure 3.2.5. (a) and (b)). The biggest increase in RNF168 expression was 759% and 73% at MOI 1:1 in comparison to the control (Figure 3.2.5. (a) and (b)). In another experiment the biggest increase in RNF168 expression was by 263% in comparison to the control at MOI 0.5:1 (Figure 3.2.1. (c)).

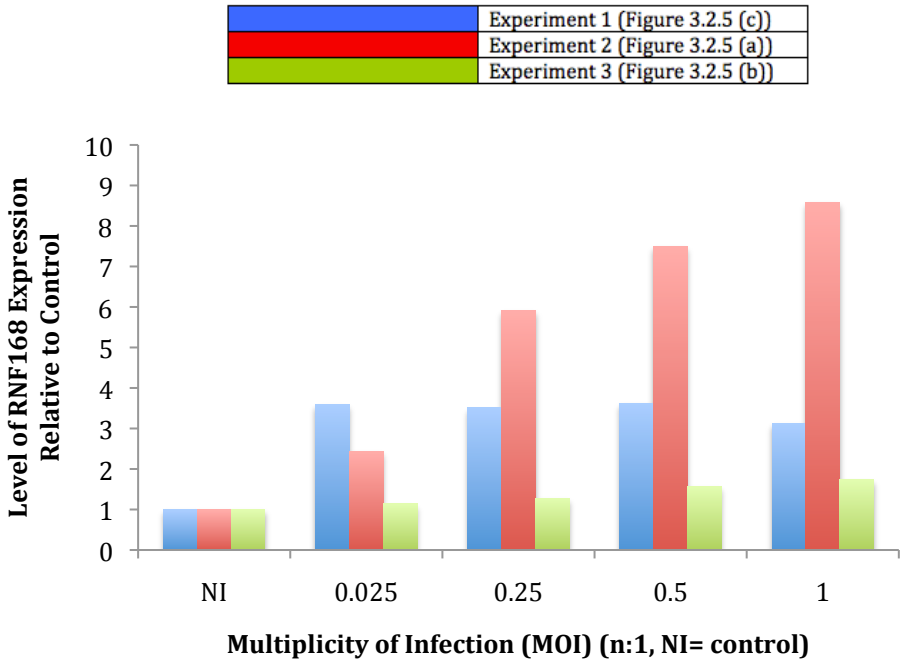

Figure 3.2.6: Combined graph of 3 experiments (Figure 3.2.5) of RNF168 expression relative to control for A549 cells infected with RSV for 4 hours. The data from 3 experiments (Figure 3.2.5) was combined to provide a clear comparison between experiments.

Experiment 2 had the highest levels of RNF168 expression in all samples whereas experiment 3 had the lowest level of RNF168 expression (Figure 3.2.6). The highest levels of expression for RNF168 were seen at MOI 1:1 for experiments 2 and 3 at 8.58 and 1.73 respectively (Figure 3.2.6). The highest level of RNF168 expression for experiment 1 was at MOI 0.025:1 at 3.59 (Figure 3.2.6).

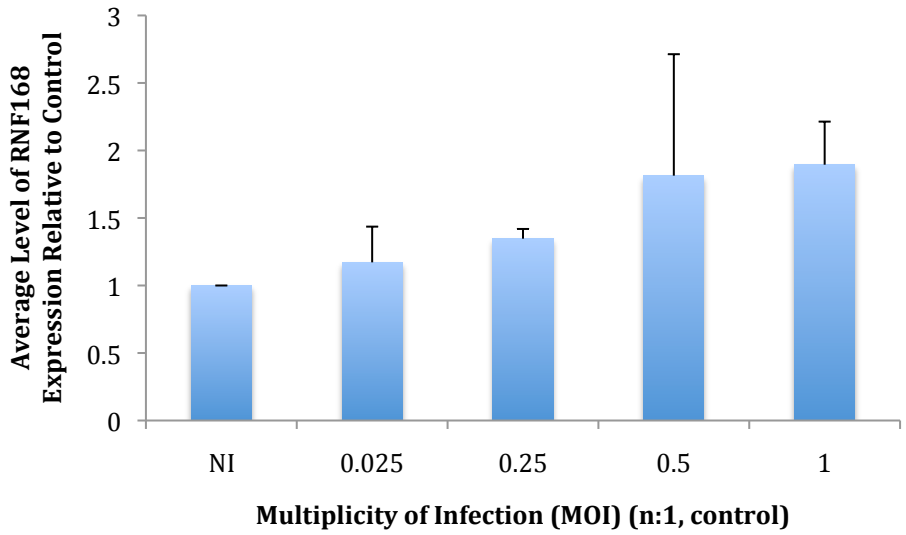

Figure 3.2.7: Mean levels of RNF168 expression relative to control for A549 cells infected with RSV for 4 hours. Mean values from the 3 experiments (Figure 3.2.5) were calculated to provide an overall interpretation of the relationship between RNF168 expression and 4 hours RSV infection.

The biggest increase in RNF168 was at MOI 1:1 of 89% more than the control (Figure 3.2.7). It was noted that as the MOI increased, the percentage increase in RNF68 expression also increased (Figure 3.2.7). The value that was least accurate was at MOI 0.5:1 where the standard error of the mean is the greatest (Figure 3.2.7).

3.3 Measurement of RNF168 Expression at 24 hours Post Infection

One sample for 24 hours post RSV infection was measured for IL-8 and IL-6 concentrations in addition to RSV N gene expression and RNF168 expression (Figure 3.2.8, 3.2.9, 3.3.1 and 3.3.2 (b)). The Il-6, IL-8, RSV N gene data provides supporting evidence that RSV infection of A549 cells was carried out correctly.

3.3.1. The Effect of RSV Infection of A594 cells for 24 hours on RSV N Gene Expression

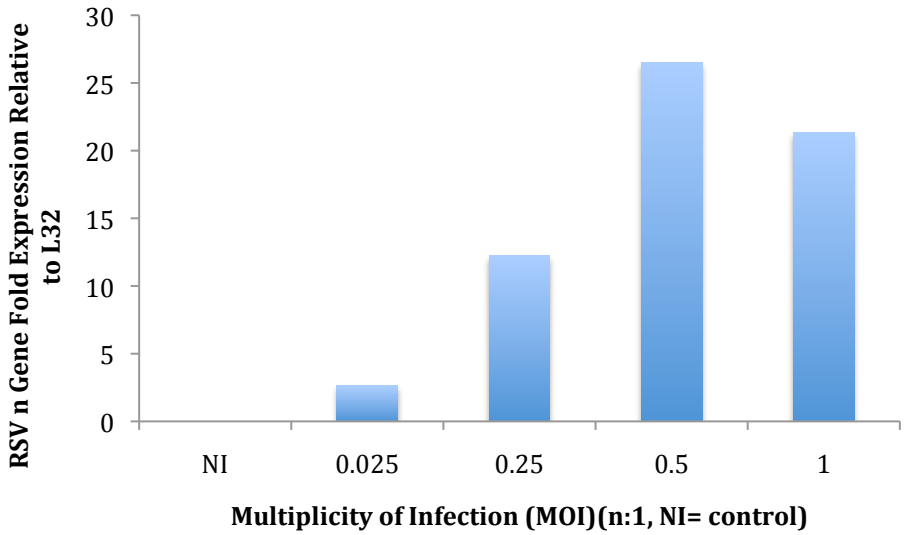

Figure 3.2.8: The level of RSV N gene expression in A549 cells infected with RSV for 24 hours. A549 cells were grown in a 24-well plate and infected with RSV as a MOI titration experiment. The RNA was harvested from these samples and used to run real-time PCR for RSV N gene expression. This experiment was carried out 3 times.

All RSV infected cells have shown RSV N gene expression, which is greater than the control (Figure 3.2.8). The control sample had no RSV N gene expression. As the RSV MOI increases, the level of RSV N gene expression also increases between MOI 0.025:1 and 0.5:1(Figure 3.2.8). The highest level of RSV N gene expression was at 0.5:1 at 26.51. After RSV MOI 0.5:1 the level of RSV N gene expression decreases at MOI 1:1(Figure 3.2.8).

3.3.2. The Effect of 24 hours RSV Infection of A549 cells on IL-6 Concentration Levels

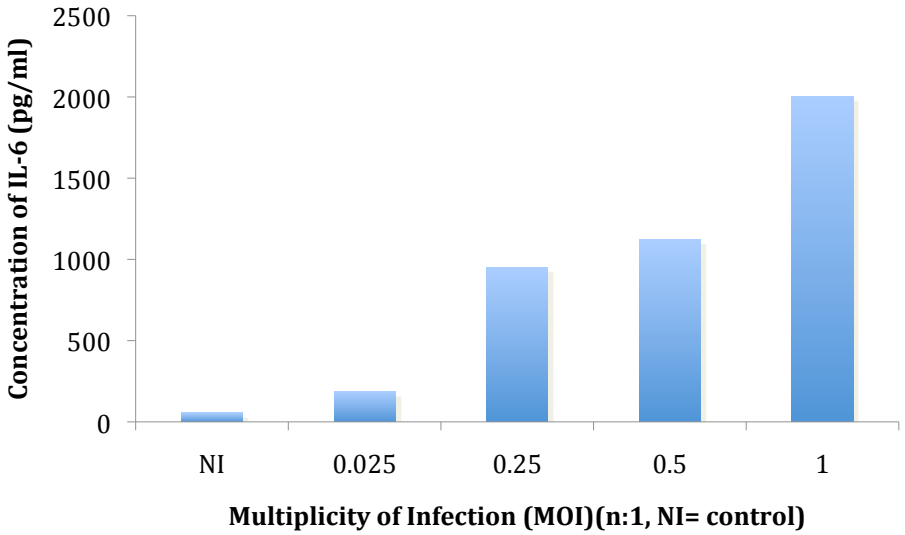

Figure 3.2.9: The concentration of IL-6 produced from A549 cells infected with RSV for 24 hours. A549 cells were infected with RSV over 24 hours as a MOI titration for 24 hours. The supernatant from these samples was run for an IL-6 Sandwich ELISA.

The control sample had the lowest concentration of IL-6 57.49 pg/ml (Figure 3.2.9). In comparison to the control, all RSV infected samples had greater concentration level of IL-6 (Figure 3.2.9). The highest IL-6 concentration was at MOI 1:1 at 2003.24 pg/ml (Figure 3.2.9). As the RSV MOI increases the concentration of IL-6 increases (Figure 3.2.9).

3.3.3. The Effect of 24 hours RSV infection of A549 cells on IL-8 Concentration Levels

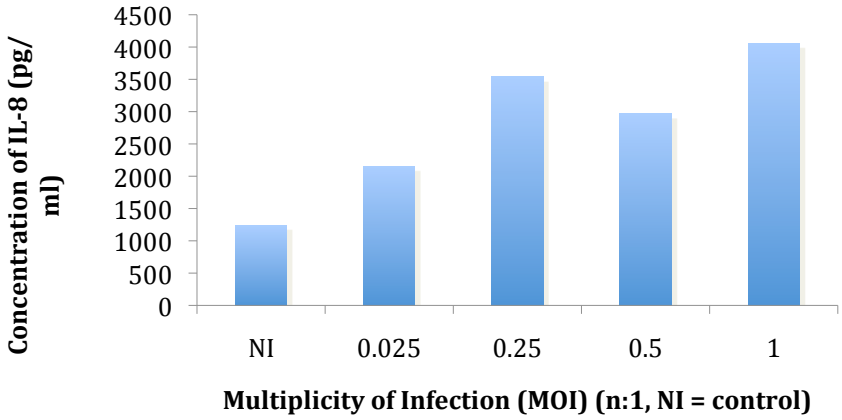

Figure 3.3.1: Concentration of IL-8 produced from A549 cells when infected with RSV for 24 hours. A549 cells were grown in a confluent 24-well plate were infected with RSV as a MOI titration experiment for 24 hours. The supernatant was taken from these samples and used to run an IL-8 Sandwich ELISA.

In comparison to the control, it is clear that the concentration of IL-8 is higher in RSV infected samples (Figure 3.3.1). The lowest concentration of IL-8 is the control at 1238.61pg/ml (Figure 3.3.1). The highest levels occurred with RSV MOI 1:1 at 4062.21pg/ml (Figure 3.3.1). The general trend is increasing RSV MOI leads to a higher concentration of IL-8 (Figure 3.3.1). However, the RSV MOI 0.5:1 is the one exception to this as the IL-8 concentration at this MOI is 2968.99 pg/ml, which is lower than the MOI 0.25:1 that has an IL-8 concentration of 3539.41pg/ml (Figure 3.3.1).

3.3.4 Western Blot Data: The effect of 24 hours RSV infection on RNF168 Expression

(a)

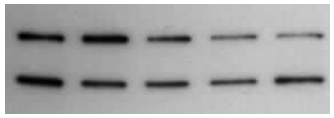

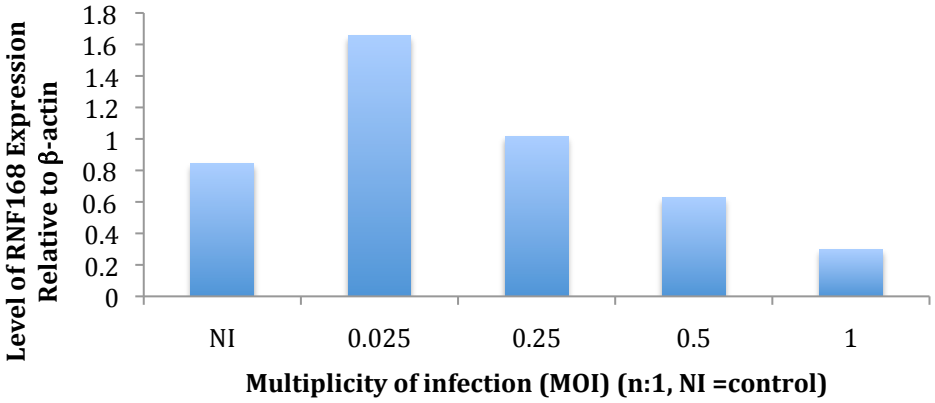

(b)

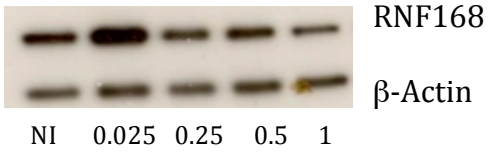

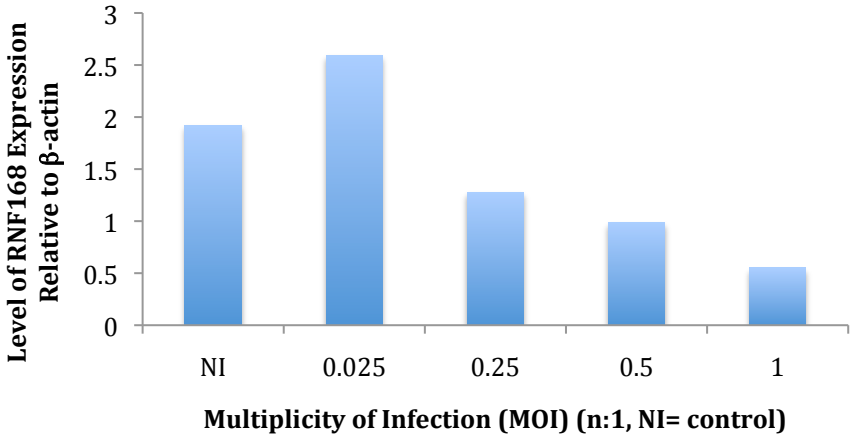

(c)

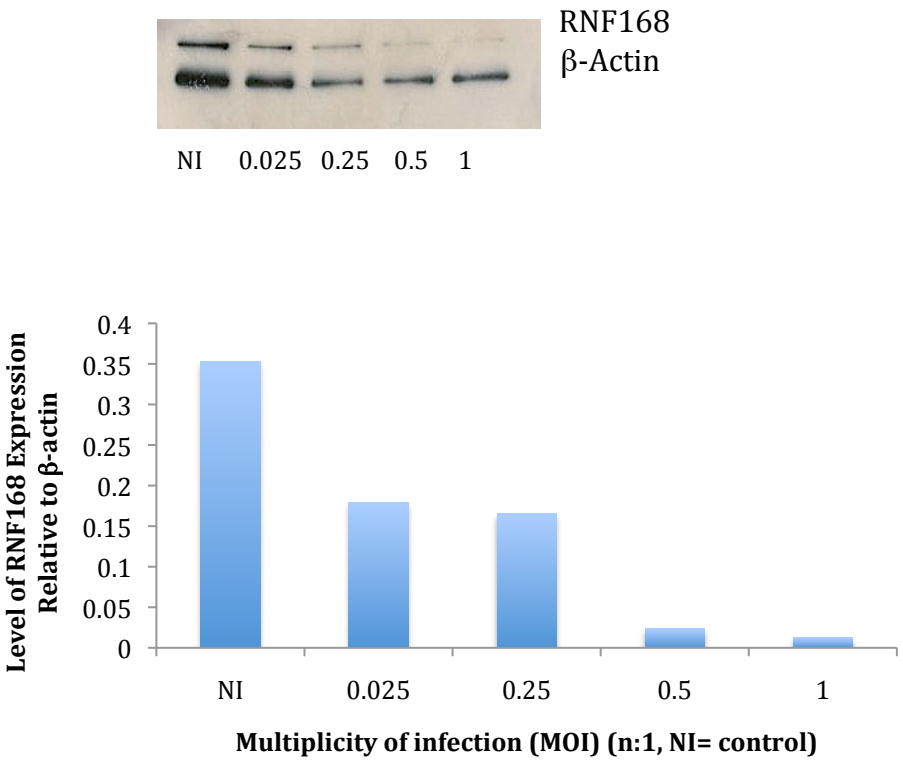

Figure 3.3.2: The level of RNF168 expression from A549 cells that have been infected with RSV for 24 hours. A549 cells were grown in 24-well plates and infected with RSV as a MOI titration experiment. The protein from the cells was harvested after 24 hours and used to run Western blot for RNF168 expression.

In all three experiments the level of RNF168 expression is the lowest at RSV MOI 1:1 (Figure 3.3.2). In two experiments the highest level of RNF168 expression is at MOI 0.025:1 at 1.65 (Figure 3.3.2 (a)) and 2.6 (Figure 3.3.2 (b)). In the other the greatest RNF168 expression level occurs at 0.35 for the control (Figure 3.3.2 (c)). In all 3 experiments the RNF168 expression decreases between MOIs 0.025:1 to 1:1. The lowest level of RNF168 expression across all experiments is at an MOI of 1:1 with the lowest value being 0.01 (Figure 3.3.2 (c)).

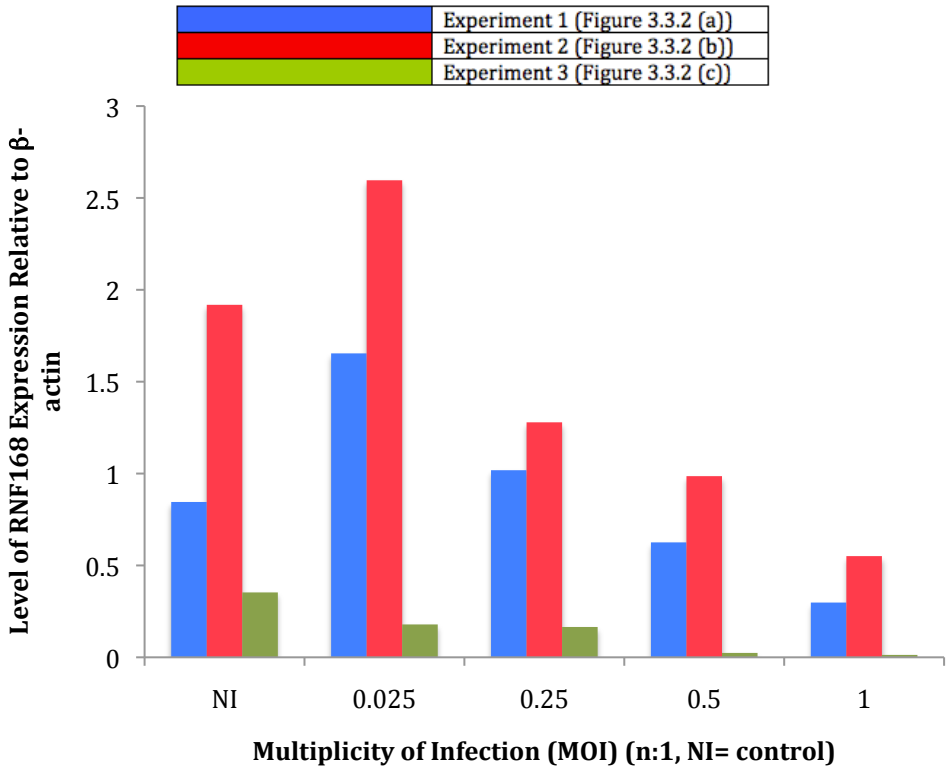

Figure 3.3.3: A combined graph of 3 experiments investigating the effect of infecting A549 cells with RSV for 24 hours. The data from all three graphs (Figure 3.3.2) was combined into a graph to provide a clear comparison between values.

Experiment 3 had the lowest level of RNF168 expression across all samples with the lowest being MOI 1:1 at 0.01 (Figure 3.3.3). Experiment 2 had the highest values of RNF168 with 2.6 at MOI 0.025:1 being the highest value (Figure 3.3.3). The relationship between MOI and RNF168 expression are identical in experiments 1 and 2 (Figure 3.3.3). These show that in comparison to the control RNF168 expression initially increases at a RSV MOI of 0.025:1 and then continues to decrease as MOI increases (Figure 3.3.3). However, experiment 3 shows RNF168 expression decreasing from control to RSV MOI 1:1(Figure 3.3.3).

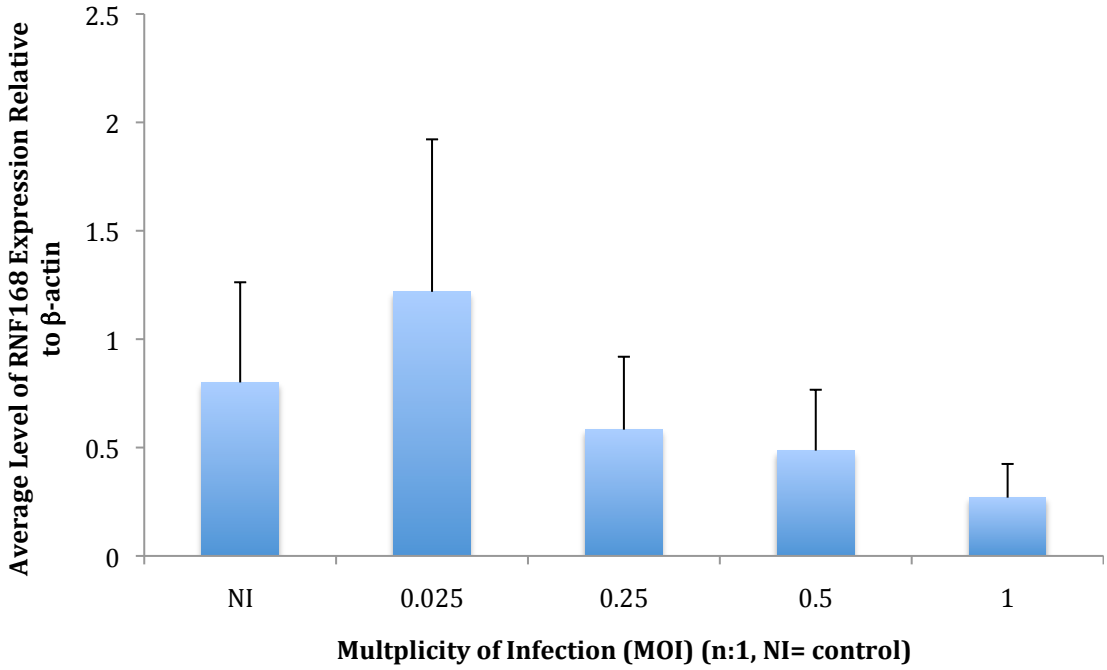

Figure 3.3.4: Mean RNF168 expression values for 24 hours RSV infection with standard error bars. The values obtained for the 3 replicate experiments (Figure 3.3.2) involving the infection of A549 cells for 24 hours were meand and standard error of the mean calculated as represented by error bars. This gave the overall relationship between RNF168 and RSV at 24 hours.

Table 3.2.3: P-values for 24 Hours RSV to determine whether there was any statistical significant (p<0.05) difference between samples and the control

RSV MOI (n:1)	P Value
0.025:1	0.29
0.25:1	0.41
0.5:1	0.16
1:1	0.14

The lowest mean RNF168 expression value is the control at 0.8 (Figure 3.3.4). In comparison to the control, there is an increase in RNF168 expression for MOI 1:0.025 at 1.21 which is the highest value (Figure 3.3.4). Thereafter, the level of RNF168 expressions continues to decrease as MOI increases. The most inaccurate value is at MOI 0.025:1 because it has the largest standard error of the mean (Figure 3.3.4).

When comparing the infected samples with the control, the difference in RNF168 expression is not statistically significant ($p<0.05$) (Table 3.2.2).In contrast, other infected samples MOI 1:1 showed the greatest difference in RNF168 expression when compared to the control ($p=0.14$) (Table 3.2.2).

3.3.5 Western Blot Data: The effect of 24 hours RSV infection on RNF168 Expression relative to control

(a)

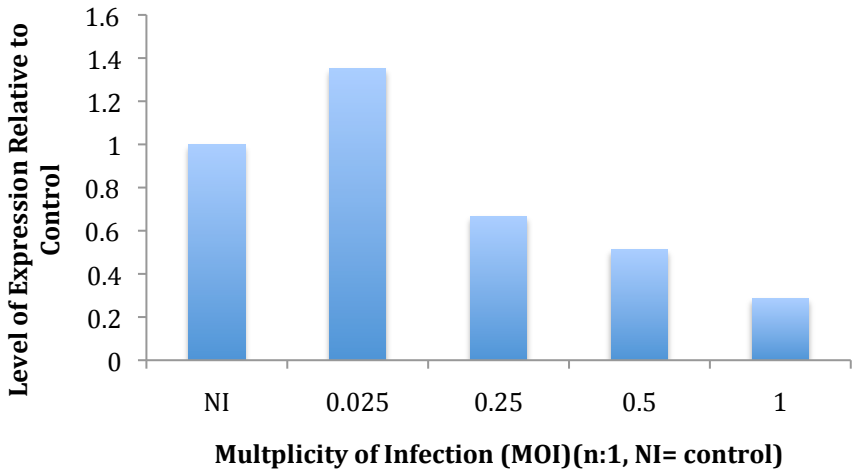

(b)

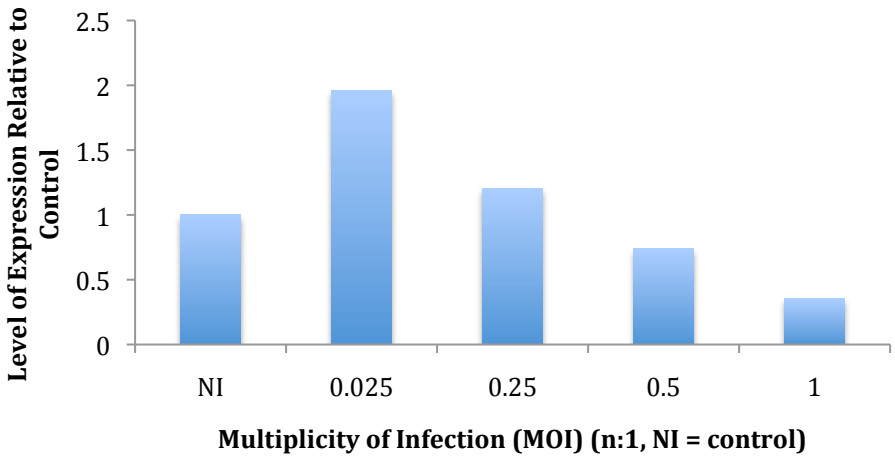

(c)

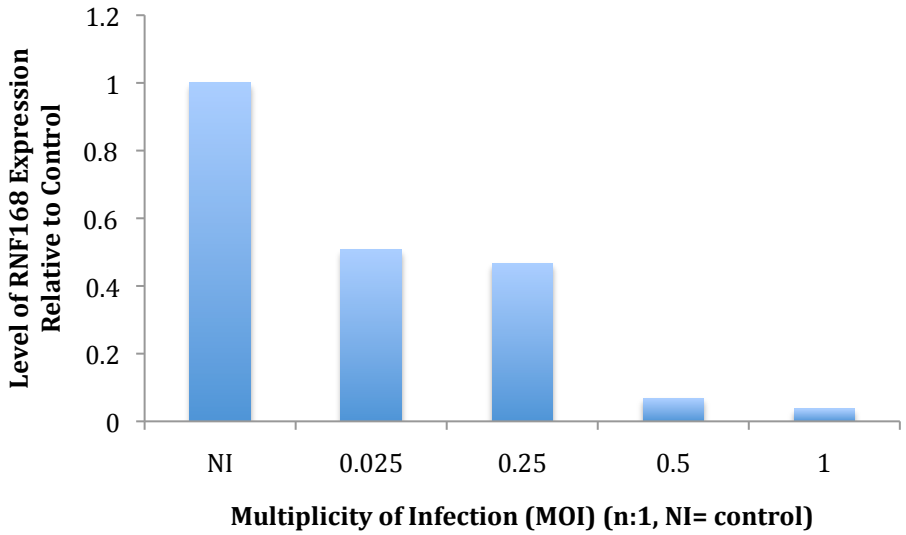

Figure 3.3.5: The level of RNF168 expression relative to control for A549 cells that have undergone 24 hours RSV infection. The level of RNF168 expression present in the three repeat experiments (Figure 3.2.2) was re-calculated relative to the control. This was to standardise the yield and number of cells per sample.

In one of the experiments as the MOI increases the expression of RNF168 decreases by 96% at MOI 1:1 (Figure 3.3.5 (c)). The highest value recorded for the same experiment was the control (Figure 3.3.5 (c)). In the other two experiments the highest value was at MOI 0.025:1 which showed an increase by 35% (Figure 3.3.5 (a)) and 96% (Figure 3.3.5(b)) in comparison to the control. After MOI 0.025:1, the expression of RNF168 decreases with increasing MOI (Figure 3.3.5 (a) and (b)). The lowest value for both these experiment shows a decrease at MOI 1:1 by 71% (Figure 3.3.5 (a)) and 65% (Figure 3.3.5(b)) in comparison to control.

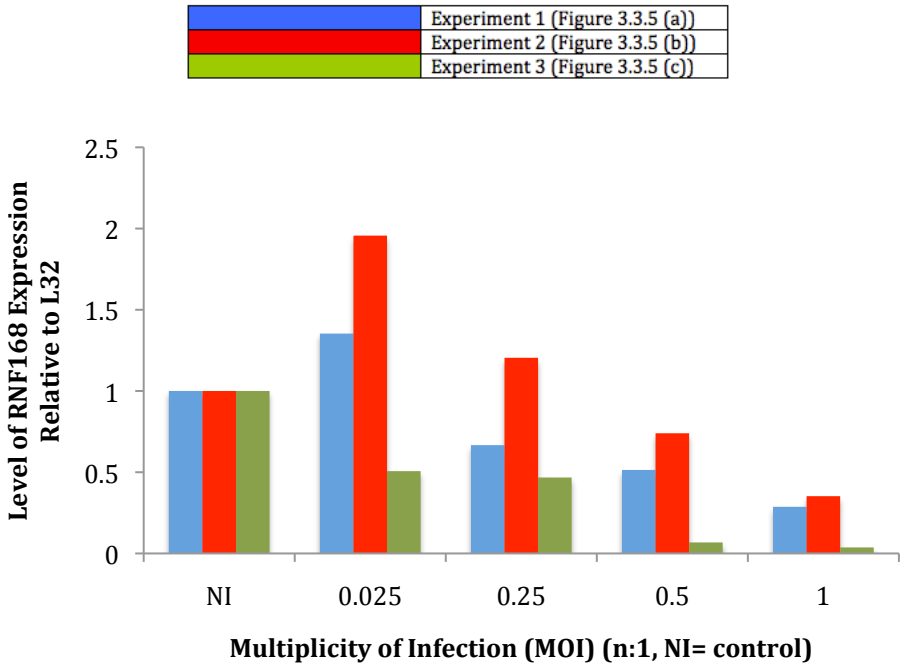

Figure 3.3.6: Combined graph for the level of RNF168 expression relative to control in three experiments where A549 cells are infected with RSV for 24 hours. The values from the three experiments (Figure 3.3.5) were combined together to provide a clear comparison.

Experiment 2 had the highest level of RNF168 expression for all samples (Figure 3.3.6). Experiment 3 had the lowest level of RNF168 expression for all samples (Figure 3.3.6). The lowest level of RNF168 expression was seen at MOI 1:1 for all samples in experiment 3 (Figure 3.3.6). Experiments 1 and 2 showed an increase of 35% and 96% in comparison to the control at MOI 0.025:1 (Figure 3.3.6). After MOI 0.025:1, RNF168 expression decreases in both experiments (Figure 3.3.6).

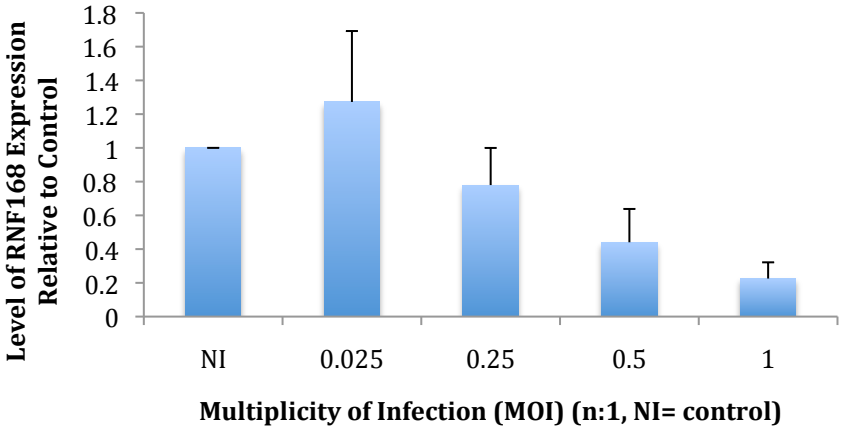

Figure 3.3.7: Mean value of RNF168 expression for A549 cells infected with RSV for 24 hours. The mean of RNF168 expression values taken from 3 experiments (Figure 3.3.5) was calculated with standard error of the mean displayed as error bars.

From the mean values it is clear that the lowest level of RNF168 expression is present at an MOI of 1:1 at 0.23, which is a decrease of 77% in comparison to the control (Figure 3.3.7). The highest level is at MOI 0.025 at 1.27, which is a 27% increase in comparison to the control (Figure 3.3.7). However, the standard error of the means for MOI 0.025:1 is the largest suggesting that it is the least accurate value (Figure 3.3.7).

3.4 Influence of time post infection on RNF168 gene expression

The same sample was measured for RSV N gene expression and IL-8 concentration in addition to RNF168 expression. The RSV N gene expression and IL-8 data provided supporting evidence that cells had been infected correctly and viral replication was greater for a longer duration of RSV infection.

3.4.1 The Effect of Duration of RSV Infection on RSV N gene Expression

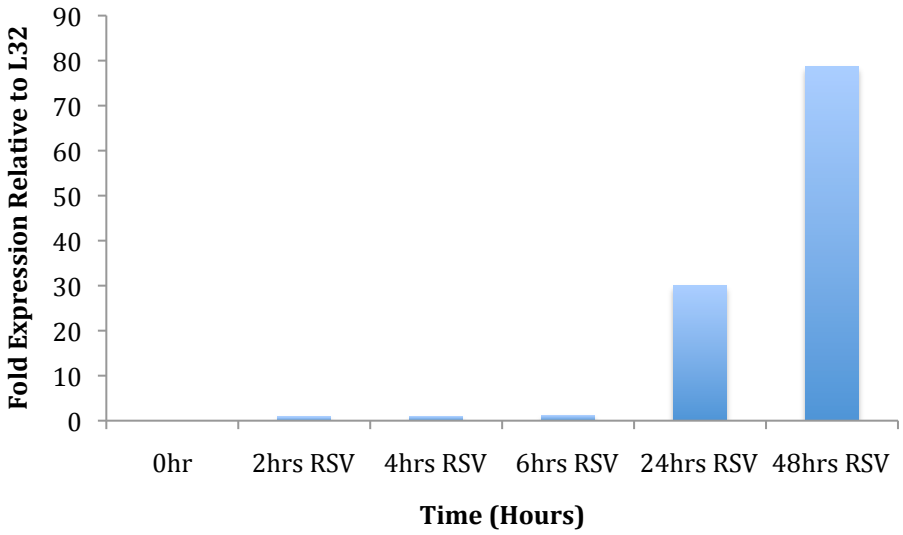

Figure 3.3.8: RSV N gene expression of samples of A549 cells, which have undergone RSV infection for 0, 2, 4, 6, 24 and 48 hours. A549 cells grown in a 24-well plate were infected with RSV (MOI 1:1) for time points 0, 2, 4, 6, 24 and 48 hours. 0 hours was a starting control which was harvested immediately after all other samples had been infected. The RNA harvested from RSV infected cells (not the paired control) was used to run real-time PCR for RSV N gene expression.

At the 0 hours control no RSV N gene expression is detected (Figure 3.3.8). At all other times points for RSV infected samples there is RSV N gene expression (Figure 3.3.8). The level of RSV N gene expression is comparable for 2,4 and 6 hours samples (Figure 3.3.8). However, at 24 hours the level of RSV N gene expression increases greatly by approximately 30 fold from 1.25 at 6 hours to 30.05 at 24 hours (Figure 3.3.8). Between 24 and 48 hours, RSV N gene expression more than doubles to 78.69, which is the highest value (Figure 3.3.8)?

3.4.2 The Effect of Duration of RSV Infection on IL-8 levels

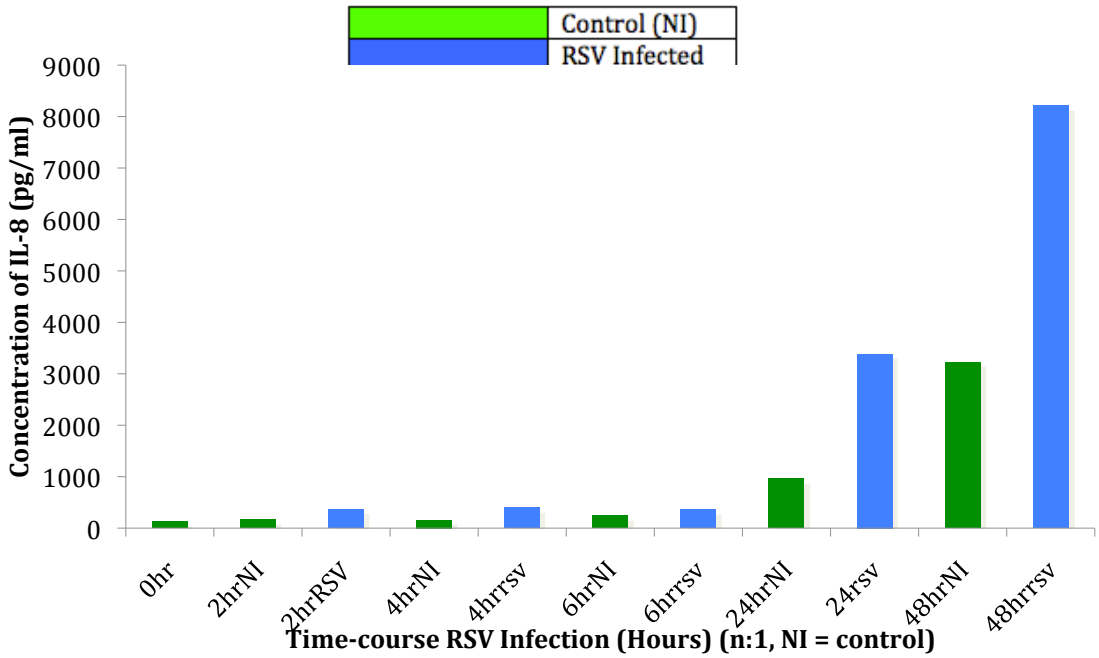

Figure 3.3.9: **IL-8 Sandwich ELISA for A549 cells infected with RSV for 0, 2, 4, 6, 24 and 48 hours with paired controls.** A549 cells grown in a 24-well plate were infected with RSV (MOI 1:1) for time points 0, 2, 4, 6, 24 and 48 hours paired with controls (sample of cells that were not infected) for each time point. 0 hours was a starting control which was harvested immediately after all other samples had been infected. The supernatant for each of these samples was removed and used to run an IL-8 Sandwich ELISA comparing infected samples with controls.

All RSV infected cells produced a higher concentration level than the control at the same time point (Figure 3.3.9). The lowest level of IL-8 was at the 0 hour starting control at 131.36 pg/ml (Figure 3.3.9). When comparing control and RSV infected samples at 24 and 48 hours, RSV sample has more than doubled in concentration level of IL-8 at both of these time points (Figure 3.3.9). The highest concentration of IL-8 was at 48 hours at 8209 pg/ml (Figure 3.3.9).

3.4.3 Western Blot Data: The Effect of Duration of RSV Infection on RNF168 Expression

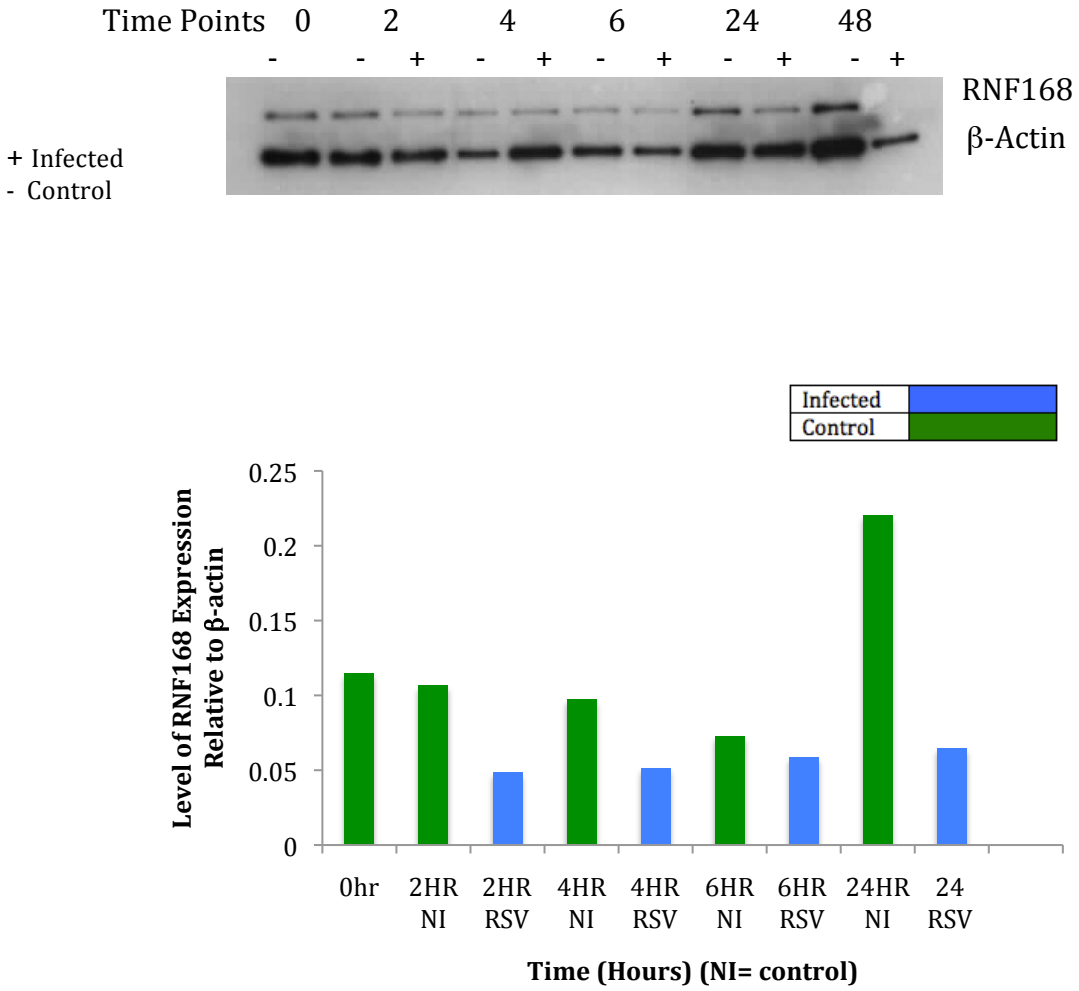

Figure 3.4.1: RNF168 expression for A549 cells infected with RSV for 0, 2, 4, 6, 24 and 48 hours with paired controls. A549 cells were grown in a 24-well plate and infected with RSV at MOI 1:1. For each RSV sample there was a paired control of non-infected cells. The cells were harvested at 0, 2, 4, 6, 24 and 48 hours time points along with their paired control. 0 hour was a starting control with no RSV added and was harvested immediately after RSV had been added to all other samples of A549 cells. These samples were run for a Western blot. The images gathered were analysed using ImageJ software to obtain densitometry values. The 48 hours time point was not plotted as both results for control and infected samples did not develop sufficiently for densitometry to be done.

The highest level of RNF168 expression is the 24 hours control at 0.2 (Figure 3.4.1). The lowest level of RNF168 expression is for the 2 hour RSV infected sample at 0.048 (Figure 3.4.1). Excluding 24 hours, the 0 hour control had the next highest level of RNF168 expression at 0.11 (Figure 3.4.1). The RSV infected samples had the lowest levels of RNF168 expression in comparison to the controls at the same time point (Figure 3.4.1). The biggest difference between control and infected samples was at 24 hours where the control was 0.16 greater than the infected sample (Figure 3.4.1). This difference was 0.16 (Figure 3.4.1).

3.5. Measurement of RNF168 Expression for 4 Hours Interferon-beta stimulation

3.5.1. Western Blot Data: The effect of Interferon beta Stimulation on RNF168 Expression at 4 Hours

(a)

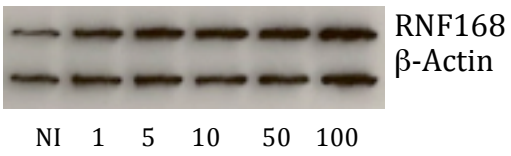

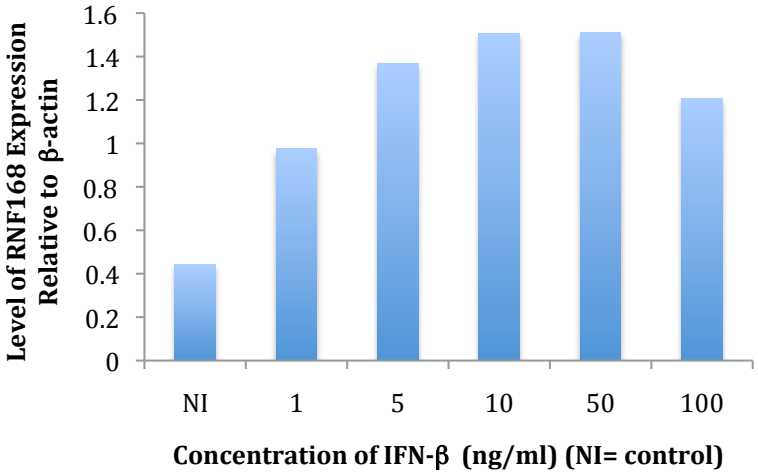

(b)

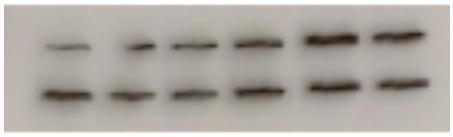

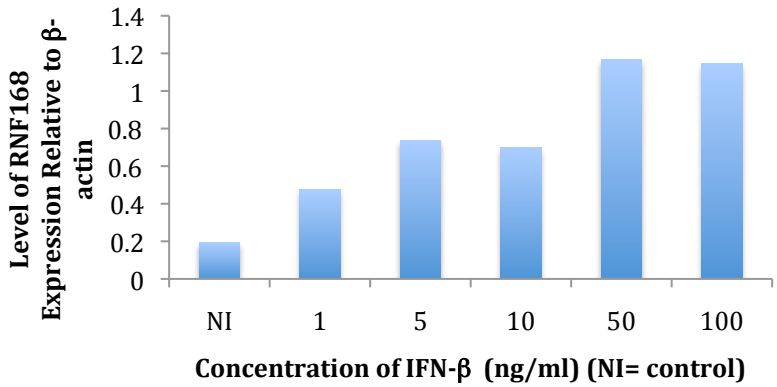

(c)

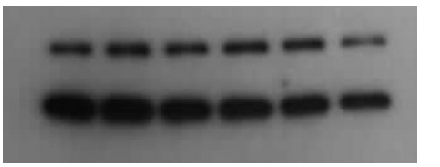

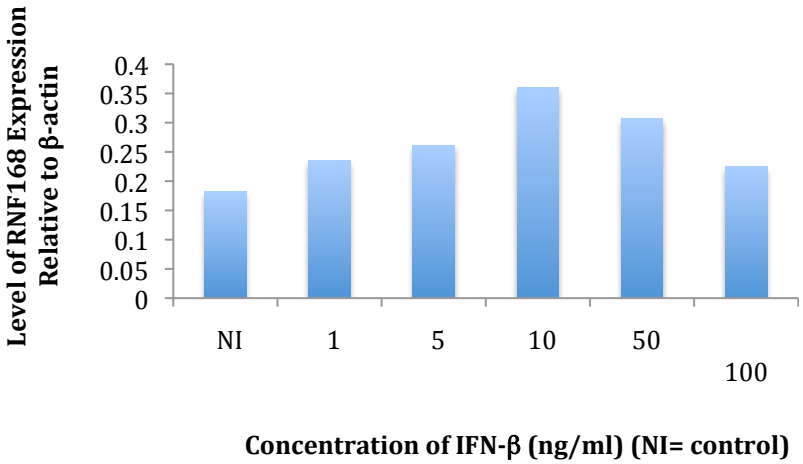

Figure 3.4.2: RN168 expression levels for A549 cells that have been stimulated with IFN-β for 4 hours. A549 cells were grown in a 24-well plate and stimulated with IFN-β as a titration experiment for 4 hours. The protein was then harvested from cells and used to run a western blot. The images produced were analysed for densitometry using ImageJ software.

In comparison to the control, the level of RNF168 expression was greater in all IFN-β samples. The highest level of RNF168 expression was at 50ng/ml in two experiments at 1.51 (Figure 3.4.2 (a)) and 1.17 (Figure 3.4.2 (b)). In the other experiments the highest level of RNF168 expression was at 10ng/ml giving 0.36.

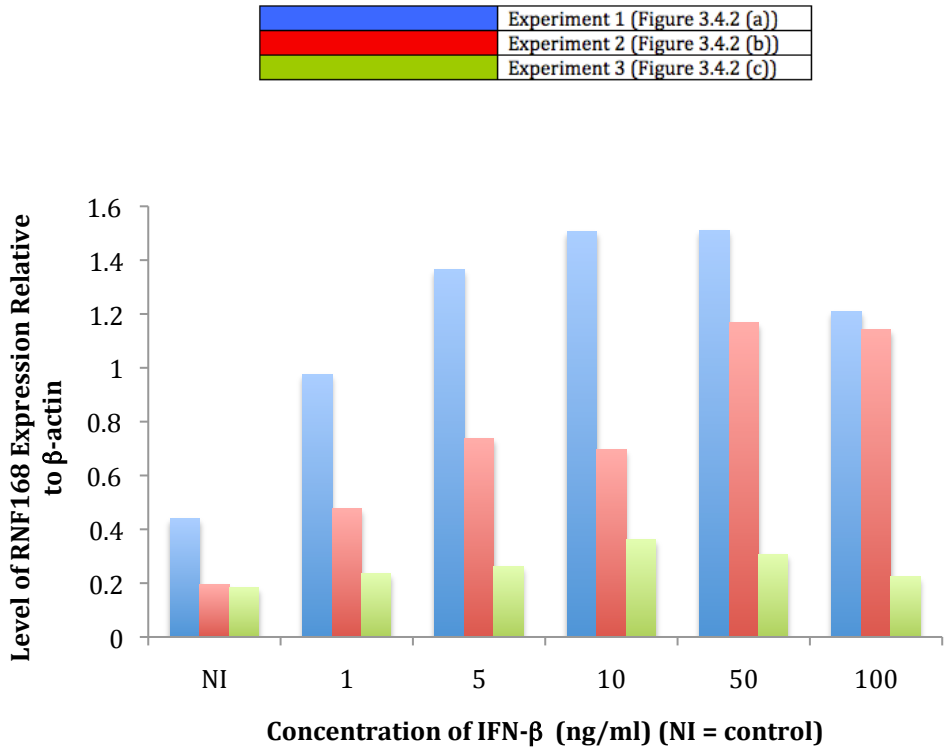

Figure 3.4.3: Combined results from the 3 experiments involving IFN-β stimulation of A549 cells for 4 hours. The data from the 3 experiments (Figure 3.4.2) was combined into a graph to provide a clear comparison of the values obtained.

Experiment 3 has the lowest level of RNF168 expression across all samples whilst experiment 1 has the highest across all samples (Figure 3.4.3). The peak levels of RNF168 expression are seen at IFN-β concentration levels 10ng/ml and 50ng/ml for all 3 experiments (Figure 3.4.3).

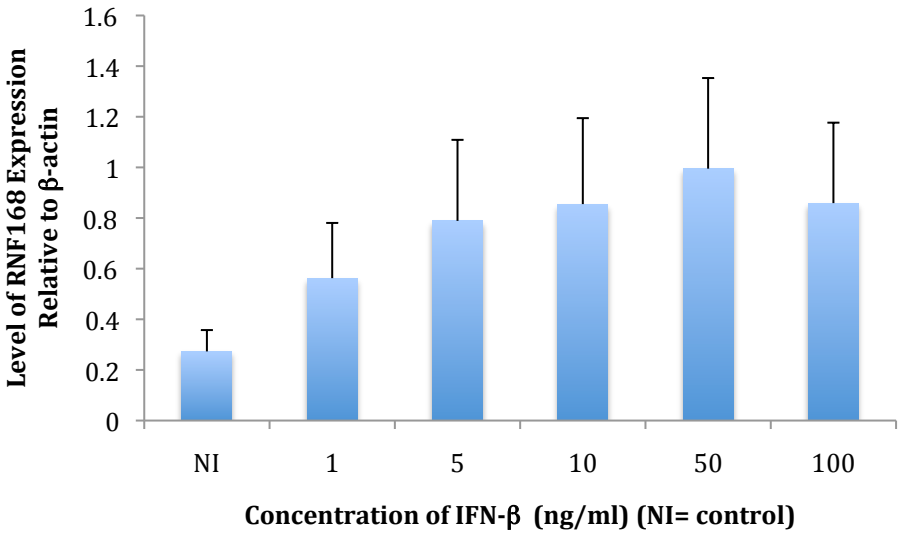

Figure 3.4.4: Means level of RNF168 expression for A549 cells that have undergone IFN-β stimulation for 4 hours with standard error bars. The mean RNF168 expression values from all 3 IFN-β experiments where standard error of mean was calculated to determine the accuracy of the mean values.

Table 3.2.4: P-values for 4 Hours IFN-beta stimulation to determine whether there was any statistical significant (p<0.05) difference between stimulated samples and the control

IFN-β Concentration (ng/ml)	P Value
1	0.17
5	0.17
10	0.15
50	0.14
100	0.17

The lowest value of RNF168 is the control at 0.27 and the highest value is for the 50ng/ml sample at 1 (Figure 3.4.4).

Between NI and 50ng/ml the expression of RNF168 increases as the concentration of IFN-β increases (Figure 3.4.4). The greatest inaccuracy for RNF168 expression values was seen between 5ng/ml and 50ng/ml as these values had the largest standard error bars (Figure 3.4.4).

The comparison between IFN-β stimulated samples and the control shows that there is no statistically significant difference ($P<0.05$) (Table 3.2.4). When comparing IFN-β stimulated samples, the 50ng/ml seemed to have the most significant difference to the control (Table 3.2.4).

3.5.2. Western Blot Data: The effect of Interferon beta Stimulation on RNF168 Expression at 4 Hours relative to control

(a)

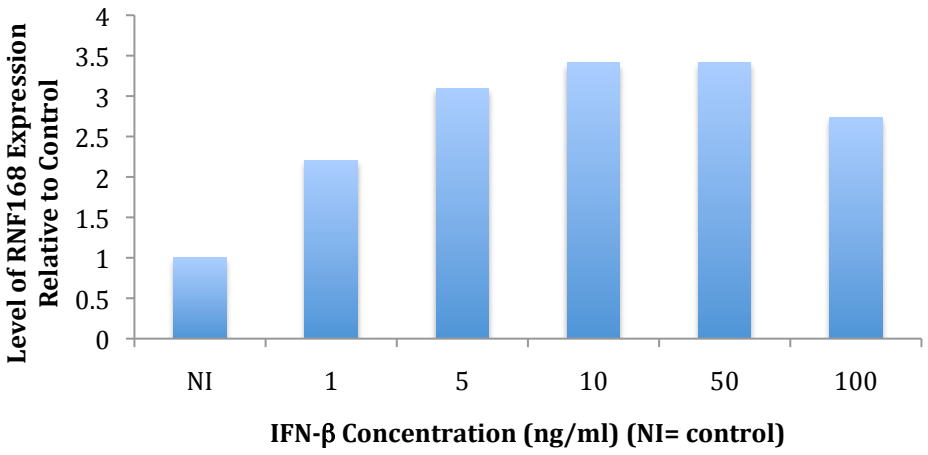

(b)

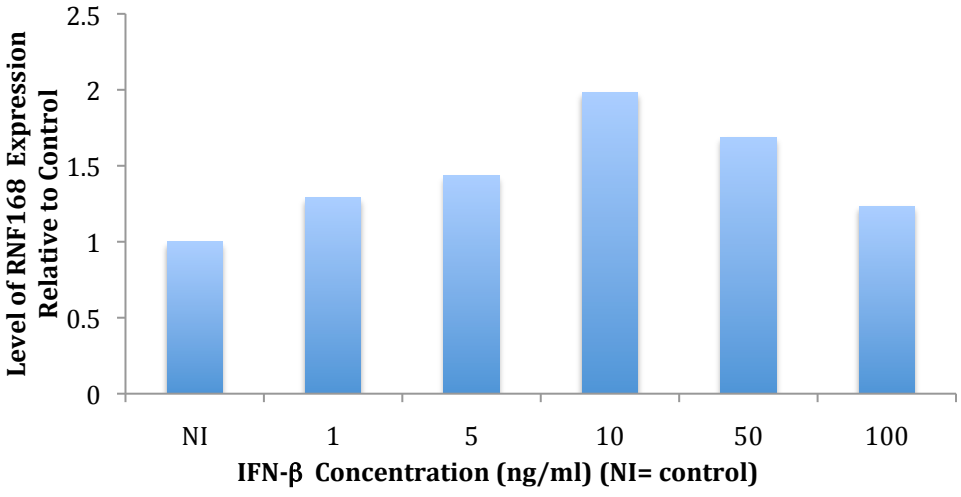

(c)

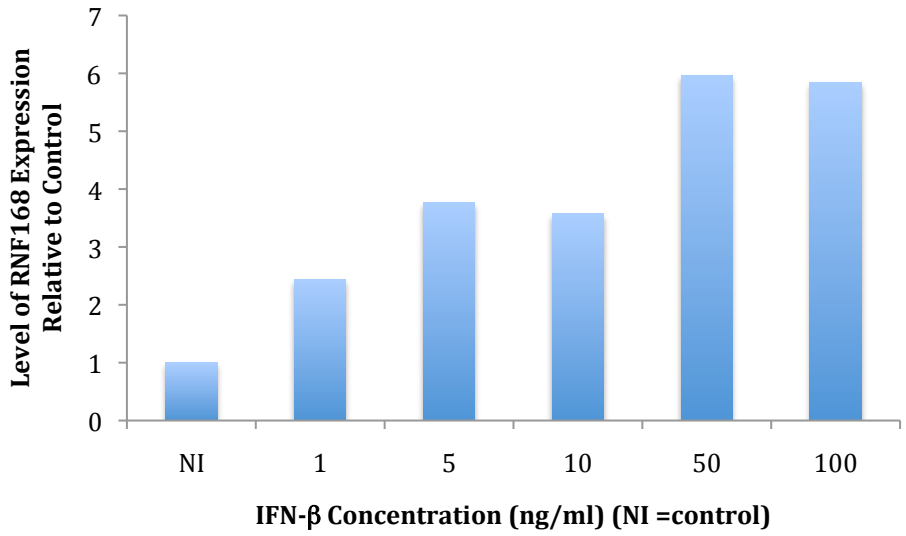

Figure 3.4.5: RNF168 expression relative to control for 4 hours IFN-β stimulation of A549 cells. The level of RNF168 expression in the 3 IFN-β experiments (Figure 3.4.2) calculated relative to the control. This was to standardise number of cells and yield of protein between samples.

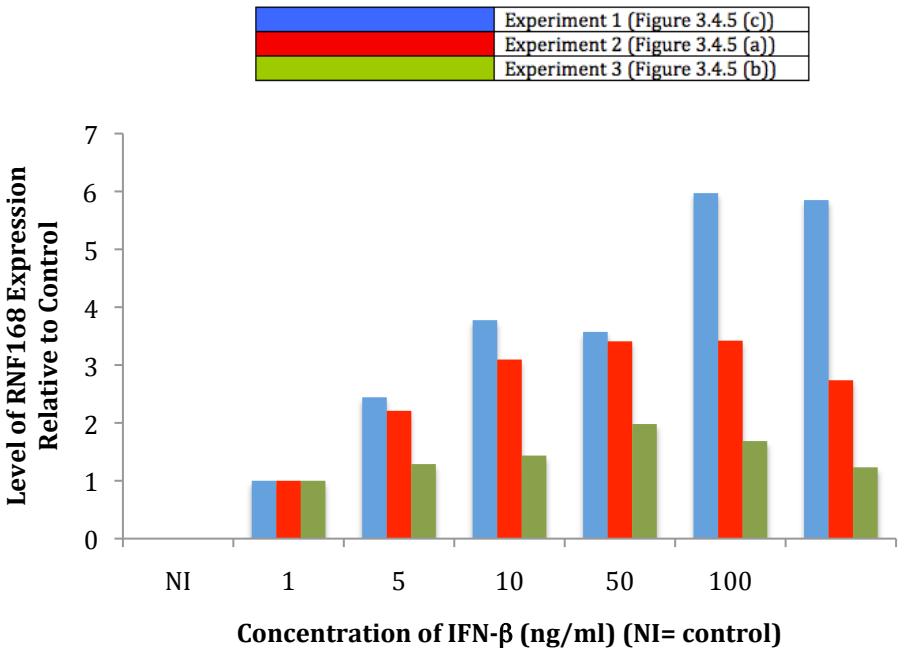

Figure 3.4.6: Combined graph of RNF168 expression relative to control for A549 cells that have been stimulated with IFN-β for 4 hours. The graphs from the 3 IFN-β experiments (Figure 3.4.5) were combined together to provide a clear comparison between data.

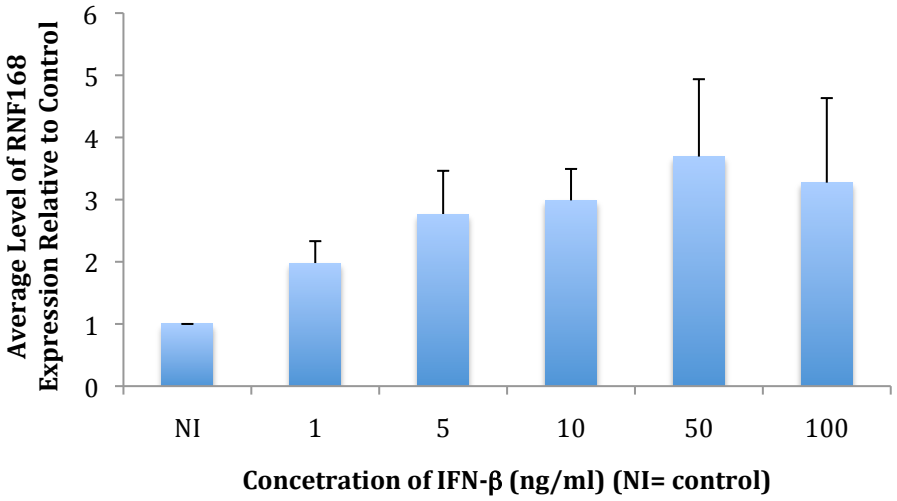

Figure 3.4.7: Mean RNF168 expression relative to control for A549 cells stimulated with IFN-β for 4 hours with standard error bars. Means of RNF168 expression for the 3 experiments were carried out and standard error of the means calculated as errors bars. The error bars show the accuracy of the mean values calculated.

3.6 Measurement of RNF168 Expression for 24 Hours Interferon-beta stimulation

3.6.1. Western Blot Data: The effect of Interferon beta Stimulation on RNF168 Expression at 24 Hours

(a)

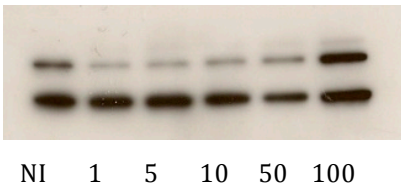

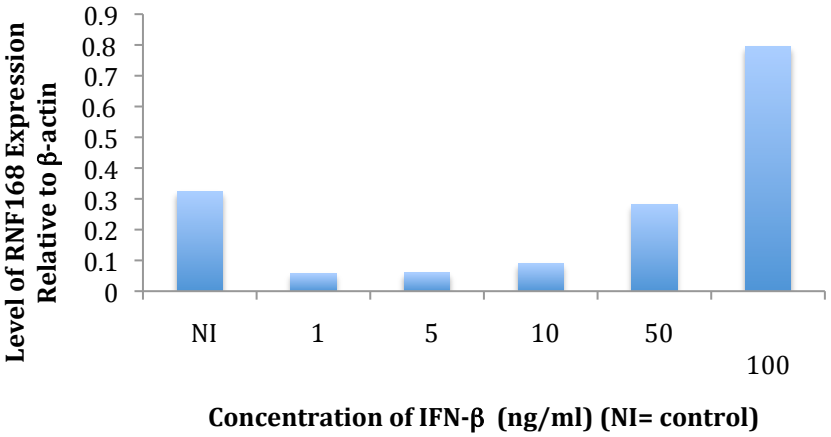

(b)

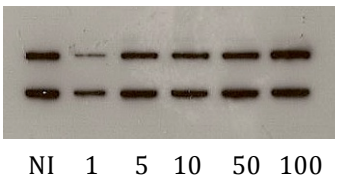

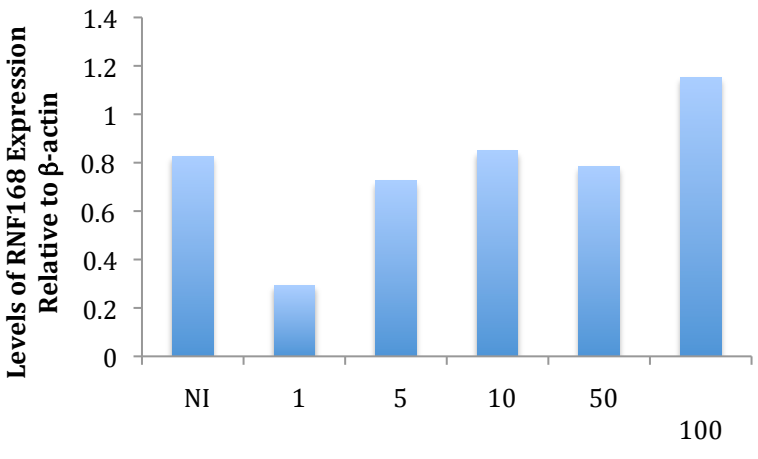

(c)

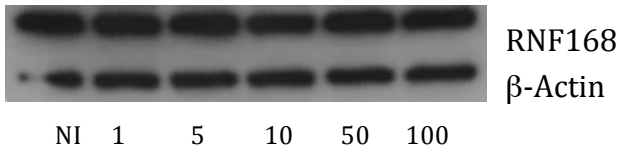

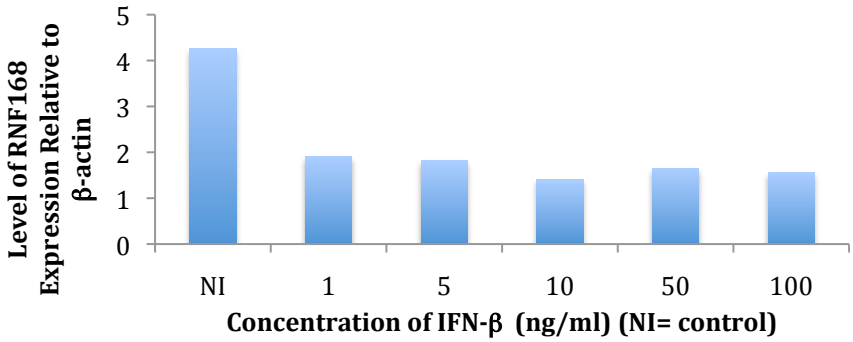

Figure 3.4.8: RNF168 expression for A549 cells stimulated with IFN-β for 24 hours. A549 cells were grown in a confluent 24-well plate and stimulated with IFN-β as a titration experiment for 24 hours. The protein from these cells was harvested and used to run a western blot. This experiment was carried out 3 times.

In two of the experiments in comparison to the control the level of RNF168 expression is lower for 1ng/ml with values 0.057 (Figure 3.4.8 (a)) and 0.29 (Figure 3.4.8 (b)) being the lowest levels of RNF168 in both experiments. The highest level of RNF168 expression was noted at IFN-β concentration 100ng/ml in the same two experiments as 0.79 (Figure 3.4.8 (a)) and 1.15 (Figure (b)). In the other experiments the highest concentration of RNF168 expression was noted for control at 4.27 (Figure 3.4.8 (c)). The lowest level of RNF168 expression for this experiment is at 10ng/ml at 1.41(Figure 3.4.8 (c)).

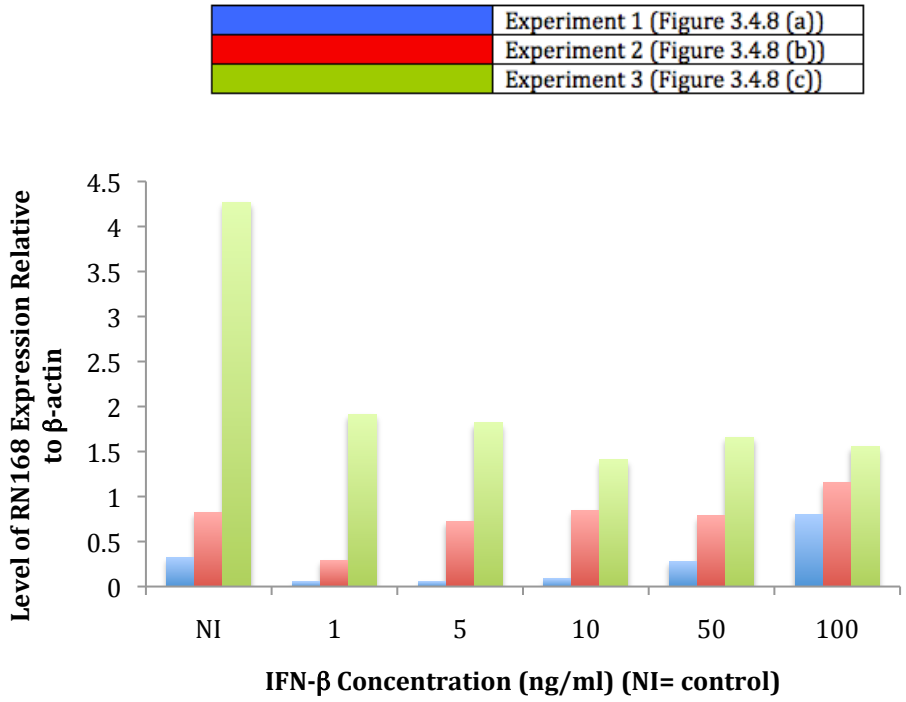

Figure 3.4.9: Combined graph of experiments for IFN-β stimulation of A549 cells for 24 hours. The data from the 3 experiments (Figure 3.4.8) was combined so that a clear and direct comparison could be made.

Experiment 3 had the highest level of RNF168 expression across all samples**.** Experiments 1 and 2 follow a similar pattern of RNF168 expression with a with an increasing RNF168 expression with higher concentration of IFN-β.

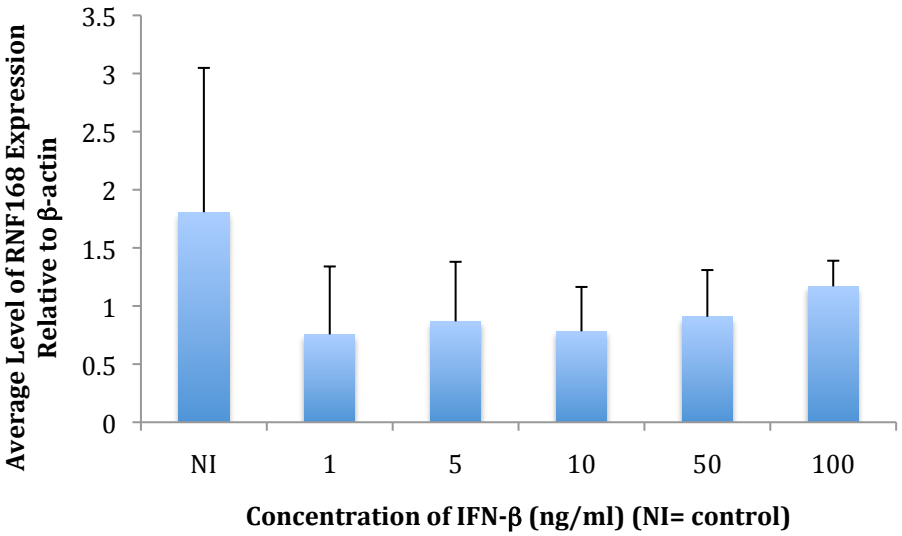

Figure 3.5.1: Mean values for IFN-β stimulation of A549 cells for 24 hours. An mean value for the 3 experiments (Figure 3.4.8) was calculated. The standard error of the mean was also determined as the accuracy of the mean values.

Table 3.2.5: P-values for 24 Hours IFN-β to determine whether there was any statistical significant ($p<0.05$) difference between samples and the control

IFN-β Concentration (ng/ml)	P Value
1	0.25
5	0.34
10	0.38
50	0.40
100	0.60

From the mean values calculated the lowest level of RNF168 expression is at 1ng/ml at 0.75 (Figure 3.5.1). The highest level of RNF168 expression is the control at 1.81 (Figure 3.5.1). Out of the IFN-β stimulated samples, the highest level of RNF168 expression was at 100ng/ml at 1.16 (Figure 3.5.1).

The sample with the largest standard error of the mean value was the control suggesting that this value is the least precise (Figure 3.5.1). There was no statistically significant ($p<0.05$) difference between the IFN-β stimulated samples and control. The greatest difference among stimulated samples to the control was at 1ng/ml ($p<0.25$) (Table 3.2.5).

3.6.2. Western Blot Data: The effect of Interferon beta Stimulation on RNF168 Expression Relative to Control at 24 Hours

(a)

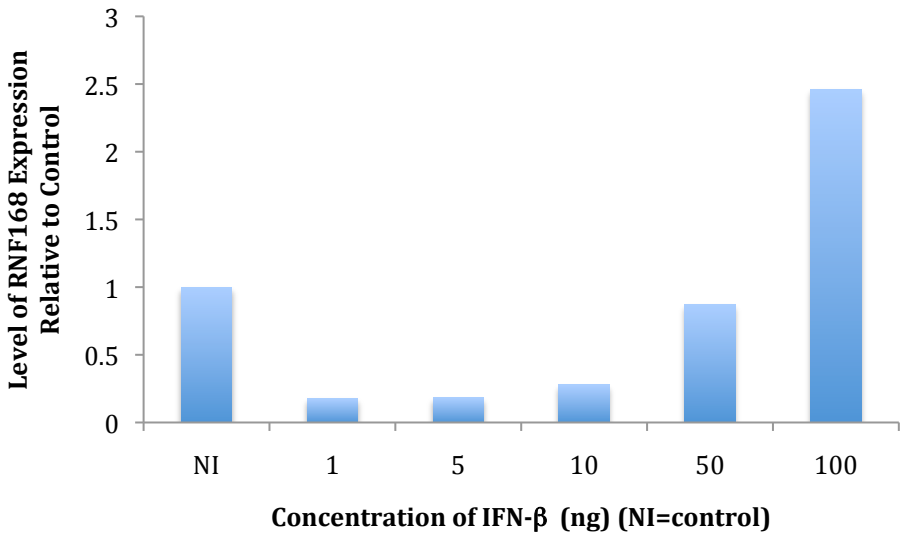

(b)

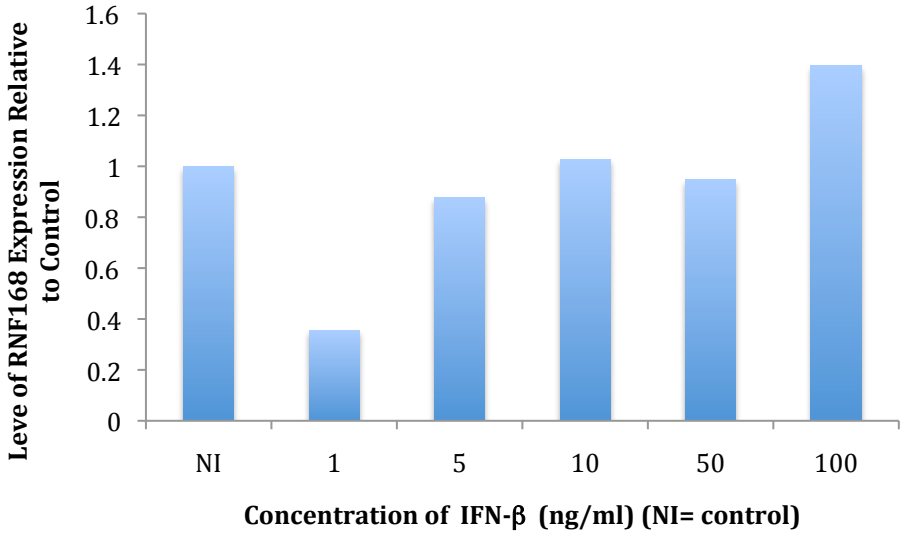

(c)

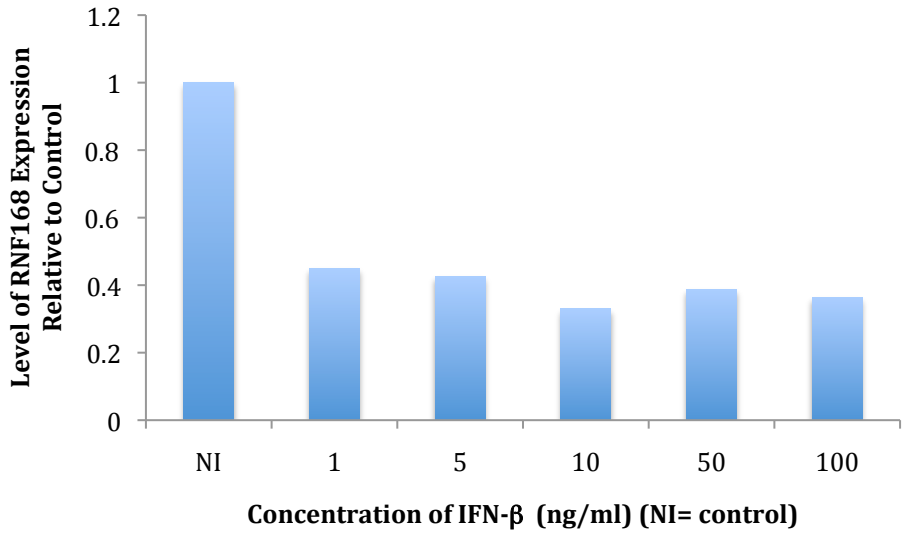

Figure 3.5.2: The level of RNF168 expression relative to control for cells stimulated with IFN-β for 24 hours relative to the control. The level of RNF168 expression was calculated relative to the control to standardise for yield and number of cells from each sample. This experiment was carried out 3 times.

Two experiments show an increase in RNF168 expression for IFN-β stimulated samples as IFN-β concentration increases (Figure 3.5.2 (a) and (b)). The other experiment shows RNF168 expression lower than the control for all IFN-β samples (Figure 3.5.2 (c)). Out of all the experiments, the highest increase in RNF168 expression was the 100ng/ml at 140% in comparison to the control. The biggest decrease was by 82% in comparison to the control (Figure 3.5.2 (a)) at 1ng/ml IFN-β concentration.

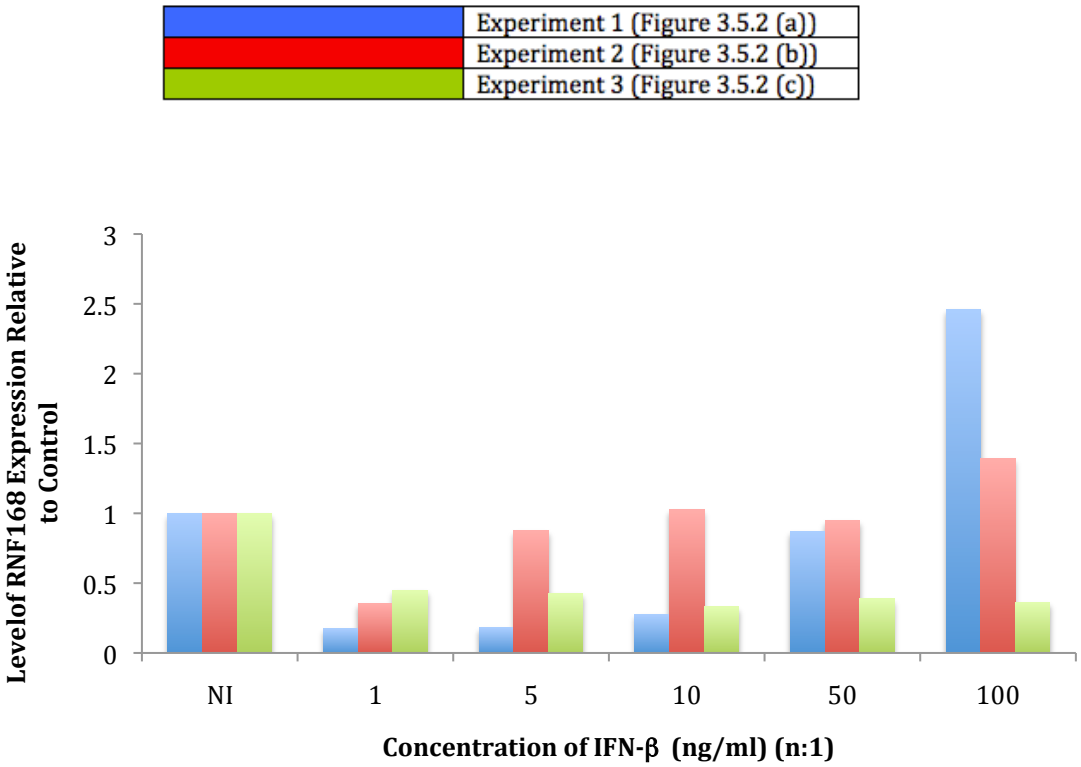

Figure 3.5.3: Combined data of 3 experiments of RNF168 expression relative to control for 24 hours IFN-β stimulation of A549 cells. Data was combined together into a graph to provide a clear comparison between experiments.

Two experiments show an increase in RNF168 expression with increasing IFN-β concentration (Figure 3.5.3 experiment 1 and 2)). However, there is a decrease of 82% (experiment 1) and 64 % (experiment 2) in RNF168 expression between control and IFN-β 1ng/ml for the same 2 experiments (Figure 3.5.3). The highest level of IFN-β expression for the same 2 experiments occurred at 100ng/ml IFN-β concentration (Figure 3.5.3). These values were 146% and 39% greater than the control (Figure 3.5.3). In experiment 3 RNF168 expression was lower in IFN-β stimulated samples.

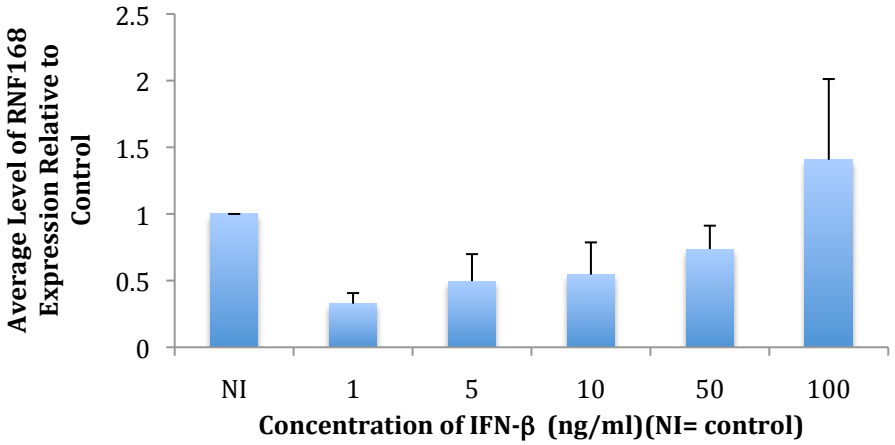

Figure 3.5.4: Mean level of RNF168 expression for A549 cells stimulated with IFN-β. The mean values from all 3 experiments were calculated and standard error of the mean represented as error bars to show the accuracy of the values obtained.

As the concentration of IFN-β increases, the level of RNF168 expression increases (Figure 3.5.4). The lowest value with respect to the control is at 1ng/ml where there is a 67% decrease in RNF168 expression in comparison to the control (Figure 3.5.4). The highest value is at 100ng/ml where RNF168 expression is 40% greater than the control (Figure 3.5.4). The value that is least accurate is at 100ng/ml as it has the largest standard error of the mean (Figure 3.5.4).

3.7 Western Blot Data: The Effect of Duration of Interferon beta stimulation on RNF168 expression

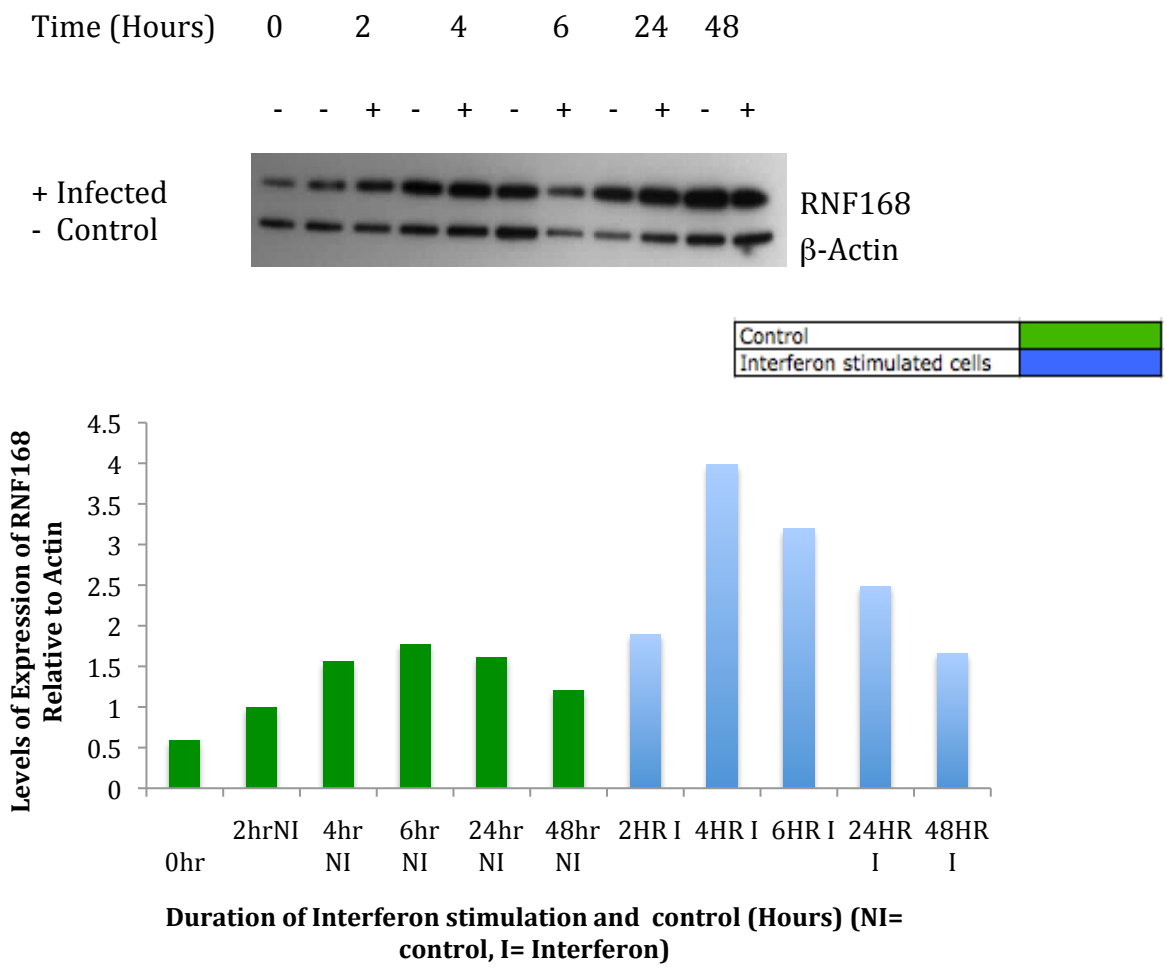

Figure 3.5.5: RNF168 expression for A549 cells stimulated IFN-β for 0, 2, 4, 6, 24 and 48 hours with paired controls. A549 cells grown in a 24-well plate were stimulated with IFN-β at 50ng/ml concentration for time points 0, 2, 4, 6, 24 and 48 hours. 0 hour was taken to be the starting control where cells were not stimulated with IFN-β and were harvested immediately after all of the other wells had been stimulated. For every other time point there was a paired control of cells that had not been stimulated. The protein from these samples was harvested at these time points and used to run a western blot**.** The western blot images underwent densitometry analysis using ImageJ software.

Both control and IFN-β stimulated samples showed an increase in the expression of RNF168 in comparison to the 0 hours control (Figure 3.5.5). This was most evident around 4, 6 and 24 hours (Figure 3.5.5). The lowest level of RNF168 expression was at 0 hours at 0.59 (Figure 3.5.5). The highest level of IFN-β expression was at 4 hours at 3.98 (Figure 3.5.5). The biggest difference between control and IFN-β stimulated samples was seen at 4 hours where the IFN-β stimulated sample was more than 2 fold greater than the 4 hour control (Figure 3.5.5). In both the IFN-β and control samples there was a decrease in RNF168 expression at 48 hours in comparison to 24 hours (Figure 3.5.5). The highest level of RNF168 expression for stimulated samples was at 4 hours whereas for control samples the highest level was at 6 hours.

3.8 Western Blot Data: The Effect of Duration of PolyI:C stimulation on RNF168 Expression

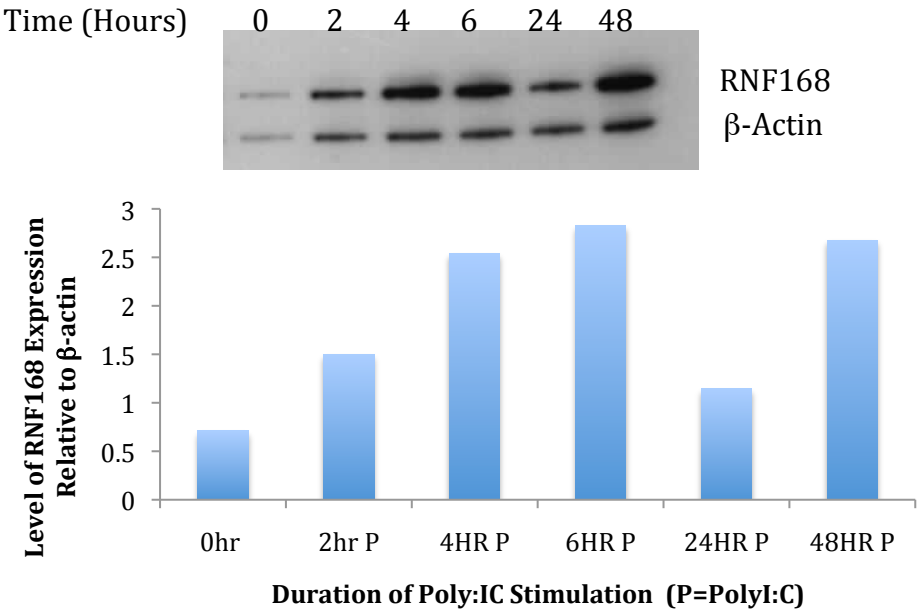

Figure 3.5.6: RNF168 expression for cells stimulated with polyI:C for 0,2, 4, 6, 24 and 48 hours. A549 cells were grown in a 24-well plate and stimulated with polyI:C. The protein from these cells was harvested at 0, 2, 4, 6, 24 and 48 hours. In this experiment there were no paired controls for each time point. 0 hours was taken to be the starting control where cells were not stimulated with polyI:C and were harvested immediately after other samples had been stimulated. The protein from these blots was used to run a western blot. The images were analysed for densitometry using ImageJ software.

The lowest level of RNF168 expression was at 0 hours at 0.71 (Figure 3.5.6). The highest level of RNF168 expression was at 2.83 at 6 hours (Figure 3.5.6). As the duration of polyI:C stimulation increases up to 6 hours, the level of RNF168 expression also increases (Figure3.5.6). There is a considerable decrease in RNF168 expression thereafter at 24 hours (Figure 3.5.6). However, there is an increase after 24 hours with the levels of RNF168 returning to levels comparable to 6 hours at 48 hours (Figure 3.5.6).

3.9 Palivizumab and CXCL5 Data

3.9.1 The Effect of Palivizumab on RNF168 Expression for A549 cells infected with RSV MOI

Samples from the same experiment were used when measuring RSV N gene expression and RNF168 expression (Figure 3.5.7 and Figure 3.5.8).

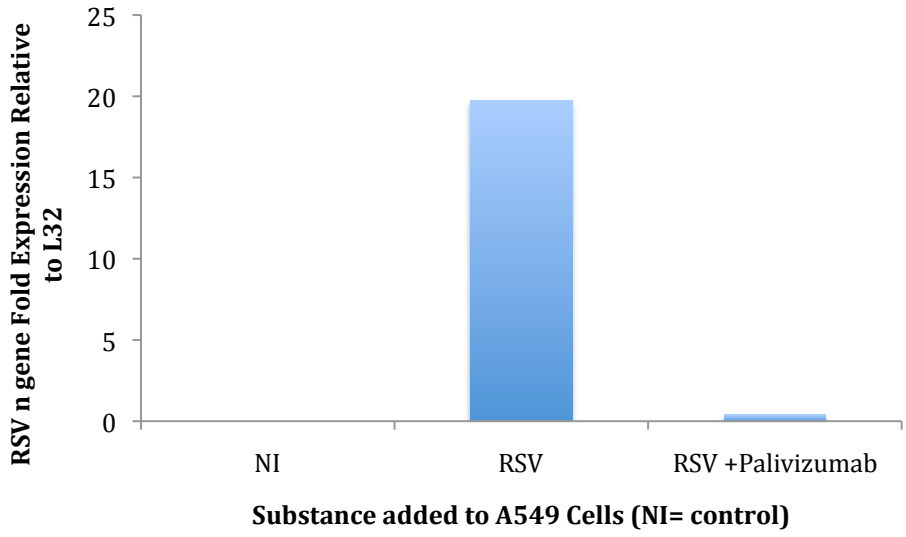

Figure 3.5.7: RSV N gene expression for A549 cells infected with RSV and treated with palivizumab. A549 cells were grown in a confluent 24-well plate. Of the 3 wells containing A549 cells, 1well was used as a control and another infected with RSV MOI 1:1. The third well was infected with RSV MOI 1:1 but palivizumab was added. The RNA from these samples was taken to run real-time PCR.

The lowest level of RSV N gene expression was the control at 1.23 (Figure 3.5.7). The highest level of RSV N gene expression was the RSV infected cells at 19.76 (Figure 3.5.7). In comparison to this sample, the cells that were RSV infected with palivizumab added had far lower levels of RSV N gene expression (Figure 3.5.7).

3.9.2 The Effect of Palivizumab on RNF168 Expression

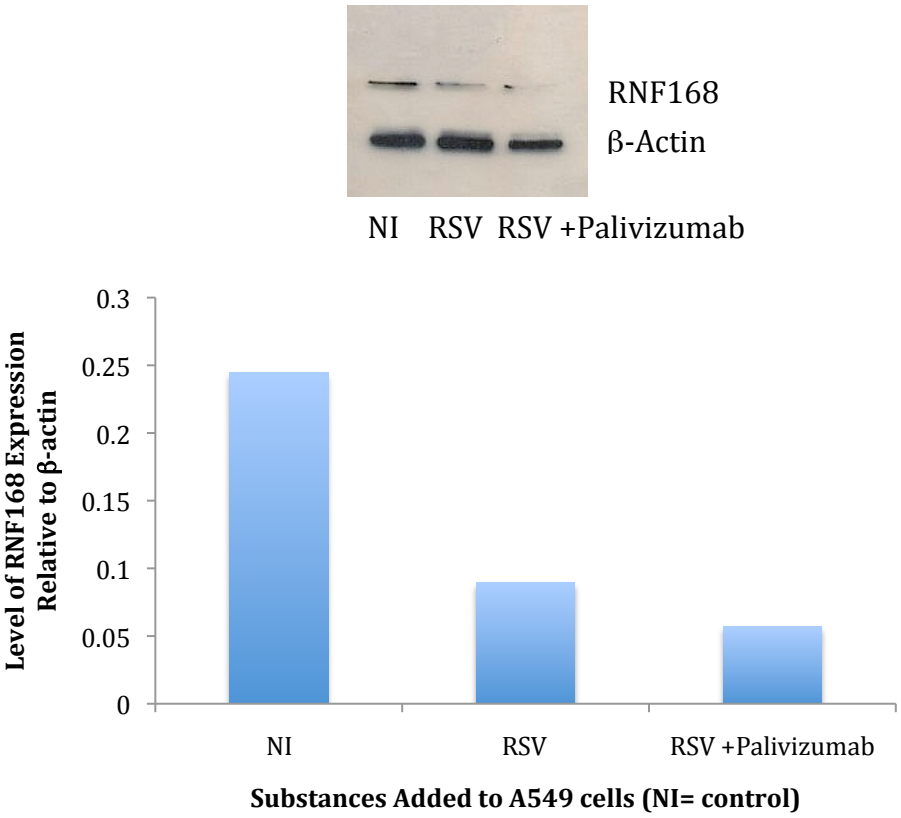

Figure 3.5.8: RNF168 expression for A549 cells infected with RSV and treated with palivizumab. A549 cells were grown in a confluent 24-well plate. Of the 3 wells containing A549 cells, one well was used as a control and another infected with RSV MOI 1:1. The final well was infected with RSV MOI 1:1 but palivizumab was added. The protein from the cells was harvested to run a western blot.

The control has the highest level of RNF168 expression at 0.24 (Figure 3.5.8). The sample with RSV and palivizumab has the lowest level of RNF168 expression at 0.06 (Figure 3.5.8).

3.9.3 The Effect of RSV Infection on CXCL5 Concentrations

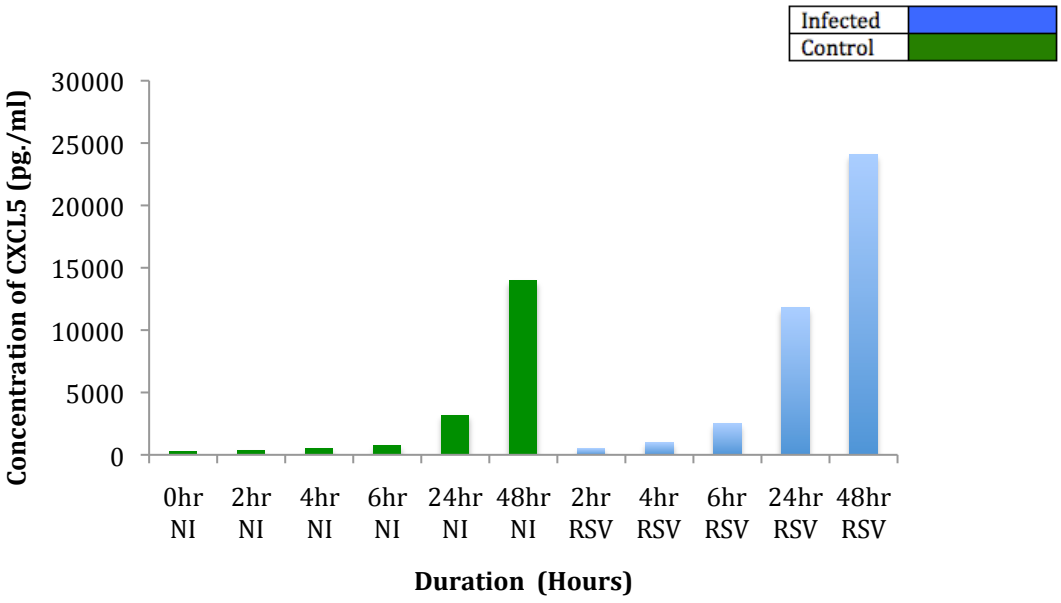

Figure 3.5.9: Concentration levels for CXCL5 for A549 cells infected with RSV for 0, 2,4, 6, 24 and 48 hours. A549 cells were grown in a 24-well plate and infected with RSV at a MOI of 1:1. There were paired controls for 2, 4, 6, 24 and 48 hours. The supernatant was taken from these infected cells and controls at 0, 2, 4, 6, 24 and 48 hours time points to run a CXCL5 Sandwich ELISA. 0 hour was taken to be the starting control where cells were not infected with RSV and were harvested after the samples had been infected.

As time increases the concentration of CXCL5 increases in both infected and non-infected samples (Figure 3.5.9). RSV infected samples have a greater CXCL5 concentration than their paired control for all time points. The lowest concentration of CXCL5 is 250.62 pg/ml for the 0 hours control (Figure 3.5.9). The highest CXCL5 concentration is 24103.79 pg/ml for the 48 hours RSV infection (Figure 3.5.9).

The biggest difference between control and infected samples is at 24 hours where the infected sample is 8574.59 pg/ml greater than the control (Figure 3.5.9). Overall the biggest difference in CXCL5 concentration between infected and control samples occur at 24 and 48 hours (Figure 3.5.9).

4. Discussion

4.1 Evaluation of Results

The mean 4 and 24 hour RSV results for real-time PCR, IL-8 and IL-6 suggest that all infections of A549 cells were carried out accurately (Figures 3.1.3, 3.1.6, 3.1.9, 3.2.8, 3.2.9 and 3.3.1). Mean values show that RSV infected cells had higher levels of RSV N gene expression and concentrations of IL-6 and IL-8 (Figures 3.1.3, 3.1.6, 3.1.9, 3.2.8, 3.2.9 and 3.3.1). The RSV infection time course experiment provided evidence showing that increase duration of infection increased RSV replication (3.3.8). The differences between 4 hours RSV infected samples to the control were statistically significant ($p<0.05$) for IL-6 concentrations (MOI 1:1, $p=0.04$) (Figure 3.1.6), IL-8 concentrations (MOI 1:1,$p= 0.03$) (Figure 3.1.9) but not RSV N gene expression (MOI 1:1, $p= 0.09$)(Figure 3.1.3). This could be due to the samples sizes being relatively small. As result, more repeat experiments for 4 and 24 hours RSV infection could be carried out. Comparisons between the concentration levels of IL-8 in the RSV prep and total IL-8 concentration levels show that the total concentration of IL-8 is greater (Figure 3.2.1). This shows that A549 cells are producing IL-8 in response to RSV infection.

The results from 4 hours RSV infection of A549 cells suggests that RSV causes an increase in RNF168 expression (Figure 3.2.4). It could be inferred that antiviral defence associated with RNF168 is greatest at 4 hours RSV infection when the MOI is 1:1 (Figure 3.2.4). The increase seen in 4 hours RSV infected samples in comparison to the control was not statistically significant (MOI 0.5 $p=0.11$, MOI 1:1 $p=0.13$) (Figure 3.2.4). This may have been due to the relatively small sample size. In comparison, 24 hours RSV infection showed that MOIs 0.25:1 to 1:1 caused a decrease in RNF168 expression, which was not statistically significant (MOI 1:1, $p=0.14$) (Figure 3.5.4). The significance and reliability of this finding could increase if this experiment were repeated.

This result seen at 24 hours RSV infection was supported by the RSV time-course experiment which showed that RNF168 expression decreased in comparison to the control at 24 hours for RSV MOI 1:1 (Figure 3.4.1). Measuring RSV N gene expression implies that greater viral replication occurs after 24 hours (3.3.8). Therefore, at 24 hours RSV infection MOI 1:1, RSV could be overcoming the antiviral defence of RNF168 because there are too many virus particles per cell at a higher RSV MOI.

The IFN-β data shows that there is greater RNF168 expression at 4 hours with higher concentrations of IFN-β (Figure 3.4.4). This finding was not statistically significant (IFN-β 50ng/ml p=0.14, 100ng/ml p=0.17) (Figure 3.4.4) but could be more significant if more experiments were repeated. These findings are supported by an IFN-β time-course experiment where the biggest difference between IFN-β stimulated and control samples was at 4 hours (Figure 3.5.5). Given that IFN-β is released from A549 cells as an innate immune response to RSV it could be proposed that IFN-β is a trigger for RNF168 expression.

When analysing the mean values for 24 hours IFN-β stimulation, lower concentrations of 1ng/ml IFN-β decrease RNF168 expression in comparison to the control (p=0.25). In comparison, higher IFN-β concentrations increased RNF168 expression (p=0.60). Repeat experiments could increase the reliability and significance of these findings. Higher concentrations of IFN-β could be linked to increased RNF168 expression at 4 hours (Figures 3.2.4 and Figure 3.4.4). It could be concluded that the concentration of IFN-β is a factor that has the potential to affect the level of RNF168 expression. Furthermore, these findings may emphasise that time is a factor affecting expression of RNF168 by IFN-β stimulation.

The 4 hours RSV and IFN-β data suggest that IFN-β may play a role in increasing RNF168 expression. This is based on IFN-β concentration 100ng/ml and RSV MOI 1:1 increasing RNF168 expression (Figures 3.2.4 and Figure 3.4.4). 24 hours RSV data suggest that the number of viral particles possibly due to replication overcomes the level of RNF168 expression regardless of IFN-β concentration (Figures 3.3.4, 3.3.8 and 3.5.4). The findings with respect to the 24 Hours experiment have led to the following hypothesis regarding the RSV MOI effect on RNF168 expression (Figure 3.2.4).

At 24 hours when the RSV MOI is low there are very few virus particles per cell. The virus particle is detected by A549 cells, which increase RNF168 expression and increase IFN-β production. This leads to the release of IFN-β from A549 cells and an increase in RNF168 expression. However, the cell, which the virus particle attaches to, experiences a decrease in RNF168 expression as its antiviral defense is overcome. Therefore, when there is a low RSV MOI at 0.025:1 there will be more cells that are not attached to viral particles and expressing RNF168 (3.2.4) (Figure 4.1). However, when the MOI is high at 1:1, there will be more virus particles per cell, which means that more cells will experience a decrease in RNF168 expression (Figure 4.2). This theory can apply to duration of infection as viral replication could exceed cell growth leading to a similar effect.

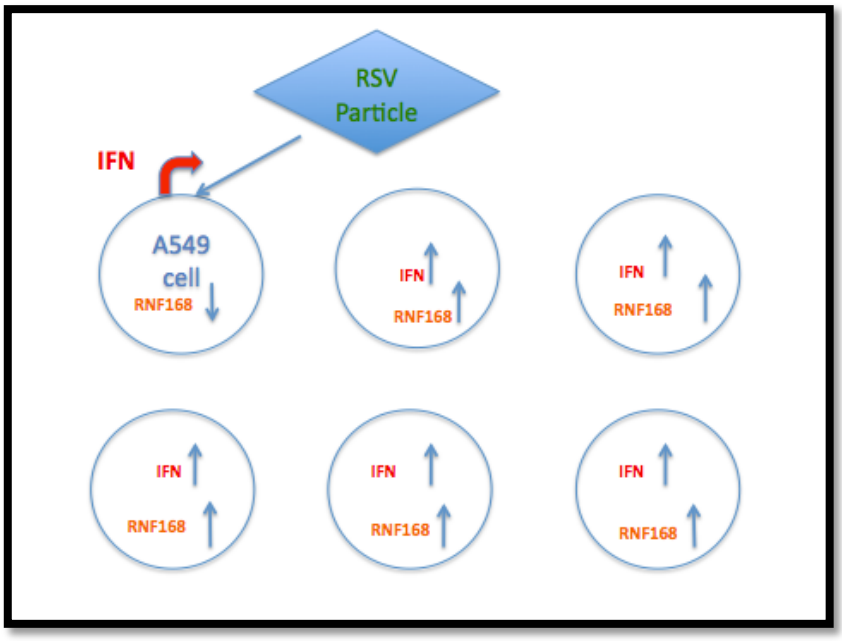

Figure 4.1: Theory behind lower RSV MOI 0.025:1 at 24 hours and effects on RNF168 expression.

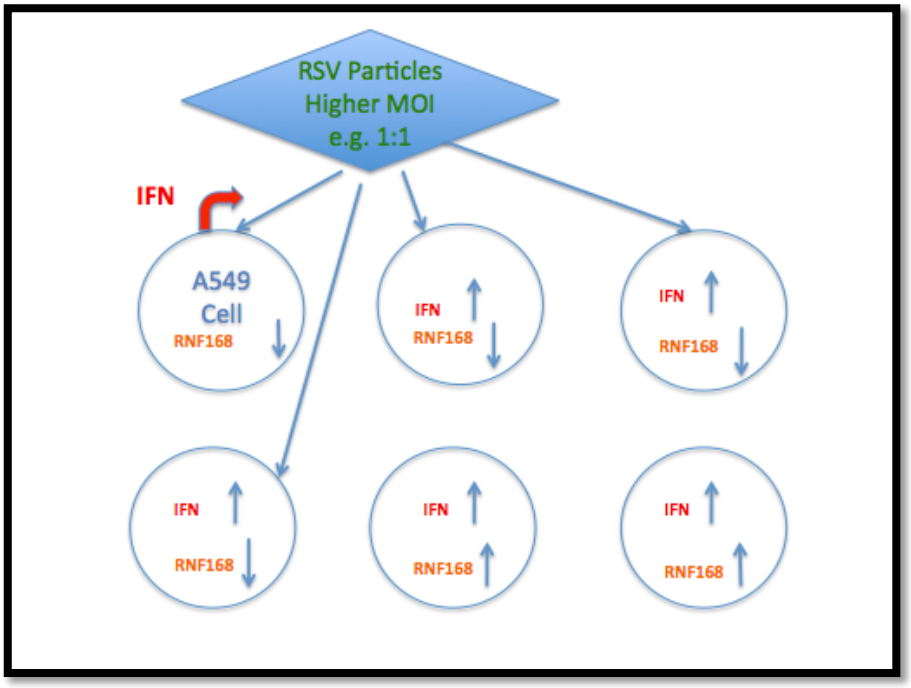

Figure 4.2: **Higher MOI of RSV infection of A549 cells.**

The other major factors affecting RNF168 expression is time. The amount of viral replication increases as time increases. At the same time it also true that cell growth and cell death occurs. This is shown by the PCR data, which highlights RSV N gene expression increasing by approximately 30 fold from 6 to 24 hours RSV infection (Figure 3.3.8). Therefore, at 24 hours, the increased viral replication primarily could contribute to decreased RNF168 expression. The finding in the 24 hours RSV MOI titration experiment are supported by the RSV time-course experiment where the biggest decrease in RNF168 expression was seen at 24 hours for RSV infected samples in comparison to the 24 hours control. However, it should be noted that cell death could contribute to the lower RNF168 expression, as this is more likely for longer time points. Furthermore, it could be that RSV has reduces cell growth and through replication leads to less cells being capable of expressing RNF168.

There was an indication that polyI:C increased RNF168 expression over an increased duration of cell stimulation with the highest levels of expression seen at 6 hours (Figure 3.5.6). In all samples other than the 24 hours control there was an increase in RNF168 expression in comparison to the control (Figure 3.5.6). It could be assumed that the result at 24 hours was an anomaly (Figure 3.5.6). Regardless of whether this was true, stimulation of polyI:C has suggested the TLR3 receptor may play a role in the pathway leading to RNF168 expression. PolyI:C has a role in stimulating type 1 interferon production. Therefore, interferon could be having an indirect on RNF168 expression (165). To reliably establish that there is a significant relationship between polyI:C and RNF168 expression this polyI:C experiment must be repeated.

The PCR data from the palivizumab experiment suggests that the palivizumab used is effective at reducing the RSV N gene expression indicative of palivizumab blocking viral infection (Figure 3.5.7). A western blot was carried out on the same samples with the purpose of showing that it was RSV that was affecting RNF168 expression and not another factor present in the RSV prep or the media in which the A549 cells were grown. If this were correct the level of RNF168 expression in the palivizumab sample would be comparable to the control rather than the sample infected with RSV MOI 1:1. Results indicated that RNF168 expression was affected by another factor than RSV (Figure3.5.8).

This was because the level of RNF168 expression in the palivizumab treated sample was lower than the RSV only treated sample (Figure 3.5.8). The protein loading represented by β-actin expression was uneven with the palivizumab sample having the least amount (Figure 3.5.8). If protein in the palivizumab treated sample had been equal to the other samples it may have been possible that RNF168 expression would have been stronger for the palivizumab treated sample. This may have affected the RNF168 expression value obtained despite a relative ratio being calculated. To verify these findings this experiment must be repeated before any other RSV experiments are carried out.

The findings from this investigation suggest that RSV affects RNF168 expression. However, to confirm that RSV is responsible for RNF168 expression the Western blot experiment with palivizumab will have to be repeated. This must show that RNF168 expression is at a relatively similar level to the control, for the palivizumab treated sample. If this experiment is successful, further experiments must be carried out with interferon, RSV and polyI:C. Only then can experiments associated with existing literature be carried out to determine if the mechanism by which RNF168 expression is being regulated by RSV is similar to herpes simplex virus type 1 (HSV-1) (121).

4.2 Comparison to Existing Literature

RSV at an MOI of 1:1 decreased the level of RNF168 expression at 24 hours in comparison to the control. This supports the previous work that when RNF168 was knocked down, RSV N gene expression increases suggesting that RNF168 has an antiviral defense role in RSV.

A HSV-1 paper showed that RNF168 had an antiviral defense role in recruiting repair factors to the site of DSBs by functioning as an E3 ligase and modifying histone proteins. The paper concluded that a HSV-1 protein ICP0 functioned as an E3 ligase causing the degradation of RNF168 by ubiquitination(121). HeLa cells underwent infection with wild type (WT) HSV-1. The WT showed a decrease in RNF168 expression at 2 hours post-infection with a MOI of 5:1 (Figure 1.1.3) (121). Similar results were seen when A549 cells were infected with RSV in a RSV time-course experiment, which noted a decrease in the RSV infected sample at 2 hours in comparison to the control.

At 2 hours a MOI titration experiment could be done to investigate effects on RNF168 expression in detail at 2 hours. The RSV time-course experiment showed a decrease at all other time points in comparison to the control. To gain a better understanding of the relationship between duration of infection and RNF168 expression titration experiments could also be done for time points between 4 and 24 hours such as 12 hours.

The biggest decrease in RNF168 expression due to RSV occurred at 24 hours at MOI 1:1 as shown by the 24 hours RSV titration experiment. These findings were supported by the RSV time-course experiment where the biggest decrease in the infected sample in comparison to the control occurred at 24 hours. Hence, in comparison to HSV-1, a lower viral MOI causes a significant decrease in RNF168 expression over a longer period of time as there is less virus particles per cell for the RSV experiments meaning that time must be allowed for viral replication.

Another possible explanation could be that the cell types in these investigations were different and that other factors could be involved such as the rate of cell replication and growth in relation to the number of viral particles. Both HSV-1 and RSV have different processes of replication with HSV-1 virus particle replicating in the nucleus allowing it to have a direct effect on histones. In comparison, RSV replicates in the epithelial cytoplasm and therefore any modification of histones by RSV could be a result of changes occurring in the cytoplasm (121).

The primary focus of the HSV-1 experiment was ICP0, an immediate early gene protein that is the essential to lytic HSV-1 viral replication. Results from this paper showed that it was specifically ICP0 that caused degradation of RNF168 E3 ubiquitin ligase as no significant changes in RNF168 expression were seen with ICP0 null virus (121). RSV does not have an ICP0 protein present in its viral structure. Instead there may be other proteins in viral structure that may exhibit E3 ligase activity, playing a similar role to ICP0. For example, nonstructural protein 1 (NS1), which is found in the cytoplasm and the nucleus during RSV infection, was found to influences HOX gene expression through monoubiquitination histone H2B of the elongin cullin E3 ligase activity (71). Protein such as these could be identified and investigated further to see if they have a direct influence on RNF168.

To determine that ubiquitination of histone H2A was implicated in the role of RNF168 in antiviral defense a HSV-1 WT time course was carried out for ubiquitinated H2A (uH2A) expression. This showed a loss of ubiquitinated H2A at 2 hours post-infection (Figure 1.1.3) (121). To show that RSV is causing histone ubiquitination a RSV infection time-course could be run with samples used for a Western blot for uH2A. Based on the RSV results obtained so far it could be hypothesised that loss of ubiquitinated H2A could occur at 24 hours, as this was lowest level of RNF168 expression seen.

The protein Ubc13 is used as a conjugating enzyme to ubiquitinate H2A. The HSV-1 paper found that there were no decreased levels of Ubc13 during the time-course of viral infection. UBc13 investigation could be carried out as a time-course experiment of RSV infection. The results could help to determine the mechanism by which RSV is affecting RNF168 expression and whether the process of ubiquitination is involved (121).

To verify that RNF168 was undergoing proteasome-mediated degradation, HSV-1 experiments were carried out with proteasome inhibitor. This showed that the proteasome inhibitor prevented the degradation of RNF168 for the HSV-1 paper (121). A similar experiment could be carried out with RSV infected cells. If the findings were similar to that seen in the HSV-1 paper then it would provide support that the changes in RNF168 expression occurring could be due to ubiquitination.

Experiments were carried with IFN-β and polyI:C found changes in RNF168 expression. Both of these stimuli were not used in the HSV-1 paper. There is limited literature available regarding the interaction of IFN-β and polyI:C with RNF168. However, this investigation does provide new evidence that such a relationship does exist. More experiments with polyI:C must be carried out to provide detailed evidence that it is affecting RNF168 expression. To show that it is IFN-β having a direct effect on RNF168, experiments must be carried out with anti-interferon.

If the findings of these experiments support the results already obtained, then there will be more evidence about how the mechanism by which RSV affects RNF168 expression could differ to HSV-1.

Previous work on CXCL5 showed that CXCL5 expression was highest in RSV infected samples at 6 hours. From the results obtained it was clear that the concentration of CXCL5 was greater than the control at 6 hours. However, the biggest increase in CXCL5 in infected samples in comparison to the control at the same time point was seen at 24 and 48 hours. Therefore, the data provides supporting evidence that CXCL5 could be involved in early neutrophil recruitment during RSV infection. However, this experiment needs to be repeated to provide detailed evidence of the relationship between duration of RSV infection and the concentration of CXCL5.

4.3 Future Work Priorities

The time allowed to complete this project was only one year. If there were more time more experiments would have been carried out to investigate how RSV affects RNF168 expression. These experiments are discussed in this section.

The data from the palivizumab experiment indicated that RSV was not the primary component causing a decrease RNF168 expression. This was because the A549 cells stimulated with RSV (MOI 1:1) and palivizumab for 24 hours showed a decrease in RNF168 expression in comparison to the control. It was expected that RNF168 expression in this sample would be equal to the control, as the RSV has been neutralised by the palivizumab. To validate these findings this experiment will have to be repeated at least two further times. Results will include RSV N gene expression and Western blot data available for each set of samples. If the results suggest that RSV is directly affecting RNF168, then other experiments can be carried out to investigate this relationship in further detail.

Of the 24 hours RSV MOI titration experiments carried out, only one experiment had PCR and ELISA data available for the same sample used to run a western blot. More repeat experiments with RSV N gene expression, IL-6 and IL-8 data for 24 hours RSV

MOI titration could be carried out to further increase the reliability of any proposed relationship between RNF168 expression and RSV.

An experiment was carried out to show that the A549 cells were producing IL-8 and that the IL-8 result recorded by IL-8 Sandwich ELISA was not due to the RSV prep added. This experiment could be done for IL-6 to show that A549 cell are releasing IL-6 in response to RSV infection.

Given that RSV MOI 0.025:1 showed an increased RNF168 expression in comparison to the control at 24 hours, a time course experiment involving RSV MOI 1:1 could be done. The time points would be 0, 2, 4, 6, 24 and 48 hours where there would be a control for each time point. 0 hour would be a starting control where the cells would be harvested immediately after all other samples had been infected with RSV. The experiment would be repeated 3 times. This would provide evidence of how a lower RSV MOI affects RNF168 expression with respect to duration of infection. RSV N gene expression, IL-6 and IL-8 data would also be obtained for all samples.

To provide a more detailed and accurate interpretation of a relationship between RNF168 and duration of RSV infection more RSV time course experiments must be carried out. A preliminary experiment was carried out which only gave data between 0 and 24 hours. The future experiments would involve RSV infection for 0, 2, 4, 6, 24 and 48 hours with controls for each time point where 0 hour is a starting control. This experiment would be carried out at least 3 times with RSV N gene expression, IL-6 and IL-8 data available for all samples. Carrying out this experiment would lead to a reliable evaluation of the relationship between RNF168 expression and duration of RSV infection.

Only 1 IFN-β time course experiment has been carried out. This should be repeated to provide reliable and accurate evidence regarding the relationship between duration of IFN-β stimulation and RNF168 expression. Stimulation should be carried out with 50ng/ml, as this was the concentration where RNF168 expression was highest in comparison to control. This was also the concentration used in the original IFN-β time-course experiment.

An experiment must also be done with anti-interferon beta. The function of anti-interferon beta is to neutralise the effects of IFN-β. IFN-β and anti-interferon beta will be added to A549 cells for 4 and 24 hours. If the level of RNF168 expression in samples is comparable to the control then it could be concluded that IFN-β stimulation has a direct effect on RNF168 expression. This is because anti-interferon has blocked the effect that IFN-β stimulation has on RNF168 expression.

A single experiment regarding polyI:C stimulation was carried out. This was a time-course experiment and needs to be repeated at least 2 further times. PolyI:C titration experiments need to be carried out at 4 and 24 hours. A459 cells will be stimulated with different concentrations of polyI:C and harvested at 4 and 24 hours. Experiments will be carried out a minimum of 3 times for both time points. The purpose of this experiment will be to establish the effect that different concentrations of polyI:C have on RNF168 expression with respect to each time point. Furthermore, titration experiments at 4 and 24 hours may provide more evidence that TLR3 is implicated in the mechanism regulating RNF168 expression.

With regards to the quality of western blot data it was clear that the protein loading was uneven as indicated by the expression of β-actin for each sample in some experiment. A technique that could have been implemented in the future could be the use of the Bradford protein assay. This involves measuring the concentration of protein in each sample before loading the protein into a western blot gel. Calculations can then be done to find out the correct amount of protein that needs to be loaded for each sample to get even loading across all samples. A Bradford assay was not done because time taken to do one would have limited the amount of data that could be taken from experiments. An alternative to a Bradford assay, samples were re-run adjusting for protein loading based on the first western blot image and the amount of protein loaded to get this image. However, if a Bradford assay could be done in the future if more cases of uneven loading arise.

Previous work on CXCL5 showed that CXCL5 expression was highest in RSV infected sample at 6 hours. From the results obtained it was clear that the concentration of CXCL5 was greater than the control at 6 hours. However, the biggest increase in CXCL5 in infected samples in comparison to the control at the same time point was seen at 24 and 48 hours. Therefore, the data provides supporting evidence that CXCL5 could be involved in early neutrophil recruitment during RSV infection and may have a bigger impact on neutrophil recruitment at later time points of infection. However, repeat experiments need to be carried out in order to provide detailed evidence of the relationship between the duration of RSV infection and the concentration of CXCL5.

5. Concluding Remarks

This investigation suggests that RSV affects RNF168 expression. However, before any further RSV experiments are done the experiment involving palivizumab must be repeated to show that RSV affects RNF168 expression and not any other factor. This investigation suggests that RNF168 is affected by RSV MOI infection at 4 hours and 24 hours. Results imply that MOI of RSV and duration of infection are factors in influencing the level of RNF168 expression. However, to increase the reliability and the significance of results, RSV, IFN-β and polyI:C experiments should be repeated to increase the sample size.

The findings from this investigation also show that IFN-β and polyI:C may be implicated in the mechanism by which RSV affects RNF168 expression and that this mechanism may differ to that demonstrated in the HSV-1 paper. Nevertheless, experiments similar to the HSV-1 paper with uH2A and protease inhibitor should be done to confirm whether ubiquitination is involved. Furthermore, to provide evidence that IFN-β is affecting RNF168 and not any other factors experiments must be done with anti-interferon.

Results from the CXCL5 experiment supports previous findings that this cytokine is expressed more at 6 hours RSV infection in comparison to the control. However, this experiment has been carried out once and will have to be repeated to provide more evidence of a relationship between duration of RSV infection and CXCL5 expression.

6. References

1. Law BJ, Carbonell-Estrany X, Simoes EA. An update on respiratory syncytial virus epidemiology: a developed country perspective. Respiratory medicine. 2002 Apr;96 Suppl B:S1-7. PubMed PMID: 11996399.
2. Blanchard SS, Gerrek M, Siegel C, Czinn SJ. Significant morbidity associated with RSV infection in immunosuppressed children following liver transplantation: Case report and discussion regarding need of routine prophylaxis. Pediatr Transplant. 2006 Nov;10(7):826-9. PubMed PMID: WOS:000241109800013. English.
3. Borchers AT, Chang C, Gershwin ME, Gershwin LJ. Respiratory Syncytial Virus-A Comprehensive Review. Clinical reviews in allergy & immunology. 2013 Apr 12. PubMed PMID: 23575961.
4. Johnson PR, Collins PL. The 1B (NS2), 1C (NS1) and N proteins of human respiratory syncytial virus (RSV) of antigenic subgroups A and B: sequence conservation and divergence within RSV genomic RNA. The Journal of general virology. 1989 Jun;70 (Pt 6):1539-47. PubMed PMID: 2525176.
5. Power UF. Respiratory syncytial virus (RSV) vaccines--two steps back for one leap forward. Journal of clinical virology : the official publication of the Pan American Society for Clinical Virology. 2008 Jan;41(1):38-44. PubMed PMID: 18340669.
6. Jones R, Shah S, MacMahon EE, Goldsmith DJ. Respiratory syncytial virus pneumonitis complicating immunosuppressive treatment for ANCA-positive vasculitis. Nephrology, dialysis, transplantation : official publication of the European Dialysis and Transplant Association - European Renal Association. 2003 Sep;18(9):1920-2. PubMed PMID: 12937244.
7. Hall CB. The nosocomial spread of respiratory syncytial viral infections. Annual review of medicine. 1983;34:311-9. PubMed PMID: 6344761.
8. Adams JM, Imagawa DT, Zike K. Epidemic bronchiolitis and pneumonitis related to respiratory syncytial virus. JAMA : the journal of the American Medical Association. 1961 Jun 24;176:1037-9. PubMed PMID: 13681401.
9. Ogra PL. From chimpanzee coryza to palivizumab: changing times for respiratory syncytial virus. The Pediatric infectious disease journal. 2000 Aug;19(8):774-9; discussion 811-3. PubMed PMID: 10959757.
10. Simoes EA. Respiratory syncytial virus infection. Lancet. 1999 Sep 4;354(9181):847-52. PubMed PMID: 10485741.
11. Chanock R, Roizman B, Myers R. Recovery from infants with respiratory illness of a virus related to chimpanzee coryza agent (CCA). I. Isolation, properties and characterization. American journal of hygiene. 1957 Nov;66(3):281-90. PubMed PMID: 13478578.
12. Hemming VG, Prince GA, Groothuis JR, Siber GR. Hyperimmune globulins in prevention and treatment of respiratory syncytial virus infections. Clinical microbiology reviews. 1995 Jan;8(1):22-33. PubMed PMID: 7704893. Pubmed Central PMCID: 172847.
13. Organisation WH. Acute Respiratory Infections (Update September 2009) World Health Organisation2009 [updated 2009; cited 2013 6th August]. Available from: http://www.who.int/vaccine_research/diseases/ari/en/index2.html.
14. Openshaw PJ, Chiu C. Protective and dysregulated T cell immunity in RSV infection. Current opinion in virology. 2013 Jun 24. PubMed PMID: 23806514.
15. Nair H, Nokes DJ, Gessner BD, Dherani M, Madhi SA, Singleton RJ, et al. Global burden of acute lower respiratory infections due to respiratory syncytial virus in

young children: a systematic review and meta-analysis. Lancet. 2010 May 1;375(9725):1545-55. PubMed PMID: 20399493. Pubmed Central PMCID: 2864404.
16. Agency HP. Laboratory reports received by HPA Colindale of infections due to respiratory syncytial virus, England and Wales, by date of report 1991-2013 (4 weekly) 2013 [updated 20th March 2013; cited 2013 6th August]. Available from: http://www.hpa.org.uk/webc/HPAwebFile/HPAweb_C/1194947411794.
17. Agency HP. Laboratory reports of RSV received by HPA Colindale from NHS and HPA laboratories, by date of specimen and age, 2012/13 2013 [updated 20th March; cited 2013 6th August]. Available from: http://www.hpa.org.uk/webc/HPAwebFile/HPAweb_C/1194947408453.
18. Cormier SA, You D, Honnegowda S. The use of a neonatal mouse model to study respiratory syncytial virus infections. Expert review of anti-infective therapy. 2010 Dec;8(12):1371-80. PubMed PMID: 21133663. Pubmed Central PMCID: 3033119.
19. Shay DK, Holman RC, Newman RD, Liu LL, Stout JW, Anderson LJ. Bronchiolitis-associated hospitalizations among US children, 1980-1996. JAMA : the journal of the American Medical Association. 1999 Oct 20;282(15):1440-6. PubMed PMID: 10535434.
20. Welliver RC. Review of epidemiology and clinical risk factors for severe respiratory syncytial virus (RSV) infection. The Journal of pediatrics. 2003 Nov;143(5 Suppl):S112-7. PubMed PMID: 14615709.
21. Hall CB, Weinberg GA, Blumkin AK, Edwards KM, Staat MA, Schultz AF, et al. Respiratory syncytial virus-associated hospitalizations among children less than 24 months of age. Pediatrics. 2013 Aug;132(2):e341-8. PubMed PMID: 23878043.
22. Hall CB. Respiratory syncytial virus and parainfluenza virus. The New England journal of medicine. 2001 Jun 21;344(25):1917-28. PubMed PMID: 11419430.
23. Handforth J, Friedland JS, Sharland M. Basic epidemiology and immunopathology of RSV in children. Paediatric respiratory reviews. 2000 Sep;1(3):210-4. PubMed PMID: 12531081.
24. Respiratory Syncitial Virus (RSV) American Lung Association2008 [cited 2013 15 January].
25. Thomsen SF, Stensballe LG, Skytthe A, Kyvik KO, Backer V, Bisgaard H. Increased concordance of severe respiratory syncytial virus infection in identical twins. Pediatrics. 2008 Mar;121(3):493-6. PubMed PMID: 18310197.
26. Zoeller RF, Stout JR, O'Kroy J A, Torok DJ, Mielke M. Effects of 28 days of beta-alanine and creatine monohydrate supplementation on aerobic power, ventilatory and lactate thresholds, and time to exhaustion. Amino acids. 2007 Sep;33(3):505-10. PubMed PMID: 16953366.
27. Carbonell-Estrany X, Quero J, Group IS. Hospitalization rates for respiratory syncytial virus infection in premature infants born during two consecutive seasons. The Pediatric infectious disease journal. 2001 Sep;20(9):874-9. PubMed PMID: 11734767.
28. Carbonell-Estrany X, Quero J, Bustos G, Cotero A, Domenech E, Figueras-Aloy J, et al. Rehospitalization because of respiratory syncytial virus infection in premature infants younger than 33 weeks of gestation: a prospective study. IRIS Study Group. The Pediatric infectious disease journal. 2000 Jul;19(7):592-7. PubMed PMID: 10917214.
29. Sethi S, Murphy TF. RSV infection--not for kids only. The New England journal of medicine. 2005 Apr 28;352(17):1810-2. PubMed PMID: 15858191.
30. Peltola V, Ruuskanen O. Editorial commentary: Respiratory viral infections in developing countries: common, severe, and unrecognized. Clinical infectious diseases :

an official publication of the Infectious Diseases Society of America. 2008 Jan 1;46(1):58-60. PubMed PMID: 18171214.
31. Thorburn K, Harigopal S, Reddy V, Taylor N, van Saene HK. High incidence of pulmonary bacterial co-infection in children with severe respiratory syncytial virus (RSV) bronchiolitis. Thorax. 2006 Jul;61(7):611-5. PubMed PMID: 16537670. Pubmed Central PMCID: 2104657.
32. Barreira ER, Precioso AR, Bousso A. Pulmonary surfactant in respiratory syncytial virus bronchiolitis: The role in pathogenesis and clinical implications. Pediatric pulmonology. 2010 Dec 30. PubMed PMID: 21194166.
33. Kleiboeker S. The nose knows: RSV and HRV. MLO: medical laboratory observer. 2010 Jun;42(6):10-2, 4; quiz 6-7. PubMed PMID: 20632623.
34. Butt ML, Symington A, Janes M, Elliott L, Steele S, Paes BA. The impact of prophylaxis on paediatric intensive care unit admissions for RSV infection: a retrospective, single-centre study. European journal of pediatrics. 2011 Jul;170(7):907-13. PubMed PMID: 21174120.
35. Mlinaric-Galinovic G, Welliver RC, Vilibic-Cavlek T, Ljubin-Sternak S, Drazenovic V, Galinovic I, et al. The biennial cycle of respiratory syncytial virus outbreaks in Croatia. Virology journal. 2008;5:18. PubMed PMID: 18226194. Pubmed Central PMCID: 2267449.
36. Meissner HC, Anderson LJ, Pickering LK. Annual variation in respiratory syncytial virus season and decisions regarding immunoprophylaxis with palivizumab. Pediatrics. 2004 Oct;114(4):1082-4. PubMed PMID: 15466107.
37. Langley GF, Anderson LJ. Epidemiology and prevention of respiratory syncytial virus infections among infants and young children. The Pediatric infectious disease journal. 2011 Jun;30(6):510-7. PubMed PMID: 21487331.
38. Rodriguez DA, Rodriguez-Martinez CE, Cardenas AC, Quilaguy IE, Mayorga LY, Falla LM, et al. Predictors of severity and mortality in children hospitalized with respiratory syncytial virus infection in a tropical region. Pediatric pulmonology. 2013 Feb 8. PubMed PMID: 23401345.
39. Ramet M, Korppi M, Hallman M. Pattern recognition receptors and genetic risk for rsv infection: value for clinical decision-making? Pediatric pulmonology. 2011 Feb;46(2):101-10. PubMed PMID: 20963841.
40. Amanatidou V, Apostolakis S, Spandidos DA. Genetic diversity of the host and severe respiratory syncytial virus-induced lower respiratory tract infection. The Pediatric infectious disease journal. 2009 Feb;28(2):135-40. PubMed PMID: 19106772.
41. Carpenter TC, Stenmark KR. Predisposition of infants with chronic lung disease to respiratory syncytial virus-induced respiratory failure: a vascular hypothesis. The Pediatric infectious disease journal. 2004 Jan;23(1 Suppl):S33-40. PubMed PMID: 14730268.
42. Checchia P. Identification and management of severe respiratory syncytial virus. American journal of health-system pharmacy : AJHP : official journal of the American Society of Health-System Pharmacists. 2008 Dec 1;65(23 Suppl 8):S7-12. PubMed PMID: 19020202.
43. Dawson-Caswell M, Muncie HL, Jr. Respiratory syncytial virus infection in children. American family physician. 2011 Jan 15;83(2):141-6. PubMed PMID: 21243988.
44. Simoes EA. Environmental and demographic risk factors for respiratory syncytial virus lower respiratory tract disease. The Journal of pediatrics. 2003 Nov;143(5 Suppl):S118-26. PubMed PMID: 14615710.

45. Krilov LR, Palazzi DL, Fernandes AW, Klein RW, Mahadevia PJ. Prevalence of respiratory syncytial virus (RSV) risk factors and cost implications of immunoprophylaxis to infants 32 to 35 weeks gestation for health plans in the United States. Value in health : the journal of the International Society for Pharmacoeconomics and Outcomes Research. 2010 Jan-Feb;13(1):77-86. PubMed PMID: 19706010.
46. Goksor E, Amark M, Alm B, Gustafsson PM, Wennergren G. The impact of pre- and post-natal smoke exposure on future asthma and bronchial hyper-responsiveness. Acta paediatrica. 2007 Jul;96(7):1030-5. PubMed PMID: 17498194.
47. Van Leeuwen JC, Goossens LK, Hendrix RM, Van Der Palen J, Lusthusz A, Thio BJ. Equal virulence of rhinovirus and respiratory syncytial virus in infants hospitalized for lower respiratory tract infection. The Pediatric infectious disease journal. 2012 Jan;31(1):84-6. PubMed PMID: 21909047.
48. McNamara PS, Smyth RL. The pathogenesis of respiratory syncytial virus disease in childhood. British medical bulletin. 2002;61:13-28. PubMed PMID: 11997296.
49. Prevention CfDCa. Respiratory Syncitial Virus Infection (RSV): Clinical Description and Diagnosis [updated 25th January 2010; cited 2013 30th January]. Available from: http://www.cdc.gov/rsv/clinical/description.html.
50. Randolph AG, Meert KL, O'Neil ME, Hanson JH, Luckett PM, Arnold JH, et al. The feasibility of conducting clinical trials in infants and children with acute respiratory failure. American journal of respiratory and critical care medicine. 2003 May 15;167(10):1334-40. PubMed PMID: 12615617.
51. Munjal I, Gialanella P, Goss C, McKitrick JC, Avner JR, Pan Q, et al. Evaluation of the 3M rapid detection test for respiratory syncytial virus (RSV) in children during the early stages of the 2009 RSV season. Journal of clinical microbiology. 2011 Mar;49(3):1151-3. PubMed PMID: 21177903. Pubmed Central PMCID: 3067731.
52. Ginocchio CC, Swierkosz E, McAdam AJ, Marcon M, Storch GA, Valsamakis A, et al. Multicenter study of clinical performance of the 3M Rapid Detection RSV test. Journal of clinical microbiology. 2010 Jul;48(7):2337-43. PubMed PMID: 20463154. Pubmed Central PMCID: 2897525.
53. Miernyk K, Bulkow L, DeByle C, Chikoyak L, Hummel KB, Hennessy T, et al. Performance of a rapid antigen test (Binax NOW(R) RSV) for diagnosis of respiratory syncytial virus compared with real-time polymerase chain reaction in a pediatric population. Journal of clinical virology : the official publication of the Pan American Society for Clinical Virology. 2011 Mar;50(3):240-3. PubMed PMID: 21163694.
54. Papenburg J, Buckeridge DL, De Serres G, Boivin G. Host and Viral Factors Affecting Clinical Performance of a Rapid Diagnostic Test for Respiratory Syncytial Virus in Hospitalized Children. The Journal of pediatrics. 2013 Apr 30. PubMed PMID: 23639327.
55. Bordley WC, Viswanathan M, King VJ, Sutton SF, Jackman AM, Sterling L, et al. Diagnosis and testing in bronchiolitis: a systematic review. Archives of pediatrics & adolescent medicine. 2004 Feb;158(2):119-26. PubMed PMID: 14757603.
56. Jefferson T, Del Mar C, Dooley L, Ferroni E, Al-Ansary LA, Bawazeer GA, et al. Physical interventions to interrupt or reduce the spread of respiratory viruses. Cochrane database of systematic reviews. 2010 (1):CD006207. PubMed PMID: 20091588.
57. Committee on Infectious D. From the American Academy of Pediatrics: Policy statements--Modified recommendations for use of palivizumab for prevention of

respiratory syncytial virus infections. Pediatrics. 2009 Dec;124(6):1694-701. PubMed PMID: 19736258.
58. Stuebe A. The risks of not breastfeeding for mothers and infants. Reviews in obstetrics and gynecology. 2009 Fall;2(4):222-31. PubMed PMID: 20111658. Pubmed Central PMCID: 2812877.
59. Meijboom MJ, Pouwels KB, Luytjes W, Postma MJ, Hak E. RSV vaccine in development: Assessing the potential cost-effectiveness in the Dutch elderly population. Vaccine. 2013 Dec 16;31(52):6254-60. PubMed PMID: 24148573.
60. Groothuis JR, Nishida H. Prevention of respiratory syncytial virus infections in high-risk infants by monoclonal antibody (palivizumab). Pediatrics international : official journal of the Japan Pediatric Society. 2002 Jun;44(3):235-41. PubMed PMID: 11982888.
61. Zhu Q, Patel NK, McAuliffe JM, Zhu W, Wachter L, McCarthy MP, et al. Natural polymorphisms and resistance-associated mutations in the fusion protein of respiratory syncytial virus (RSV): effects on RSV susceptibility to palivizumab. The Journal of infectious diseases. 2012 Feb 15;205(4):635-8. PubMed PMID: 22184728.
62. Resch B, Resch E, Muller W. Should respiratory care in preterm infants include prophylaxis against respiratory syncytial virus infection? The case in favour. Paediatric respiratory reviews. 2013 Jun;14(2):130-6. PubMed PMID: 23375547.
63. Zhu Q, McAuliffe JM, Patel NK, Palmer-Hill FJ, Yang CF, Liang B, et al. Analysis of respiratory syncytial virus preclinical and clinical variants resistant to neutralization by monoclonal antibodies palivizumab and/or motavizumab. The Journal of infectious diseases. 2011 Mar 1;203(5):674-82. PubMed PMID: 21208913. Pubmed Central PMCID: 3072724.
64. Blanken M, Rovers M, Sanders E, Bont L. Ethical considerations and rationale of the MAKI trial: a multicenter double-blind randomized placebo-controlled trial into the preventive effect of palivizumab on recurrent wheezing associated with respiratory syncytial virus infection in children with a gestational age of 33-35 weeks. Contemporary clinical trials. 2012 Nov;33(6):1287-92. PubMed PMID: 22820319.
65. Blanken MO, Rovers MM, Molenaar JM, Winkler-Seinstra PL, Meijer A, Kimpen JL, et al. Respiratory syncytial virus and recurrent wheeze in healthy preterm infants. The New England journal of medicine. 2013 May 9;368(19):1791-9. PubMed PMID: 23656644.
66. Sun Z, Pan Y, Jiang S, Lu L. Respiratory syncytial virus entry inhibitors targeting the F protein. Viruses. 2013 Jan;5(1):211-25. PubMed PMID: 23325327. Pubmed Central PMCID: 3564118.
67. (SIGN) SIGN. Bronchiolitis in Children, A National Clinical Guidline 2006 [cited 2013 6th August]. Available from: http://www.sign.ac.uk/pdf/sign91.pdf.
68. Okiro EA, Ngama M, Bett A, Nokes DJ. The incidence and clinical burden of respiratory syncytial virus disease identified through hospital outpatient presentations in Kenyan children. PloS one. 2012;7(12):e52520. PubMed PMID: 23300695. Pubmed Central PMCID: 3530465.
69. Collins PL, Melero JA. Progress in understanding and controlling respiratory syncytial virus: still crazy after all these years. Virus research. 2011 Dec;162(1-2):80-99. PubMed PMID: 21963675. Pubmed Central PMCID: 3221877.
70. Domachowske JB, Rosenberg HF. Respiratory syncytial virus infection: immune response, immunopathogenesis, and treatment. Clinical microbiology reviews. 1999 Apr;12(2):298-309. PubMed PMID: 10194461. Pubmed Central PMCID: 88919.

71. Tan YR, Peng D, Chen CM, Qin XQ. Nonstructural protein-1 of respiratory syncytial virus regulates HOX gene expression through interacting with histone. Molecular biology reports. 2013 Jan;40(1):675-9. PubMed PMID: 23054021.
72. Noton SL, Fearns R. The first two nucleotides of the respiratory syncytial virus antigenome RNA replication product can be selected independently of the promoter terminus. Rna. 2011 Oct;17(10):1895-906. PubMed PMID: 21878549. Pubmed Central PMCID: 3185921.
73. Noton SL, Deflube LR, Tremaglio CZ, Fearns R. The respiratory syncytial virus polymerase has multiple RNA synthesis activities at the promoter. PLoS pathogens. 2012;8(10):e1002980. PubMed PMID: 23093940. Pubmed Central PMCID: 3475672.
74. Fix J, Galloux M, Blondot ML, Eleouet JF. The insertion of fluorescent proteins in a variable region of respiratory syncytial virus L polymerase results in fluorescent and functional enzymes but with reduced activities. The open virology journal. 2011;5:103-8. PubMed PMID: 21966341. Pubmed Central PMCID: 3178903.
75. Blondot ML, Dubosclard V, Fix J, Lassoued S, Aumont-Nicaise M, Bontems F, et al. Structure and functional analysis of the RNA- and viral phosphoprotein-binding domain of respiratory syncytial virus M2-1 protein. PLoS pathogens. 2012;8(5):e1002734. PubMed PMID: 22675274. Pubmed Central PMCID: 3364950.
76. Esperante SA, Chemes LB, Sanchez IE, de Prat-Gay G. The respiratory syncytial virus transcription antiterminator M(2-1) is a highly stable, zinc binding tetramer with strong pH-dependent dissociation and a monomeric unfolding intermediate. Biochemistry. 2011 Oct 11;50(40):8529-39. PubMed PMID: 21877705.
77. Moore EC, Barber J, Tripp RA. Respiratory syncytial virus (RSV) attachment and nonstructural proteins modify the type I interferon response associated with suppressor of cytokine signaling (SOCS) proteins and IFN-stimulated gene-15 (ISG15). Virology journal. 2008;5:116. PubMed PMID: 18851747. Pubmed Central PMCID: 2577635.
78. Swedan S, Musiyenko A, Barik S. Respiratory syncytial virus nonstructural proteins decrease levels of multiple members of the cellular interferon pathways. Journal of virology. 2009 Oct;83(19):9682-93. PubMed PMID: 19625398. Pubmed Central PMCID: 2748017.
79. Swedan S, Andrews J, Majumdar T, Musiyenko A, Barik S. Multiple functional domains and complexes of the two nonstructural proteins of human respiratory syncytial virus contribute to interferon suppression and cellular location. Journal of virology. 2011 Oct;85(19):10090-100. PubMed PMID: 21795342. Pubmed Central PMCID: 3196442.
80. Taylor KE, Mossman KL. Recent advances in understanding viral evasion of type I interferon. Immunology. 2013 Mar;138(3):190-7. PubMed PMID: 23173987. Pubmed Central PMCID: 3573272.
81. Tayyari F, Marchant D, Moraes TJ, Duan W, Mastrangelo P, Hegele RG. Identification of nucleolin as a cellular receptor for human respiratory syncytial virus. Nature medicine. 2011 Sep;17(9):1132-5. PubMed PMID: 21841784.
82. Krzyzaniak MA, Zumstein MT, Gerez JA, Picotti P, Helenius A. Host cell entry of respiratory syncytial virus involves macropinocytosis followed by proteolytic activation of the F protein. PLoS pathogens. 2013 Apr;9(4):e1003309. PubMed PMID: 23593008. Pubmed Central PMCID: 3623752.
83. Meanwell NA, Krystal M. Respiratory syncytial virus: recent progress towards the discovery of effective prophylactic and therapeutic agents. Drug discovery today. 2000 Jun;5(6):241-52. PubMed PMID: 10825730.

84. Radhakrishnan A, Yeo D, Brown G, Myaing MZ, Iyer LR, Fleck R, et al. Protein analysis of purified respiratory syncytial virus particles reveals an important role for heat shock protein 90 in virus particle assembly. Molecular & cellular proteomics : MCP. 2010 Sep;9(9):1829-48. PubMed PMID: 20530633. Pubmed Central PMCID: 2938102.
85. Tian J, Huang K, Krishnan S, Svabek C, Rowe DC, Brewah Y, et al. RAGE inhibits human respiratory syncytial virus syncytium formation by interfering with F-protein function. The Journal of general virology. 2013 Aug;94(Pt 8):1691-700. PubMed PMID: 23559480.
86. Haynes LM, Caidi H, Radu GU, Miao C, Harcourt JL, Tripp RA, et al. Therapeutic monoclonal antibody treatment targeting respiratory syncytial virus (RSV) G protein mediates viral clearance and reduces the pathogenesis of RSV infection in BALB/c mice. The Journal of infectious diseases. 2009 Aug 1;200(3):439-47. PubMed PMID: 19545210.
87. Triantafilou K, Kar S, Vakakis E, Kotecha S, Triantafilou M. Human respiratory syncytial virus viroporin SH: a viral recognition pathway used by the host to signal inflammasome activation. Thorax. 2013 Jan;68(1):66-75. PubMed PMID: 23229815.
88. Sergel TA, McGinnes LW, Morrison TG. A single amino acid change in the Newcastle disease virus fusion protein alters the requirement for HN protein in fusion. Journal of virology. 2000 Jun;74(11):5101-7. PubMed PMID: 10799584. Pubmed Central PMCID: 110862.
89. Li Z, Xu J, Patel J, Fuentes S, Lin Y, Anderson D, et al. Function of the small hydrophobic protein of J paramyxovirus. Journal of virology. 2011 Jan;85(1):32-42. PubMed PMID: 20980504. Pubmed Central PMCID: 3014192.
90. Gan SW, Tan E, Lin X, Yu D, Wang J, Tan GM, et al. The small hydrophobic protein of the human respiratory syncytial virus forms pentameric ion channels. The Journal of biological chemistry. 2012 Jul 13;287(29):24671-89. PubMed PMID: 22621926. Pubmed Central PMCID: 3397895.
91. Krishnan S, Craven M, Welliver RC, Ahmad N, Halonen M. Differences in participation of innate and adaptive immunity to respiratory syncytial virus in adults and neonates. The Journal of infectious diseases. 2003 Aug 1;188(3):433-9. PubMed PMID: 12870126.
92. Matsukawa A, Hogaboam CM, Lukacs NW, Kunkel SL. Chemokines and innate immunity. Reviews in immunogenetics. 2000;2(3):339-58. PubMed PMID: 11256744.
93. Zeng R, Cui Y, Hai Y, Liu Y. Pattern recognition receptors for respiratory syncytial virus infection and design of vaccines. Virus research. 2012 Aug;167(2):138-45. PubMed PMID: 22698878.
94. Groskreutz DJ, Monick MM, Powers LS, Yarovinsky TO, Look DC, Hunninghake GW. Respiratory syncytial virus induces TLR3 protein and protein kinase R, leading to increased double-stranded RNA responsiveness in airway epithelial cells. Journal of immunology. 2006 Feb 1;176(3):1733-40. PubMed PMID: 16424203.
95. Hull J, Thomson A, Kwiatkowski D. Association of respiratory syncytial virus bronchiolitis with the interleukin 8 gene region in UK families. Thorax. 2000 Dec;55(12):1023-7. PubMed PMID: 11083887. Pubmed Central PMCID: 1745668.
96. Harrison AM, Bonville CA, Rosenberg HF, Domachowske JB. Respiratory syncytical virus-induced chemokine expression in the lower airways: eosinophil recruitment and degranulation. American journal of respiratory and critical care medicine. 1999 Jun;159(6):1918-24. PubMed PMID: 10351940.
97. Focus on articulators. The Dental technician. 1976 Feb;29(2):4-5, 7. PubMed PMID: 1072872.

98. Levitz R, Wattier R, Phillips P, Solomon A, Lawler J, Lazar I, et al. Induction of IL-6 and CCL5 (RANTES) in human respiratory epithelial (A549) cells by clinical isolates of respiratory syncytial virus is strain specific. Virology journal. 2012;9:190. PubMed PMID: 22962966. Pubmed Central PMCID: 3463437.
99. de Veer MJ, Holko M, Frevel M, Walker E, Der S, Paranjape JM, et al. Functional classification of interferon-stimulated genes identified using microarrays. Journal of leukocyte biology. 2001 Jun;69(6):912-20. PubMed PMID: 11404376.
100. Schoggins JW, Rice CM. Interferon-stimulated genes and their antiviral effector functions. Current opinion in virology. 2011 Dec;1(6):519-25. PubMed PMID: 22328912. Pubmed Central PMCID: 3274382.
101. UT southwestern Medical Center Research Labs SL. Interferon Stimulated Genes [cited 2013 7th August]. Available from: http://www.utsouthwestern.edu/labs/schoggins/research/isgs.html.
102. Kumar H, Kawai T, Akira S. Pathogen recognition by the innate immune system. International reviews of immunology. 2011 Feb;30(1):16-34. PubMed PMID: 21235323.
103. Ling Z, Tran KC, Teng MN. Human respiratory syncytial virus nonstructural protein NS2 antagonizes the activation of beta interferon transcription by interacting with RIG-I. Journal of virology. 2009 Apr;83(8):3734-42. PubMed PMID: 19193793. Pubmed Central PMCID: 2663251.
104. Graham BS. Biological challenges and technological opportunities for respiratory syncytial virus vaccine development. Immunological reviews. 2011 Jan;239(1):149-66. PubMed PMID: 21198670. Pubmed Central PMCID: 3023887.
105. Lukens MV, Kruijsen D, Coenjaerts FE, Kimpen JL, van Bleek GM. Respiratory syncytial virus-induced activation and migration of respiratory dendritic cells and subsequent antigen presentation in the lung-draining lymph node. Journal of virology. 2009 Jul;83(14):7235-43. PubMed PMID: 19420085. Pubmed Central PMCID: 2704789.
106. Bera MM, Lu B, Martin TR, Cui S, Rhein LM, Gerard C, et al. Th17 cytokines are critical for respiratory syncytial virus-associated airway hyperreponsiveness through regulation by complement C3a and tachykinins. Journal of immunology. 2011 Oct 15;187(8):4245-55. PubMed PMID: 21918196. Pubmed Central PMCID: 3186836.
107. Marblestone JG, Suresh Kumar KG, Eddins MJ, Leach CA, Sterner DE, Mattern MR, et al. Novel approach for characterizing ubiquitin E3 ligase function. Journal of biomolecular screening. 2010 Dec;15(10):1220-8. PubMed PMID: 20864734.
108. Walczak H, Iwai K, Dikic I. Generation and physiological roles of linear ubiquitin chains. BMC biology. 2012;10:23. PubMed PMID: 22420778. Pubmed Central PMCID: 3305636.
109. Pinato S, Scandiuzzi C, Arnaudo N, Citterio E, Gaudino G, Penengo L. RNF168, a new RING finger, MIU-containing protein that modifies chromatin by ubiquitination of histones H2A and H2AX. BMC molecular biology. 2009;10:55. PubMed PMID: 19500350. Pubmed Central PMCID: 2699339.
110. Al-Hakim A, Escribano-Diaz C, Landry MC, O'Donnell L, Panier S, Szilard RK, et al. The ubiquitous role of ubiquitin in the DNA damage response. DNA repair. 2010 Dec 10;9(12):1229-40. PubMed PMID: 21056014.
111. Okumura F, Yoshida K, Liang F, Hatakeyama S. MDA-9/syntenin interacts with ubiquitin via a novel ubiquitin-binding motif. Molecular and cellular biochemistry. 2011 Jun;352(1-2):163-72. PubMed PMID: 21359963.

112. Hoeller D, Dikic I. Regulation of ubiquitin receptors by coupled monoubiquitination. Sub-cellular biochemistry. 2010;54:31-40. PubMed PMID: 21222271.
113. Hokkaido University Graduate School of Medicine B, Medical Chemistry Biochemical Reaction of Ubiquitination 2013 [cited 2013 7th May]. Available from: http://www.med.hokudai.ac.jp/en/dept/outline/mc/fig1.html.
114. Baumann K. Technologies: Seeing ubiquitin chains. Nature reviews Molecular cell biology. 2012 Sep;13(9):540. PubMed PMID: 22850817.
115. Metzger MB, Hristova VA, Weissman AM. HECT and RING finger families of E3 ubiquitin ligases at a glance. Journal of cell science. 2012 Feb 1;125(Pt 3):531-7. PubMed PMID: 22389392. Pubmed Central PMCID: 3381717.
116. Deshaies RJ, Joazeiro CA. RING domain E3 ubiquitin ligases. Annual review of biochemistry. 2009;78:399-434. PubMed PMID: 19489725.
117. Plechanovova A, Jaffray EG, Tatham MH, Naismith JH, Hay RT. Structure of a RING E3 ligase and ubiquitin-loaded E2 primed for catalysis. Nature. 2012 Sep 6;489(7414):115-20. PubMed PMID: 22842904. Pubmed Central PMCID: 3442243.
118. Carlile CM, Pickart CM, Matunis MJ, Cohen RE. Synthesis of free and proliferating cell nuclear antigen-bound polyubiquitin chains by the RING E3 ubiquitin ligase Rad5. The Journal of biological chemistry. 2009 Oct 23;284(43):29326-34. PubMed PMID: 19706603. Pubmed Central PMCID: 2785563.
119. Bratzel F, Lopez-Torrejon G, Koch M, Del Pozo JC, Calonje M. Keeping cell identity in Arabidopsis requires PRC1 RING-finger homologs that catalyze H2A monoubiquitination. Current biology : CB. 2010 Oct 26;20(20):1853-9. PubMed PMID: 20933424.
120. Munoz MC, Laulier C, Gunn A, Cheng A, Robbiani DF, Nussenzweig A, et al. RING finger nuclear factor RNF168 is important for defects in homologous recombination caused by loss of the breast cancer susceptibility factor BRCA1. The Journal of biological chemistry. 2012 Nov 23;287(48):40618-28. PubMed PMID: 23055523. Pubmed Central PMCID: 3504775.
121. Lilley CE, Chaurushiya MS, Boutell C, Landry S, Suh J, Panier S, et al. A viral E3 ligase targets RNF8 and RNF168 to control histone ubiquitination and DNA damage responses. The EMBO journal. 2010 Mar 3;29(5):943-55. PubMed PMID: 20075863. Pubmed Central PMCID: 2837166.
122. Lilley CE, Chaurushiya MS, Boutell C, Everett RD, Weitzman MD. The intrinsic antiviral defense to incoming HSV-1 genomes includes specific DNA repair proteins and is counteracted by the viral protein ICP0. PLoS pathogens. 2011 Jun;7(6):e1002084. PubMed PMID: 21698222. Pubmed Central PMCID: 3116817.
123. Weller SK. Herpes simplex virus reorganizes the cellular DNA repair and protein quality control machinery. PLoS pathogens. 2010;6(11):e1001105. PubMed PMID: 21124825. Pubmed Central PMCID: 2991270.
124. Stewart GS, Stankovic T, Byrd PJ, Wechsler T, Miller ES, Huissoon A, et al. RIDDLE immunodeficiency syndrome is linked to defects in 53BP1-mediated DNA damage signaling. Proceedings of the National Academy of Sciences of the United States of America. 2007 Oct 23;104(43):16910-5. PubMed PMID: 17940005. Pubmed Central PMCID: 2040433.
125. Pinato S, Gatti M, Scandiuzzi C, Confalonieri S, Penengo L. UMI, a novel RNF168 ubiquitin binding domain involved in the DNA damage signaling pathway. Molecular and cellular biology. 2011 Jan;31(1):118-26. PubMed PMID: 21041483. Pubmed Central PMCID: 3019843.

126. Panier S, Durocher D. Regulatory ubiquitylation in response to DNA double-strand breaks. DNA repair. 2009 Apr 5;8(4):436-43. PubMed PMID: 19230794.
127. Bekker-Jensen S, Mailand N. Ubiquitin and the DNA damage response: a new handle on histones. Cell cycle. 2012 Sep 1;11(17):3153. PubMed PMID: 22895171. Pubmed Central PMCID: 3466509.
128. Mosbech A, Lukas C, Bekker-Jensen S, Mailand N. The deubiquitylating enzyme USP44 counteracts the DNA double-strand break response mediated by the RNF8 and RNF168 ubiquitin ligases. The Journal of biological chemistry. 2013 Jun 7;288(23):16579-87. PubMed PMID: 23615962. Pubmed Central PMCID: 3675593.
129. Serio RN. Unraveling the mysteries of aging through a Hutchinson-Gilford progeria syndrome model. Rejuvenation research. 2011 Apr;14(2):133-41. PubMed PMID: 21208065.
130. Rocha CR, Lerner LK, Okamoto OK, Marchetto MC, Menck CF. The role of DNA repair in the pluripotency and differentiation of human stem cells. Mutation research. 2013 Jan-Mar;752(1):25-35. PubMed PMID: 23010441.
131. Stewart GS, Panier S, Townsend K, Al-Hakim AK, Kolas NK, Miller ES, et al. The RIDDLE syndrome protein mediates a ubiquitin-dependent signaling cascade at sites of DNA damage. Cell. 2009 Feb 6;136(3):420-34. PubMed PMID: 19203578.
132. Mattiroli F, Vissers JH, van Dijk WJ, Ikpa P, Citterio E, Vermeulen W, et al. RNF168 ubiquitinates K13-15 on H2A/H2AX to drive DNA damage signaling. Cell. 2012 Sep 14;150(6):1182-95. PubMed PMID: 22980979.
133. Blundred RM, Stewart GS. DNA double-strand break repair, immunodeficiency and the RIDDLE syndrome. Expert review of clinical immunology. 2011 Mar;7(2):169-85. PubMed PMID: 21426255.
134. Smith MC, Boutell C, Davido DJ. HSV-1 ICP0: paving the way for viral replication. Future virology. 2011 Apr;6(4):421-9. PubMed PMID: 21765858. Pubmed Central PMCID: 3133933.
135. Chaurushiya MS, Lilley CE, Aslanian A, Meisenhelder J, Scott DC, Landry S, et al. Viral E3 ubiquitin ligase-mediated degradation of a cellular E3: viral mimicry of a cellular phosphorylation mark targets the RNF8 FHA domain. Molecular cell. 2012 Apr 13;46(1):79-90. PubMed PMID: 22405594. Pubmed Central PMCID: 3648639.
136. Bian T, Gibbs JD, Orvell C, Imani F. Respiratory syncytial virus matrix protein induces lung epithelial cell cycle arrest through a p53 dependent pathway. PloS one. 2012;7(5):e38052. PubMed PMID: 22662266. Pubmed Central PMCID: 3360651.
137. Salaun C, MacDonald AI, Larralde O, Howard L, Lochtie K, Burgess HM, et al. Poly(A)-binding protein 1 partially relocalizes to the nucleus during herpes simplex virus type 1 infection in an ICP27-independent manner and does not inhibit virus replication. Journal of virology. 2010 Sep;84(17):8539-48. PubMed PMID: 20573819. Pubmed Central PMCID: 2919032.
138. Ren X, Zhou H, Li B, Su SB. Toll-like receptor 3 ligand polyinosinic:polycytidylic acid enhances autoimmune disease in a retinal autoimmunity model. International immunopharmacology. 2011 Jun;11(6):769-73. PubMed PMID: 21296697.
139. Okabe H, Beppu T, Ueda M, Hayashi H, Ishiko T, Masuda T, et al. Identification of CXCL5/ENA-78 as a factor involved in the interaction between cholangiocarcinoma cells and cancer-associated fibroblasts. International journal of cancer Journal international du cancer. 2012 Nov 15;131(10):2234-41. PubMed PMID: 22337081.
140. Chavey C, Fajas L. CXCL5 drives obesity to diabetes, and further. Aging. 2009 Jul;1(7):674-7. PubMed PMID: 20157549. Pubmed Central PMCID: 2806041.

141. Mei J, Liu Y, Dai N, Favara M, Greene T, Jeyaseelan S, et al. CXCL5 regulates chemokine scavenging and pulmonary host defense to bacterial infection. Immunity. 2010 Jul 23;33(1):106-17. PubMed PMID: 20643340.
142. Brodie AE, Reed DJ. Buthionine sulfoximine inhibition of cystine uptake and glutathione biosynthesis in human lung carcinoma cells. Toxicology and applied pharmacology. 1985 Mar 15;77(3):381-7. PubMed PMID: 3975906.
143. Advansta. Protein Analysis: Electropheresis, Blotting and Immunodetection [cited 2013 7th May]. Available from: http://advansta.com/PA_Guide.pdf.
144. Scientific T. Overview of ELISA [cited 2013 6th August]. Available from: http://www.piercenet.com/browse.cfm?fldID=F88ADEC9-1B43-4585-922E-836FE09D8403.
145. Watson R, Lindner S, Bordereau P, Hunze EM, Tak F, Ngo S, et al. Standardisation of the factor H autoantibody assay. Immunobiology. 2013 Jun 26. PubMed PMID: 23891327.
146. Sino Biological inc. Biological Solution Specialist EE. Sandwich ELISA, Highly Sensitive 2013 [cited 2013 6th August]. Available from: http://www.elisa-antibody.com/ELISA-Introduction/ELISA-types/sandwich-elisa.
147. Fiedler MA, Wernke-Dollries K, Stark JM. Mechanism of RSV-induced IL-8 gene expression in A549 cells before viral replication. The American journal of physiology. 1996 Dec;271(6 Pt 1):L963-71. PubMed PMID: 8997267.
148. Arnold R, Humbert B, Werchau H, Gallati H, Konig W. Interleukin-8, interleukin-6, and soluble tumour necrosis factor receptor type I release from a human pulmonary epithelial cell line (A549) exposed to respiratory syncytial virus. Immunology. 1994 May;82(1):126-33. PubMed PMID: 7519169. Pubmed Central PMCID: 1414862.
149. Systems RD. Human CXCL8/IL-8, Catalog Number: DY208 [cited 2013 4th May]. Available from: www.rndsystems.com/pdf/dy208.pdf.
150. Systems RD. Human IL-6 Catalog Number: DY206 [cited 2013 8th August]. Available from: http://www.rndsystems.com/pdf/dy206.pdf.
151. Systems RD. human CXCL5/ENA-78, Catalog Number: DY254 [cited 2013 3th August]. Available from: http://www.rndsystems.com/pdf/dy254.pdf.
152. Santos CF, Sakai VT, Machado MA, Schippers DN, Greene AS. Reverse transcription and polymerase chain reaction: principles and applications in dentistry. Journal of applied oral science : revista FOB. 2004 Mar;12(1):1-11. PubMed PMID: 21365144.
153. Protocol HUL. RNA Isolation and Purification from Cell Lines Using Qiagen's RNA Mini Kit [cited 2013 5th May]. Available from: http://compbio.dfci.harvard.edu/compbio/research/labprotocols/contentBlocks/0/contentBlock_files/file16/RNA_Isolation_and_Purification_from_Cell_Lines_Using_Qiagen.pdf.
154. Qiagen. RNeasy Mini Handbook-qiagen (Page 11) 2010 [cited 2013 5th May]. 4th Edition:[Available from: http://www.qiagen.com/Products/Catalog/Sample-Technologies/RNA-Sample-Technologies/Total-RNA/RNeasy-Mini-Kit#resources.
155. Scientific TF. NanoDrop 1000 Spectrophotometer V3.7 User's Manual 2008 [cited 2013 4th May]. Available from: http://www.nanodrop.com/library/nd-1000-v3.7-users-manual-8.5x11.pdf.
156. Dewhurst-Maridor G, Simonet V, Bornand JE, Nicod LP, Pache JC. Development of a quantitative TaqMan RT-PCR for respiratory syncytial virus. Journal of virological methods. 2004 Sep 1;120(1):41-9. PubMed PMID: 15234808.

157. Technologies L. Essential for Real-Time PCR 2013 [cited 2013 5th July]. Available from: http://www.lifetechnologies.com/uk/en/home/life-science/pcr/real-time-pcr/qpcr-education/essentials-of-real-time-pcr.html.
158. Tong W, Cao X, Wen S, Guo R, Shen M, Wang J, et al. Enhancing the specificity and efficiency of polymerase chain reaction using polyethyleneimine-based derivatives and hybrid nanocomposites. International journal of nanomedicine. 2012;7:1069-78. PubMed PMID: 22393296. Pubmed Central PMCID: 3289439.
159. Amer H. Real-time PCR. 2 Park Square Milton Park Abingdon, OX14 4RN: Taylor & Francis Group 2006.
160. Cockerill FR, 3rd. Application of rapid-cycle real-time polymerase chain reaction for diagnostic testing in the clinical microbiology laboratory. Archives of pathology & laboratory medicine. 2003 Sep;127(9):1112-20. PubMed PMID: 12946235.
161. Incorporated M. Advantages of Real-Time PCR 2013 [cited 2013 3rd May]. Available from: http://www.medialabinc.net/spg448465/advantages_of_real_time_pcr.aspx.
162. Technologies L. Real-time PCR Handbook [cited 2013 25th May]. Available from: http://find.lifetechnologies.com/Global/FileLib/qPCR/RealTimePCR_Handbook_Update_FLR.pdf.
163. Technologies L. A Normal Amplification Curve [cited 2013 3rd May]. Available from: http://www.invitrogen.com/site/us/en/home/Products-and-Services/Applications/PCR/real-time-pcr/qpcr-education/real-time-pcr-troubleshooting-tool/gene-expression-quantitation-troubleshooting/normal-amplification-curve.html.
164. Technologies L. Essentials of Real-Time PCR [cited 2013 24th May]. Available from: http://www.invitrogen.com/site/us/en/home/Products-and-Services/Applications/PCR/real-time-pcr/qpcr-education/essentials-of-real-time-pcr.html.
165. Matsumoto M, Seya T. TLR3: interferon induction by double-stranded RNA including poly(I:C). Advanced drug delivery reviews. 2008 Apr 29;60(7):805-12. PubMed PMID: 18262679.